UiT The Arctic University of Norway

Faculty of Science and Technology

Department of Geosciences

Neoproterozoic orogenesis in south-eastern South America

An examination of pre-orogenic rifting, sedimentation, and mountain building processes recorded in the orogenic foreland of the Dom Feliciano Belt

Jack James Percival

A dissertation for the degree of Philosophiae Doctor December 2021

Neoproterozoic orogenesis in south-eastern South America

An examination of pre-orogenic rifting, sedimentation, and mountain building processes recorded in the Dom Feliciano Belt

Jack James Percival

A dissertation for the degree of Philosophiae Doctor

UiT The Artic University of Norway

Faculty of Science and Technology

Department of Geosciences

December 2021

Front page image: Folds in the Brusque Complex (Santa Catarina, Brazil) and the Rocha Group (Uruguay).

Acknowledgements

First and foremost, I would like to thank Jiří Konopásek for being an A-grade, world-class supervisor, a passionate and dedicated scientist, and an all-round good bloke. Without your guidance, support, and patience, I may not have made it through. Thank you for inspiring in me a passion for petrology and allowing me to travel the world to pursue my interest in tectonics. Thank you also to Fátima Bitencourt, for your infectious enthusiasm and for welcoming me into your network of brilliant and passionate proteges, you are both inspirational scientists.

I would like to thank the other co-authors of the papers included in this thesis: Jiří Sláma, Robert Anczkiewicz, and Morgan Ganerød for your tireless and masterful geochronological work; Ragnhild Eiesland, Roberto Sacks de Campos, Matheus Battisti, and Pedro Oyhantçabal for your great work in the field, invaluable geological discussions, and much more.

Many thanks as well to all the people who helped with sample preparation, data collection and fieldwork along the way. Thanks (and sorry) to Trine Dahl, Ingvild Hald, and Karina Monsen for making many countless thin sections and tolerating my many questions. Thanks to the fantastic people at the Polish Academy of Sciences in Krakow—Dariusz Sala and Marta Koziarska for all the training and help in the lab, and Akeek Maitra for being a dependable friend during every visit. Thanks also to Radek Škoda and Renata Čopjaková for EMP analyses, and to Martin Whitehouse and Heejin Jeon for their support using the ion microprobe at NordSIM. Finally, thanks to all the amazing geologists in Brazil and Uruguay, without whose help this study would not have been possible—Roberto Sacks de Campos for being so generous with your time, both as a colleague and as a friend; Matheus Battisti and Diego Lira for putting up with me for so long in the field: Giuseppe de Toni for your enthusiasm, intelligent conversation, and for always sharing your chimarrão; and countless others—working with you reminds me why geology is worth studying in the first place.

I am so grateful for all the friendships I have made during my time in Tromsø. Thank you in particular to Louise, Ellery, Naima, Paul, Stephan and Marina for all the cabin trips, festivals, Friday beers, fieldwork, and good times. You are my dear friends, and I am so thankful that you were around through both the difficult and the fun moments. Many thanks also to the many others, too many to list, who made my time in Tromsø enjoyable. Thank you to my family and friends back in Australia, and my new family here in Norway, who helped get me through the final 'corona years' of the PhD. Finally, thank you Mathilde, for your beautiful smile, for all the joy you bring to my life, and for supporting me through everything; meeting you here in Tromsø has made it all worth it.

Preface

This thesis is the result of a four-year PhD project that started in April 2017. The project was funded by the department of Geosciences at the Arctic University of Norway (UiT), with additional funding from Diku Norway and CAPES Brazil (project UTF-2018-10004). The additional funding enabled four fieldtrips to Brazil and Uruguay, where I conducted fieldwork and collected samples for processing and analysis back at UiT and around Europe. Additional funding from the Norwegian Research School for Dynamics and Evolution of Earth and Planets (DEEP), University of Oslo (UiO), also funded three visits to the Institute of Geological Sciences, Polish Academy of Sciences, Kraków, where I spent a total of three months training at the Geochronology and Isotope Geochemistry Laboratory learning techniques in Lu–Hf and Sm–Nd garnet geochronology.

The educational requirements for the PhD program were met by the completion of four short courses run by the DEEP PhD school at UiO (and in collaboration with UiT), as well as a research ethics course and short course in P–T modelling at UiT. One year of the total four-year project was assigned to duty work, which included practical teaching of petrology, structural geology, and field geology courses. Part of this duty work also included maintenance of and responsibility for the rock cutting, crushing and mineral separation labs at the Department of Geosciences, UiT.

Over the course of the PhD, I presented results related to this work at the following international conferences/meetings: *European Geosciences Union (EGU) General Assembly* in Vienna, Austria, in 2019 and 2021 (online); *Thermal and mechanical evolution of collisional and accretionary orogens* in Třešť, Czech Republic. I also attended and presented work at yearly local meetings associated with DEEP and the Geoscience Research Academy of Tromsø (GReAT).

In this work I discuss the evolution of the South Atlantic Neoproterozoic Orogenic System by investigating the pre-orogenic and tectono-metamorphic history of the Dom Feliciano Belt foreland in southern Brazil and Uruguay. The thesis consists of an introduction, including a brief synthesis, and three papers.

The three research articles are as follows:

I. Percival, J. J., Konopásek, J., Eiesland, R., Sláma, J., Campos, R. S., Battisti, M. A., Bitencourt, M. F., 2021, **Pre-orogenic connection of the foreland domains of the Kaoko–Dom Feliciano–Gariep orogenic system**, *Precambrian Research*, vol. 354, pp. 106060, https://doi.org/10.1016/j.precamres.2020.106060

II. Percival, J. J., Konopásek, J., Anczkiewicz, R., Ganerød, M., Sláma, J., Campos, R. S., Battisti, M. A., Bitencourt, M. F., **Tectono-metamorphic evolution of the northern Dom Feliciano Belt foreland, Santa Catarina, Brazil: Implications for models of subduction-driven orogenesis**, in review at *Tectonics*

III. Percival, J. J., Konopásek, J., Oyhantçabal, P., Sláma, J., Anczkiewicz, R., **Diachronous two-stage Neoproterozoic evolution of the southern Dom Feliciano Belt, Uruguay**, in preparation for submission to *Journal of Metamorphic Geology* or *Tectonics*

Contents

SECTION I Synthesis

1 Introduction

Orogeny is a complex process controlled by the interactions between numerous continental and oceanic plates and minor crustal bodies over potentially many tens of millions of years. As such, the final geometry of an orogen can vary significantly depending on the dominant tectonic processes taking place during orogenesis. Three end-member types are generally recognised across both ancient and modern orogens (Fig. 1)—collisional, accretionary and intracontinental (Cawood et al., 2009; Raimondo et al., 2014)—and understanding the timing and conditions of tectonic events within an orogen are integral in developing a consistent tectonic framework within which to describe it. Due to the interrelated nature of the processes driving the three dominant orogen types, recognising identifying characteristic features can be difficult, particularly in ancient orogens where much of the information has been lost. To understand the entire evolution of an orogen, from pre-orogenesis to post-collision, it is essential to develop and integrate robust geochronological, structural, and thermobarometric datasets.

The South Atlantic Neoproterozoic Orogenic System (SANOS, sensu Konopásek et al., 2020) formed from the convergence of a series of continental plates during the amalgamation of Gondwana (Fig. 2a), and is now divided by the South Atlantic Ocean. For many years, the various belts that comprise the SANOS have been predominantly described as collisional or mixed collisional–accretionary orogenic belts preceded by the complete subduction of a large proto-Atlantic oceanic domain known as the

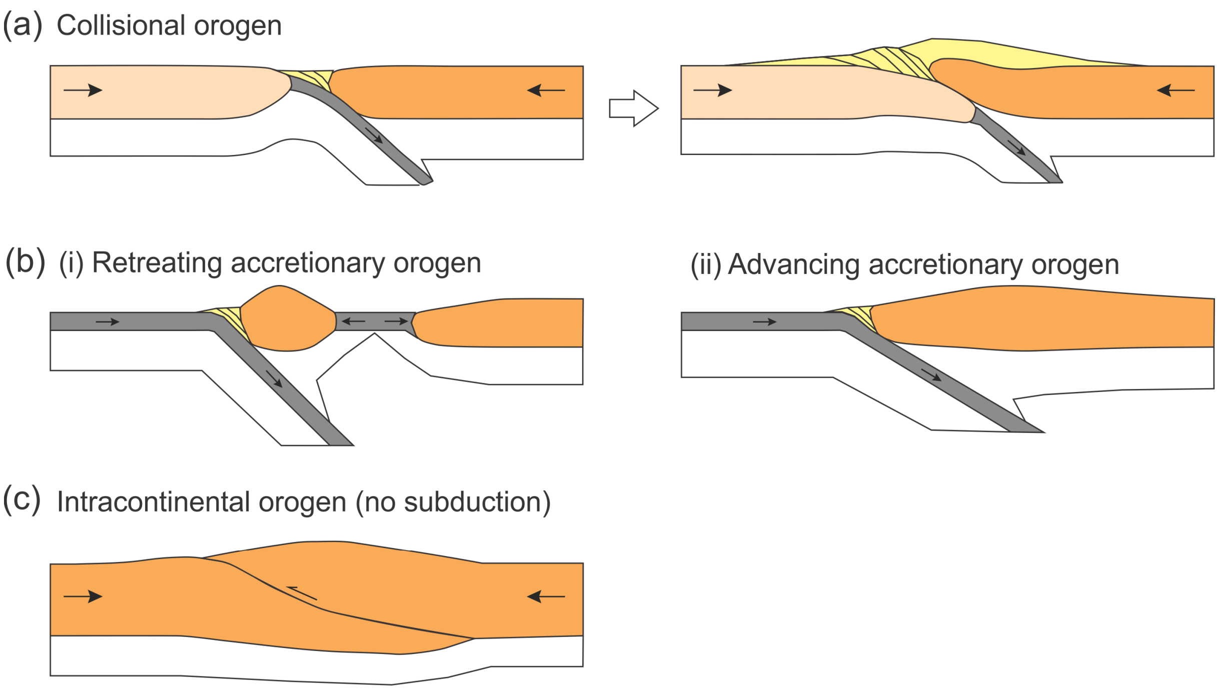

Figure 1. Schematic cross sections depicting the three major orogen types (modified after Cawood et al., 2009). (a) Collisional orogen – subduction leading to collision between two continents; (b) (i) Retreating accretionary orogen – subduction resulting in magmatism, accretion of smaller continental terranes, and back-arc spreading; (ii) Advancing accretionary orogen – subduction resulting in magmatism, accretion of smaller continental terranes, and crustal thickening; (c) Intracontinental orogen – crustal thickening in a within plate setting, far removed from active margins and subduction processes.

Adamastor Ocean (Basei et al., 2000; Hartnady et al., 1985; Heilbron and Machado, 2003; Pedrosa-Soares et al., 1998). A large, pre-orogenic proto-Atlantic Ocean located between the African and South American cratons was first proposed to describe the southern part of the SANOS in terms of continental collision (Porada, 1979), and since then the subduction–collision model has come to dominate the

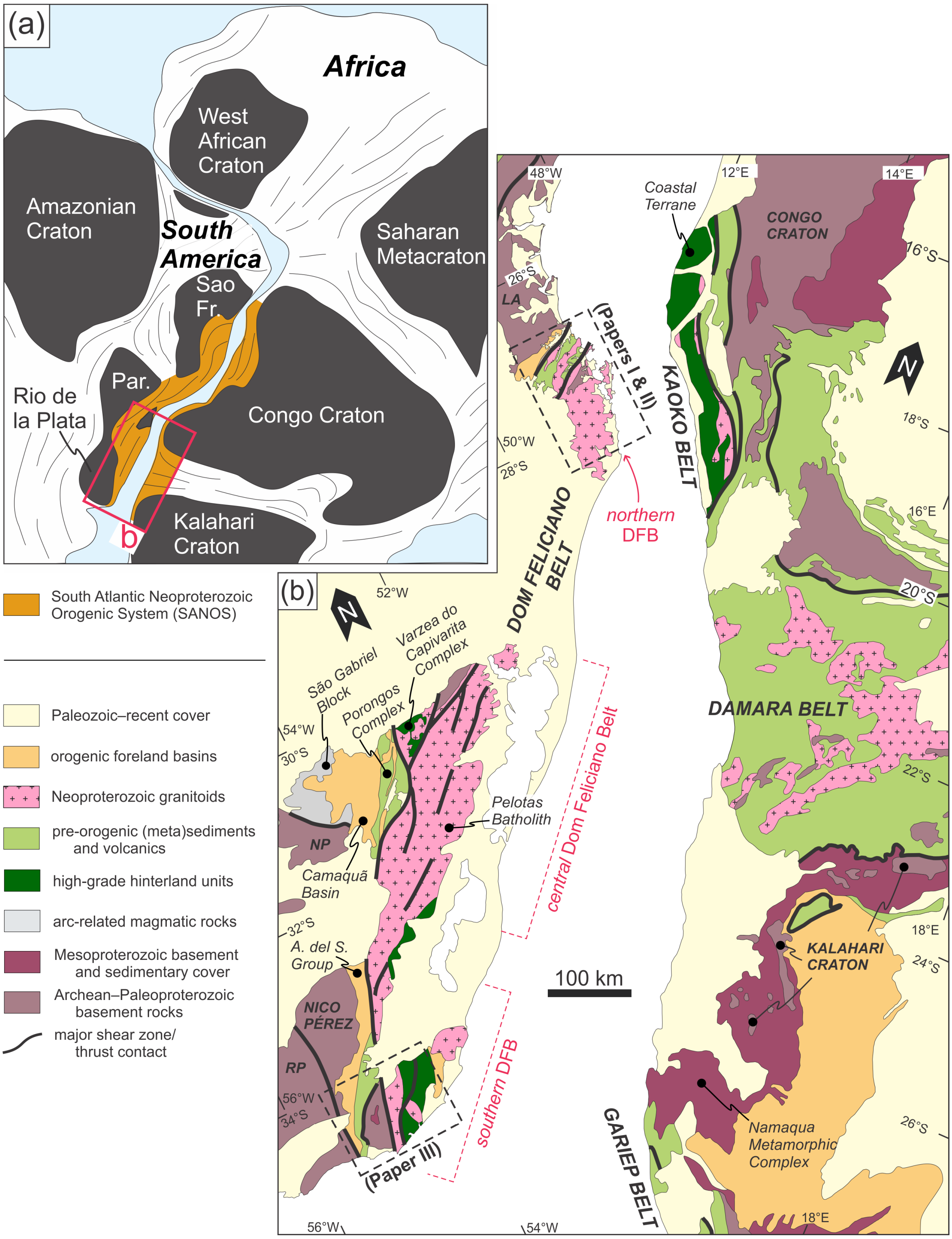

Figure 2. Geological overview of the SANOS. (a) Schematic reconstruction of Western Gondwana showing the location of the SANOS, Par. = Paranapanema Craton, Sao Fr = Sao Francisco Craton (modified after Konopásek et al., 2020). (b) Simplified geology of the southern SANOS (based on Bitencourt and Nardi, 2000; De Toni et al., 2021; Konopásek et al., 2017; McCourt et al., 2013; Oyhantçabal et al., 2011a), showing the position of the African and South American continents at the onset of the opening of the South Atlantic Ocean (after Heine et al., 2013). LA = Luis Alves Craton; NP = Nico Pérez Terrane; RP = Rio de la Plata Craton; DFB = Dom Feliciano Belt.

scientific thinking surrounding the SANOS. However, a growing body of research in recent years suggests that a large Adamastor Ocean may not have existed at all, which has led to increasing support for alternative models involving accretionary orogeny with the SANOS in the back-arc position, or purely intracontinental orogeny (Cavalcante et al., 2019; Fossen et al., 2020; Konopásek et al., 2018; Konopásek et al., 2020; Meira et al., 2019a; Meira et al., 2019b).

The Kaoko–Dom Feliciano–Gariep orogenic system, outcropping along the Atlantic coastlines of Uruguay, southern Brazil, and Namibia, is one such sub-system of the SANOS that is classically characterised as a collisional orogen preceded by the subduction of a large Adamastor Ocean (Hartnady et al., 1985; Porada, 1979, 1989). However, even more so than in the northern SANOS, contrasting interpretations of crucial units have resulted in conflicting models of orogenesis almost since the inception of the concept of the Adamastor Ocean. This conflict is driven primarily by a lack of sufficient geochronological, structural, and metamorphic data.

Constraining the timing and conditions of tectonic events prior to and during orogenesis is key to understanding the evolution of orogenic belts. In particular, the geometric configuration of continental plates prior to orogenesis and the nature of earliest crustal thickening are crucial pieces of information needed to understand the dominant processes that facilitate mountain building. In this study, a multidisciplinary approach was taken to investigate the orogenic evolution of various units within the Dom Feliciano Belt, with particular focus on supracrustal metasedimentary rock of the orogenic foreland. The key study areas are located in Santa Catarina, Brazil, and in south-eastern Uruguay (Fig. 2b).

2 Background

2.1 The South Atlantic Neoproterozoic Orogenic System (SANOS)

The South Atlantic Neoproterozoic Orogenic System (SANOS; sensu Konopásek et al., 2020) comprises the system of Neoproterozoic orogenic belts that outcrop along the coastlines of the South Atlantic Ocean (Fig. 2). The SANOS includes the Dom Feliciano, Ribeira and Araçuaí belts in South America, and the Gariep, Damara, Kaoko and West Congo belts in Africa. The system is generally divided into a northern (Ribeira–Araçuaí–West Congo belts) and a southern (Kaoko–Dom Feliciano–Gariep–Damara belts) domain. Overall, the tectonic structures of the belts fit within the framework of typical orogens, showing internal *hinterland* and external *foreland* domains. The hinterland is characterised by high metamorphic grades and extensive magmatic activity, whereas the foreland is characterised by low- to medium-grade metamorphism and fold-and-thrust tectonics with vergence away from the hinterland. Altogether, the orogenic system is roughly symmetrical, with eastern (African) and western (South American) forelands flanking a single internal hinterland.

Both the eastern and western forelands are comprised of basement domains overlain by variably deformed and metamorphosed supracrustal sequences. The basement consists of Archean–Paleoprotereozoic cratonic crust (Egydio-Silva et al., 2018; Kröner et al., 2004; Oyhantçabal et al., 2018; Passarelli et al., 2018; Seth et al., 1998; Thomas et al., 2016)—including the Congo–Sao Francisco, Kalahari, and Luis Alves cratons, and the Nico Pérez Terrane (Fig. 2a)—and the supracrustal units represent their Paleo–Neoproterozoic volcanosedimentary cover (Frimmel, 2018; Hoffman and Halverson, 2008; Hueck et al., 2018; Juliani et al., 2000; Konopásek et al., 2014; Konopásek et al., 2017; Oriolo et al., 2019). A large proportion of the cover sequences were deposited during the Tonian breakup of Rodinia after major continental rifting starting from ca. 1000 Ma, and are interpreted as rift-related to transitional passive margin successions (Alkmim et al., 2017; Basei et al., 2018; Frimmel, 2018; Pecoits et al., 2016; Philipp et al., 2004; Tack et al., 2001). Deposited on top of these units are syn-orogenic foreland basin sediments (Basei et al., 2000; Guadagnin et al., 2010; Konopásek et al., 2017).

The hinterland consists of amphibolite- to granulite-facies metaigneous and metasedimentary rocks, showing high-temperature and generally moderate- to low-pressure metamorphic conditions (Bento dos Santos et al., 2011; Goscombe and Gray, 2007; Gross et al., 2006; Gross et al., 2009), that are intruded by large volumes of late Neoproterozoic granitic rocks. The igneous protoliths of the metamorphic rocks are largely dated between ca. 860–770 Ma and are interpreted as remnants of large-scale continental rifting (Konopásek et al., 2008; Konopásek et al., 2018; Meira et al., 2019b; Passarelli et al., 2019; Will et al., 2019) or early arc magmatism (De Toni et al., 2020b; Heilbron and Machado, 2003; Heilbron et al., 2020; Koester et al., 2016; Martil et al., 2017; Masquelin et al., 2011). High-grade metamorphism and partial melting in the hinterland took place between ca. 655–570 Ma (Cavalcante et al., 2018; Franz et al., 1999; Goscombe et al., 2005a; Konopásek et al., 2008; Lenz et al., 2011; Masquelin et al., 2011). The granitoids intruded predominantly between ca. 630–575 Ma along the western part of the hinterland (Florisbal et al., 2012c; Oyhantçabal et al., 2007; Philipp and Machado, 2005; Tedeschi et al., 2016), and between ca. 585–480 Ma along the eastern part (Konopásek et al., 2016; Kröner et al., 2004; Pedrosa-Soares et al., 2011).

2.2 History of the tectonic models of the SANOS

The study of the SANOS has a long history, although it was only with the seminal studies of Porada (1979, 1989) that the tectonic evolution of the system was discussed in detail within an all-encompassing model involving a classic Wilson cycle involving continental rifting, ocean opening, and collisional orogenesis. This discussion followed on naturally from the gradual acceptance of plate tectonic theory, transitioning into a blossoming of studies on both sides of the Atlantic advocating for the novel tectonic processes of subduction, accretion, and plate collision being the driving forces behind orogenesis within the individual belts (e.g. Kröner, 1975; Kröner, 1977; Martin and Porada, 1977). Porada (1979) initially only proposed a genetic connection between the belts of the southern and central SANOS, including the Gariep, Damara, and Kaoko belts in Africa, and the Dom Feliciano and Ribeira belts in South America. They proposed that the evolution of the system began with the opening of a three-armed rift above a mantle plume, from which a 'proto-South Atlantic Ocean' opened along the northern and southern branches. The eventual closure of this ocean and subsequent collision between the African and South American cratons, according to this model, is what led to orogenesis (Fig. 3). Porada (1989) further expanded the model to include other belts of the South Atlantic, including the Araçuaí Belt in Brazil and the West Congo Belt in Africa, painting a picture of an extensive but interconnected system of orogenic belts spanning from the easternmost cape of Brazil to the southernmost cape of Africa. However, it was Hartnady et al. (1985) that introduced the term Adamastor Ocean to refer to the hypothetical oceanic domain that was consumed prior to orogenesis, and this title has continued to be in use since.

Since its inception, the Adamastor subduction–collision model has been continuously built upon by researchers on both sides of the South Atlantic and along the entire length of the orogenic system. Having started as a model to explain the evolution of the southern belts (Hartnady et al., 1985; Porada, 1979), the Adamastor Ocean was gradually brought northwards into the Ribeira, Araçuaí, and West Congo belts (Heilbron et al., 2008; Pedrosa-Soares et al., 2001; Pedrosa-Soares et al., 1998; Porada, 1989). However, from the earliest days of the model the direction of subduction remained contentious, with some researchers advocating for westward subduction of the Adamastor Ocean beneath the South American Cratons and others for eastward subduction beneath the African cratons. Some of the earliest arguments proposed that, based in part on the asymmetry of major deformation structures and clear evidence of nappe transport towards the east in the African foreland, subduction must have been directed towards the west (Fragoso-Cesar, 1980; Frimmel et al., 1996; Frimmel and Frank, 1998; Porada, 1979, 1989). As more of the belt was being studied in the context of collisional orogenesis, others instead interpreted the direction of subduction towards the east, citing thrust structures in the South American foreland with the opposite vergence as indicating nappe transport top-to-the-west, and the voluminous granitic rocks within the belts of South America as indicating arc magmatism resulting from subduction (e.g. Pedrosa-Soares et al., 1998). Both models require the consumption of a large oceanic domain, but notably they differ with respect to the location of the suture between the South American and African cratons. For eastward subduction, this suture is found between the remnants of the proposed arc and the western foreland, whereas with westward subduction the suture must be found between the arc and the eastern foreland.

Along the western side of the orogen, the subduction–collision model hinges on the interpretation of the linear granitic belts as remnant parts of long-lived magmatic arcs active between ca. 860–600 Ma. In

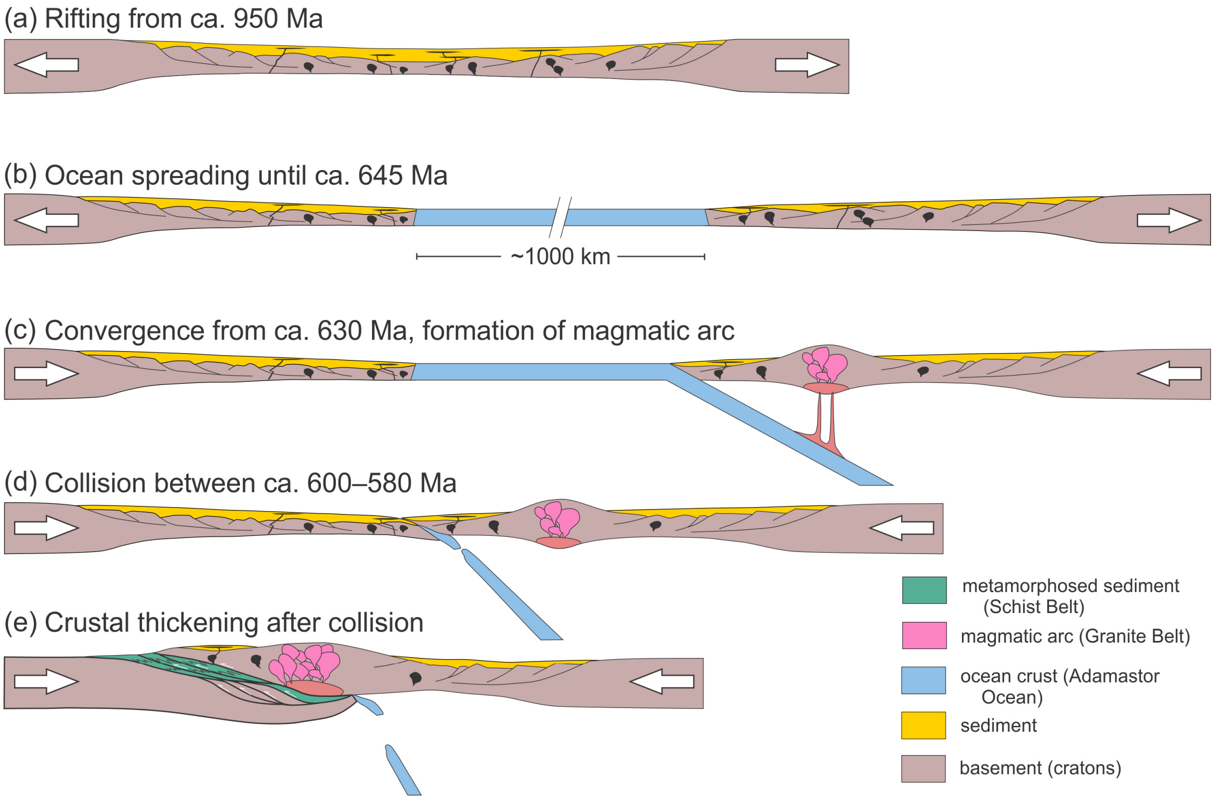

Figure 3. Schematic cross section showing the (west-directed) subduction–collision model for the formation of the SANOS. Time estimates based on reviews in Fossen et al. (2020) and Konopásek et al. (2020), and from Basei et al. (2018). (a-b) Rifting and ocean spreading from ca. 950 Ma (ca. 850 Ma for the southern SANOS) to ca. 645 Ma; (c) Subduction initiation and formation of a magmatic arc from at least 630 Ma, with the start of the Granite Belt; (d) Collision between the arc and the passive margin (the Congo and Kalahari cratons colliding with the Luis Alves and Nico Perez) between ca. 600–580 Ma; (e) Thrusting of the arc over the passive margin, forming the suture between the South American and African cratons, and deformation and metamorphism of the foreland sediment.

the northern SANOS, this is supported by extensive geochemical datasets that, when plotted within tectonic discrimination diagrams, are consistent with arc magmatism (Heilbron et al., 2020; Pedrosa-Soares et al., 2001). In the southern SANOS (the Dom Feliciano Belt) the evidence is less clear, as most geochemical and structural studies interpret large volumes of ca. 635–580 Ma granites, referred to as the Granite Belt (Basei et al., 2000), as the result of post-collisional magmatism (Bitencourt and Nardi, 1993, 2000; Florisbal et al., 2012b; Oyhantçabal et al., 2007). Despite this, there are still a number of studies that posit that the Granite Belt represents the eroded roots of a long lived magmatic arc, and they generally cite thrusting of the Granite Belt to the west over the foreland as indicating eastward subduction (Basei et al., 2000; Basei et al., 2018; Silva et al., 2005b). Several studies also interpret earlier ca. 800–770 Ma igneous activity in the hinterland as indicating arc magmatism associated with much earlier east-directed subduction (De Toni et al., 2020b; Koester et al., 2016; Lenz et al., 2013; Masquelin et al., 2011), which is consistent with the majority of interpretations from the northern SANOS (Heilbron et al., 2020). In support of these subduction–collision models, slivers of amphibolite and ultramafic rocks within the foreland supracrustal sequences are often interpreted as remnants of dismembered ophiolites, and are used as evidence for the location of a suture zone between the hinterland and western foreland (Fig. 3) (Amaral et al., 2020; Arena et al., 2018; Pedrosa-Soares et al., 2001; Pedrosa-Soares et al., 1998).

Ultimately, models involving eastward subduction have come to dominate the literature and is the generally accepted orogenic model in most publications today. However, there still remains some ambiguity, particularly within the southern SANOS. The majority of studies advocating for west-directed subduction of the Adamastor Ocean have come from geological studies along the African side of the southern SANOS (e.g. Diener et al., 2017; Frimmel et al., 1996; Frimmel and Frank, 1998; Germs, 1995; Passchier et al., 2002), and central to this east/west ambiguity is the distinct lack of evidence of high pressure metamorphism in either of the eastern or western belts (Frimmel, 2018). The presence of high pressure/low temperature metamorphic rocks is common across most orogens involving subduction and is thus generally considered indicative of relict subduction (see Fossen et al., 2020 and refernces therein). The absence of such subduction markers along the entire length of the belt is striking, and has, in part, led to models of intracontinental orogeny in place of subduction–collision (Fig. 4), which was notably discussed during the 90s by Trompette (1994, 1997) in the northern SANOS, and Dürr and Dingeldey (1996) in the southern SANOS. The intracontinental orogenic model proposes that instead of long-lived subduction of the Adamastor Ocean preceding crustal thickening, orogenesis was initiated by the inversion of an extended rift basin, with little to no oceanic crust developed between the African and South American cratons (Fig. 4). The discussion of intracontinental orogeny has further picked up speed in recent years, particularly for the belts in the northern SANOS (Araçuaí, Ribeira and West Congo belts) where the long-lived connection between the Congo–São Francisco cratons provides strong evidence for significant intracontinental deformation and a distinct lack in space for the presence of a large oceanic domain preceding orogenesis (Cavalcante et al., 2018; Cavalcante et al., 2019; Fossen et al., 2020; Konopásek et al., 2020; Meira et al., 2015; Meira et al., 2019a; Meira et al., 2019b). Such arguments are less common in the southern SANOS (Dom Feliciano, Kaoko, Gariep and Damara belts), where relict oceanic crust of the Marmora Terrane obducted over the margin of the Kalahari Craton indicates at least a minor amount of oceanic crust developed after rifting (Konopásek et al., 2020), although some interpretations characterise these rocks as forming within a back-arc tectonic setting (Frimmel, 2018).

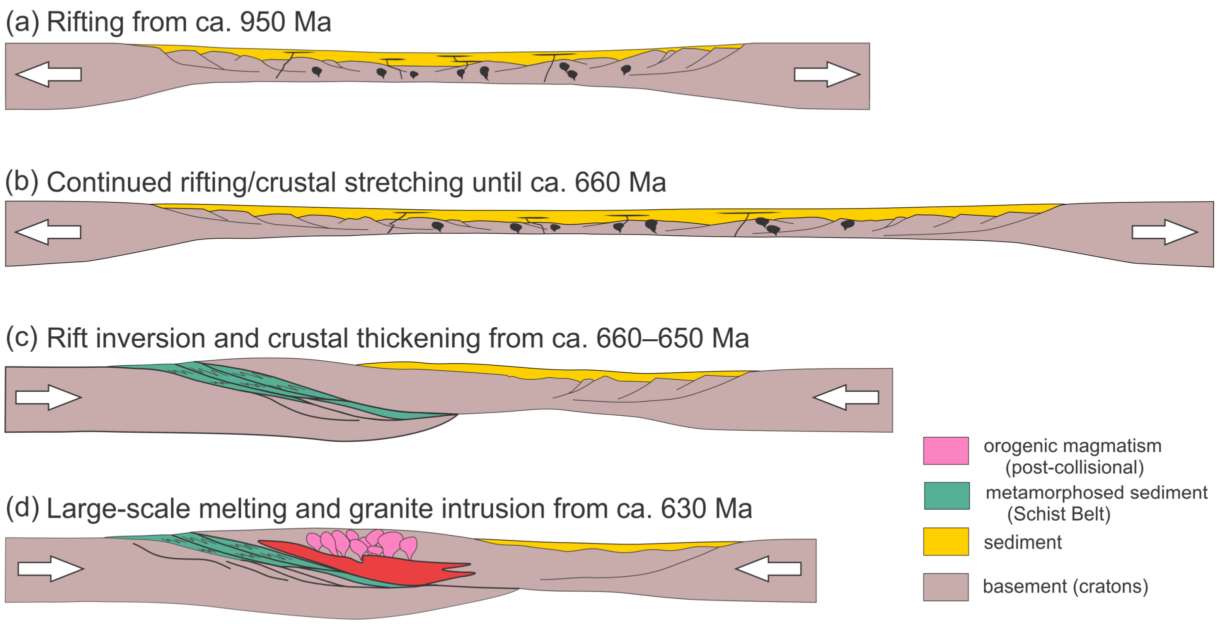

Figure 4. Schematic cross section showing the intracontinental model for the formation of the SANOS. Time estimates based on reviews in Fossen et al. (2020) and Konopásek et al. (2020). (a) Rifting and sedimentation from ca. 950 Ma (ca. 850 Ma for the southern SANOS); (b) Rifting continues throughout the Neoproterozoic without the transition into major ocean floor spreading and continental drift; (c) Rift basin inversion triggers crustal thickening and top-to-the-west directed thrusting at ca. 660–650 Ma; (d) Thermal relaxation leads to lower crustal melting (post-collisional magmatism) from ca. 630 Ma.

2.3 The Dom Feliciano Belt

The Dom Feliciano Belt outcrops along the Atlantic coastlines of southern Brazil and Uruguay and represents the south-westernmost orogenic belt of the SANOS (Fig. 5). The belt is typically grouped with the Kaoko and Gariep belts in Africa, forming part of the larger Kaoko–Dom Feliciano–Gariep orogenic system (Konopásek et al., 2020). This orogenic system was formed by the interactions between four major cratons—the Rio de la Plata and Paranapanema cratons in South American, and the Congo and Kalahari cratons in Africa—and two smaller interstitial cratonic bodies showing close association with the two African cratons (Oriolo et al., 2016b)—the Luis Alves Craton and Nico Pérez Terrane. Given early interpretations of the pre-orogenic setting of the southern SANOS as a three-armed rift system, the Kaoko–Dom Feliciano–Gariep belts, which run predominantly north–south, are often also grouped with the east–west trending Damara Belt located between the Congo and Kalahari cratons (Porada, 1979, 1989). The Dom Feliciano Belt lies along the eastern shoulders of the Luis Alves Craton and Nico Pérez Terrane, which collectively represent the cratonic foreland of the belt (Fig. 5). The Nico Pérez Terrane and Luis Alves Craton are, in turn, accreted to the eastern margins of the Rio de la Plata (Oriolo et al., 2016b; Oyhantçabal et al., 2018) and Paranapanema cratons (Passarelli et al., 2018), respectively.

The tectono-stratigraphic divisions most commonly used to describe the structure of the Dom Feliciano Belt were defined by Basei et al. (2000), who separated the belt into three major sub-units (excluding the cratonic foreland). These are, from east to west, the Granite Belt, the Schist Belt, and the foreland basins. In addition to these three units, the Coastal–Punta del Este Terrane, which outcrops

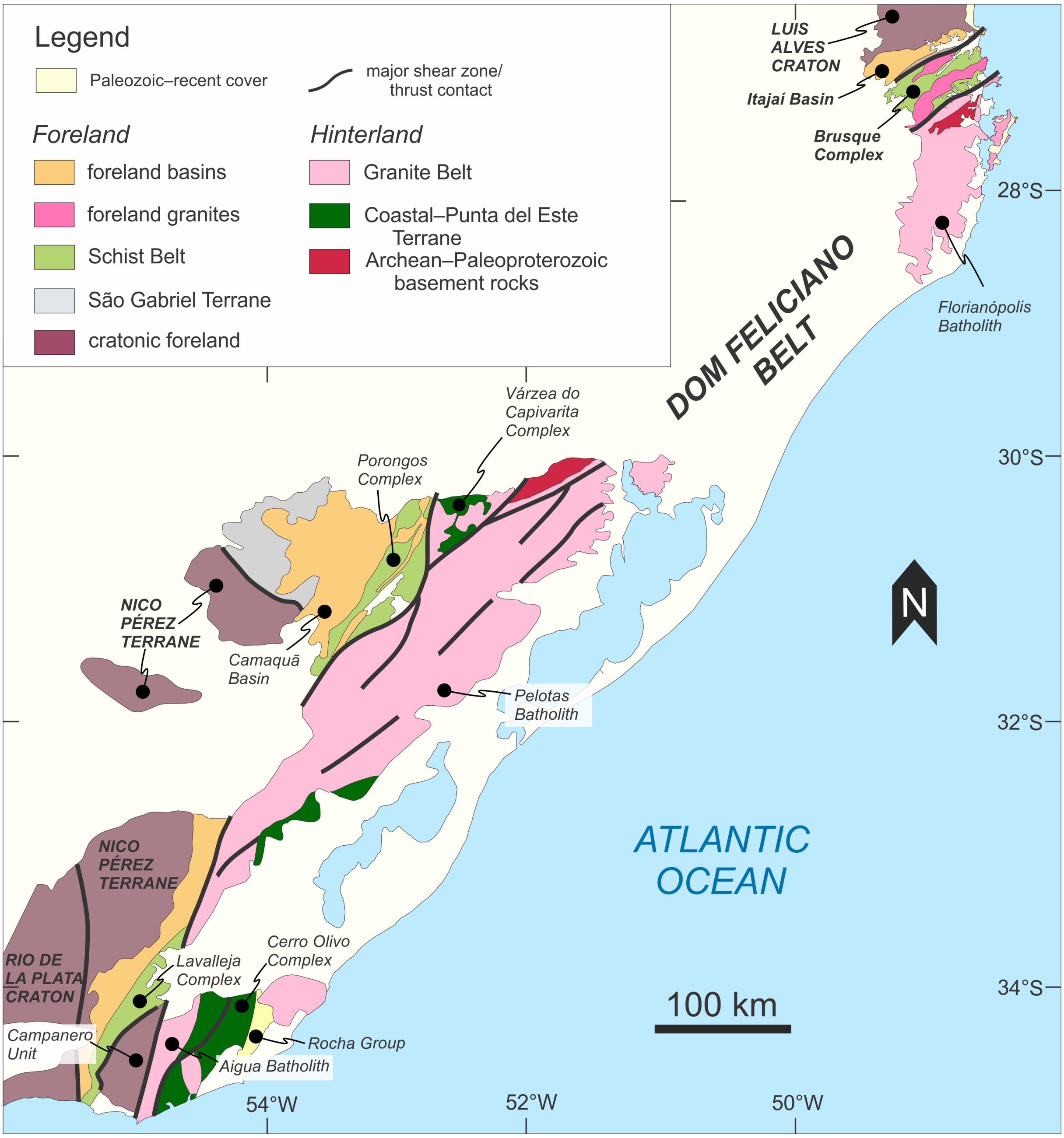

Figure 5. Simplified geological map of the Dom Feliciano Belt in southern Brazil and Uruguay (based on Bitencourt and Nardi, 2000; De Toni et al., 2021; Konopásek et al., 2017; Oyhantçabal et al., 2011a).

predominantly to the east of the Granite Belt, represents the easternmost tectonostratigraphic domain. With few exceptions, this tectonic architecture is consistent along the entire length of the belt (Fig. 5), with one exception being the Sao Gabriel Terrane, which outcrops to the west of the Schist Belt solely in the foreland of the central Dom Feliciano Belt. The belt is typically divided into northern, central, and southern sections based on major exposures in Santa Catarina (Brazil), Rio Grande do Sul (Brazil), and Uruguay, respectively. To facilitate discussion of the orogenic evolution of the belt in the introduction and the three papers that comprise this thesis, the individual tectono-stratigraphic units are further characterised as belonging to the orogenic hinterland or foreland, following the system of Konopásek et al. (2020). In this context, the foreland refers to the units west of and including the Schist Belt, whereas the hinterland comprises the units east of and including the Granite Belt (Fig. 5).

2.3.1 The Granite Belt

The Granite Belt is made up of large volumes of granitic rocks that intruded the Dom Feliciano Belt between ca. 635 and 580 Ma (Chemale et al., 2012; Florisbal et al., 2012c; Frantz et al., 2003; Oyhantçabal et al., 2007), representing much of the exposure of the belt in its central and northern sections (Fig. 5). The Granite Belt is made up of three major batholiths: the Florianópolis, Pelotas and Aiguá batholiths in the northern, central, and southern Dom Feliciano Belt, respectively (Basei et al., 2000). Early interpretations describe the Granite Belt as the exposed roots of a magmatic arc produced by subduction of the Adamastor Ocean (Porada, 1989), and this interpretation has continued to be applied to various models to this day (Basei et al., 2000; Basei et al., 2018). However, since at least the early 90s, marked by the influential study of Bitencourt and Nardi (1993), an alternative interpretation proposes that the Granite Belt represents post-collisional magmatism—that is, magmatism forming after Neoproterozoic collision between the African and South American Cratons (Florisbal et al., 2009; Florisbal et al., 2012a; Florisbal et al., 2012b; Florisbal et al., 2012c; Oyhantçabal et al., 2007). A major focus of **Papers II & III** concerns the nature of the Granite Belt as indirectly determined by the timing and conditions of metamorphism and deformation recorded in the foreland.

2.3.2 The Schist Belt

The Schist Belt is a narrow (<40km) belt of metasedimentary rocks deformed and metamorphosed in the supracrustal foreland position of the Dom Feliciano Belt. The belt consists of a series of metamorphosed sedimentary to volcanosedimentary rocks overlying the reworked cratonic basement of the foreland, primarily consisting of pelitic to psammitic schists and phyllites, metacarbonates, calc-silicates, and meta-mafic to -felsic volcanic and intrusive rocks interlayered within the sediment (Basei et al., 2011a; Basei et al., 2013; Saalmann et al., 2006; Sánchez Bettucci et al., 2001). The protolith of the Schist Belt is generally accepted to consist of pre-orogenic volcano-sedimentary successions likely deposited from ca. 850 Ma after major rifting and the breakup of Rodinia (Basei et al., 2008a; Basei et al., 2011a), although interpretations of the timing of sedimentation, the number of sedimentary episodes, and the tectonic setting vary (Basei et al., 2000; Battisti et al., 2018; Höfig et al., 2018; Oyhantçabal et al., 2021). The Schist Belt is comprised of the Brusque, Porongos and Lavalleja complexes, outcropping in the northern, central, and southern Dom Feliciano Belt, respectively (Fig. 5), and is the primary focus of the three papers presented in this thesis. Although most studies assume continuation of the Schist Belt across the entirety of the Dom Feliciano Belt based on similarities in deformation, metamorphic grade and lithology, the correlation of these three complexes has so far not been confirmed using concrete geochronological data or modern thermobarometric modelling.

Notably, the timing of metamorphism and deformation in much of the Schist Belt is entirely unknown, and the sources and timing of sedimentation of the protoliths of the Schist Belt are unknown or seemingly inconsistent. Although there is already a large detrital zircon database from the Porongos Complex in the central Dom Feliciano Belt (Höfig et al., 2018; Pertille et al., 2015a; Pertille et al., 2015b; Pertille et al., 2017), and some from the Lavalleja Complex in the south (Oyhantçabal et al., 2021), the same cannot be said for the Brusque Complex which distinctly lacks a robust dataset which could allow a comparison of the sedimentary source regions across the entire Schist Belt. A small number of data are presented by Basei et al. (2008b), who then interpret a sedimentary source from the adjacent Paranapanema Craton. However, they present a total of 22 dates from two samples from the Brusque Complex, which is not particularly statistically convincing. Furthermore, Basei et al. (2011a) constrained the timing of sedimentation of the Brusque Complex protolith to between ca. 640 to 600 Ma based on the youngest individual detrital zircon grains and reported ages of felsic volcanic rocks (Basei et al., 2008b; Silva et al., 2002). However, this age range partly conflicts with the timing of intrusion of major granite batholiths into the complex from ca. 615 Ma (Hueck et al., 2019). In the Porongos Complex, the timing of earliest sedimentation is well constrained by the dating of interlayered volcanic rocks, which provide ages between ca. 810 and 780 Ma (Pertille et al., 2015b; Saalmann et al., 2011). However, major detrital zircon age peaks between ca. 615 and 580 Ma are also recorded in parts of the complex (Pertille et al., 2015a; Pertille et al., 2015b), prompting recent studies proposing that parts of the Schist Belt are comprised of syn-orogenic sedimentary rocks (Battisti et al., 2018; Höfig et al., 2018). Finally, the Lavalleja Complex provides the greatest hurdle in correlating the units of the Schist Belt, as geochronological constraints suggest large parts of the sedimentary record of the complex date to the Mesoproterozoic (Oriolo et al., 2019), which conflicts with estimates of the timing of earliest sedimentation in the Schist Belt protolith as during the early to middle Neoproterozoic (Chemale, 2000; Pertille et al., 2017; Saalmann et al., 2011).

Clearly, based on these observations, the early assumption that all of the metasedimentary rocks of the Schist Belt shared a single paleobasin is likely incorrect. However, establishing to what degree they do have a shared history is key to reconstructing the evolution of the Dom Feliciano Belt and furthering our understanding of the pre-orogenic position of the major cratons. The Brusque Complex is the least studied of the three Schist Belt complexes, lacking both a reliable constraint on the timing of sedimentation and a significant detrital zircon database, therefore representing a distinct gap in knowledge. The focus of **Paper I** is to constrain the timing of sedimentation in the Brusque Complex, and to develop a robust detrital zircon dataset for comparison with the rest of the Schist Belt, as well as with equivalent supracrustal rocks along the eastern foreland of the Kaoko–Dom Feliciano–Gariep orogenic system.

Although there are some estimates of the timing of peak metamorphism in the Schist Belt, they are predominantly based on indirect constraints such as the intrusion of granitic batholiths and detrital zircon ages. There are currently no published studies containing geochronological constraints that can be directly linked to peak metamorphism, although a single, imprecise muscovite–whole rock Rb–Sr age of 658 ± 26 Ma from the Porongos Complex remains the only current estimate of the timing of this event (Lenz, 2006; MSc. thesis). Similarly, the current estimates of peak metamorphic conditions (lower greenschist to lower amphibolite facies) are based primarily on petrological observations of mineral assemblages or classical thermobarometry (Basei et al., 2011a; Campos et al., 2011), and there are currently no studies applying modern methods of thermodynamic modelling to estimate more precise P–T conditions from which we could derive a P–T path. **Papers II & III** address these absences by providing geochronological data and P–T estimates from the forelands of the northern and southern Dom Feliciano Belt.

2.3.3 The Coastal–Punta del Este Terrane

In addition to the three primary tectonostratigraphic units defined by Basei et al. (2000), a fourth unit—the Punta del Este Terrane—is located to the east of the Granite Belt in southern Dom Feliciano Belt in Uruguay (Preciozzi et al., 1999). The Punta del Este Terrane comprises the granulite-facies rocks of the basement Cerro Olivo Complex, as well as low-grade (maximum greenschist facies) metasedimentary syn- to post-orogenic cover sequences known as the Rocha and Sierra de Aguirre formations (Abre et al., 2020; Bossi and Gaucher, 2004; Masquelin et al., 2011; Preciozzi et al., 1999; Silva Lara et al., 2021). The Cerro Olivo Complex is represented by rocks with igneous and sedimentary protoliths recording ages between ca. 800–770 Ma, with a strong high-temperature metamorphic overprint between ca. 655–640 Ma (Lenz et al., 2011; Masquelin et al., 2011; Oyhantçabal et al., 2009; Will et al., 2019).

Hasui et al. (1975) first distinguished these metasedimentary cover units in southern Uruguay as being separate from the Schist Belt primarily based on their location east of the Granite Belt, and their interpretation of the Granite Belt and associated host gneisses as a *median massif*—a major geological division within pre-plate tectonic geosynclinal theory. The exotic nature of these rocks relative to the other supracrustal units of the Dom Feliciano Belt was further emphasised by Basei et al. (2005), who correlated the Rocha Formation with the Oranjemund Formation in the Gariep Belt on the opposite side of the Atlantic. Later, the basement of the Punta del Este Terrane was also identified as having connections with units in Africa, being correlated with the Coastal Terrane of the Kaoko Belt (Basei et al., 2011b; Gross et al., 2009; Oyhantçabal et al., 2009; Oyhantçabal et al., 2011b). Importantly, Oyhantçabal et al. (2009) recognised similarities in age between the igneous protoliths of the Cerro Olivo Complex and the rift-related igneous rocks preserved in the Coastal Terrane (Konopásek et al., 2008). These two units preserve an important magmatic episode between ca. 800–770 Ma, which helps to cement a pre-orogenic connection between the easternmost domain of the Dom Feliciano Belt with the westernmost parts of the African belts. Based on this correlation, the collective unit has been recently referred to as the Coastal–Punta del Este Terrane (Konopásek et al., 2014; Konopásek et al., 2018).

Until recently, the only known rocks of this age in the Dom Feliciano Belt were from the Punta del Este Terrane in Uruguay, and many studies have thus emphasised the uniqueness of the terrane relative to the rest of the belt, asserting that these rocks must have amalgamated against the eastern flank of the Granite Belt sometime after subduction of the Adamastor Ocean and intrusion of the granites (Basei et al., 2011b). Since then, however, rocks of similar age and metamorphic grade to those found in the Cerro Olivo Complex have been identified in the Várzea do Capivarita and Porto Belo complexes in the central and northern Dom Feliciano Belt, respectively (Costa et al., 2020; De Toni et al., 2020b; De Toni et al., 2021; Martil et al., 2017; Philipp et al., 2016). Unlike the Cerro Olivo Complex, the latter two units are located within the western part of the Granite Belt (Fig. 5). If the possible connection between all of these units is accepted, this position within the Granite Belt seemingly contradicts the interpretation that the Coastal–Punta del Este Terrane was juxtaposed against the eastern margin of the Dom Feliciano Belt sometime after intrusion of the granites (e.g. Basei et al., 2011b).

Alternatively, these observations suggest that the Coastal–Punta del Este Terrane may represent surviving relicts of the hinterland of the orogen, forming the country rocks into which intruded the Aiguá Batholith and the other granites of the Granite Belt (Masquelin et al., 2011). High-grade metamorphism recorded in these rocks between ca. 655–640 Ma has been interpreted as early crustal thickening during convergence between the South American and African cratons (Battisti et al., 2018; Lenz et al., 2011). If the Granite Belt represents post-collisional magmatism and not a magmatic arc, then it is possible that this high-grade metamorphic event, occurring some 10 to 25 million years before large-scale magmatism, marks the timing of early convergence in the Dom Feliciano Belt, and thus may be coeval with thrusting of the hinterland over the foreland of the Dom Feliciano Belt (**Paper II**).

2.3.4 Connection with the Kaoko and Gariep belts

The orogenic connection between the western (Dom Feliciano Belt) and eastern (Kaoko and Gariep belts) parts of the southern SANOS is primarily based on the similarity in ages and lithologies found across both sides of the orogen. As previously mentioned, the syn-orogenic sedimentary cover in the southern Dom Feliciano Belt (Rocha Formation) has been correlated with similar rocks (Oranjemund Group) in the Gariep Belt based on a detrital zircon provenance study (Basei et al., 2005). Similarly, the Coastal Terrane (Kaoko Belt) and the Punta del Este Terrane (southern Dom Feliciano Belt) are correlated based on the ages of their respective igneous protoliths, the age of intrusive rocks similar to the Granite Belt, and the timing and degree of granulite-facies metamorphism (Konopásek et al., 2016; Konopásek et al., 2018; Oyhantçabal et al., 2009; Will et al., 2019). However, the timing of the main phase of transpressive deformation recorded in the Kaoko Belt, between ca. 580–550 Ma, makes it clear that the high temperature metamorphism recorded in the hinterland (Coastal–Punta del Este Terrane) between ca. 655–640 Ma relates to an earlier event, or to a much earlier phase of orogenesis (Goscombe et al., 2005a). The metasedimentary rocks of the Kaoko Belt represent the eastern foreland equivalents of the Schist Belt, comprising a transpressive fold and thrust belt with tectonic vergence to the east (Goscombe et al., 2003a; Goscombe et al., 2003b; Goscombe et al., 2005b). Without any constraints on the timing of deformation and metamorphism in the equivalent part of the Dom Feliciano Belt (the foreland in general, and the Schist Belt in particular), it is not possible to make a connection between the tectonic evolution of the two halves of the belt, or to fully understand the relationship between Cryogenian high temperature metamorphism in the hinterland and Ediacaran transpression in the foreland.

3 Aims and Objectives

The *P–T–D–t* history of the metamorphosed supracrustal rocks of the Dom Feliciano Belt foreland (the Schist Belt) is largely unknown. In particular, works using modern methods for estimating P–T conditions (phase equilibria modelling) and precise geochronological estimates of the timing of metamorphic events are lacking. Furthermore, although there are already reliable constraints showing an orogenic connection between the eastern and western parts of the Kaoko–Dom Feliciano–Gariep orogenic system, their potential pre-orogenic relationship is not so well understood. Thus, the aim of this work is to improve our understanding of the pre-orogenic, metamorphic, and structural history of the Dom Feliciano Belt foreland. With this work, I hope to constrain the relative pre-orogenic positions of the major cratonic bodies involved in Neoproterozoic orogenesis, determine the potential correlation between the foreland supracrustal rocks of the Kaoko–Dom Feliciano–Gariep belts, and help to develop a consistent model of orogenesis in the Dom Feliciano Belt. To achieve this, the following questions were posed:

- What was the pre-orogenic relationship between the foreland supracrustal rocks of the Dom Feliciano, Kaoko and Gariep belts? (**Paper I**)
- What were the relative pre-orogenic positions of the major cratonic bodies involved in orogenesis (Luis Alves, Nico Perez, Congo, and Kalahari cratons)? (**Paper I**)
- What were the conditions of Neoproterozoic metamorphism in the foreland supracrustal rocks, and at what time did metamorphism occur? (**Papers II & III**)
- When did earliest crustal thickening in the orogenic foreland begin? (**Papers II & III**)
- What was the relationship between the hinterland and foreland domains in the Dom Feliciano Belt? (**Papers II & III**)

Paper I presents geochronological data from the Brusque Complex (the northern Schist Belt), exploring the connection between the supracrustal rocks of the forelands of the southern SANOS and the pre-orogenic positions of the cratons. **Paper II** presents the results of structural analysis, thermodynamic modelling, and geochronology from the Brusque Complex, providing an overview of tectonic events from the start to the end of orogenesis in the northern Dom Feliciano Belt. **Paper III** presents the results of thermodynamic modelling and geochronology from the Lavalleja and Campanero complexes (foreland) and the Cerro Olivo Complex (hinterland) in the southern Dom Feliciano Belt. This data is used to explore the relationship between the hinterland and foreland domains, and the paper builds on the results and interpretations from **Papers I & II** to develop a tectonic model for the southern Dom Feliciano Belt that is consistent with the rest of the southern SANOS. Overall, the results of the thesis provide novel data used to better understand the evolution of the Dom Feliciano Belt and southern SANOS in particular, and the SANOS as a whole.

4 Approach and methods

The aims of this thesis are addressed using a combination of analytical and investigative methods including field work, isotope geochronology, phase equilibria modelling, structural analysis, and mineral geochemistry. The motivation behind the use of these wide-ranging techniques is to find a complimentary combination that can help to resolve the complex and long-lived evolution of the Dom Feliciano Belt and the southern SANOS. This section outlines the major approaches and methodologies used during this work.

4.1 Mapping and structural analysis

Four field trips to Santa Catarina, Brazil, and two to southern Uruguay were undertaken between 2017 and 2019 to collect structural data and samples for analysis. The field studies in Santa Catarina form the basis of **Papers I & II**. The fieldwork was focused on mapping and sampling the metasedimentary cover sequences of the foreland (Brusque Complex), including their relationship with adjacent tectonostratigraphic units and major structural features. Fieldwork in Uruguay formed the basis of **Paper III**, with a focus on the foreland supracrustal (Lavalleja Complex) and basement (Campanero Unit) complexes, as well as the hinterland basement (Cerro Olivo Complex).

Due to the poor outcrop situation in southern Brazil and Uruguay, particularly inland away from the coast, collecting a good spread of reliable structural data proved difficult. Partly for this reason, field mapping and structural analysis in the Brusque Complex in Santa Catarina was prioritised over the course of the study due to a distinct lack of published data from this area. This data formed the structural foundations for **Paper II**. The smaller structural dataset obtained from southern Uruguay was supplemented by previously published studies, although the data collected still formed the groundwork for **Paper III**.

4.2 Geochronology and geochemistry

Reliably constraining the timing of major orogenic events is key to developing a consistent and reliable tectonic model. Knowing the timing of sedimentation, deformation, and metamorphism in the foreland of the Dom Feliciano Belt, and correlating these events across the southern SANOS, is vital in answering the main questions posed in this study. Multiple geochronological methods were used to constrain the timing of these events, which involved various analytical techniques in the collection of isotopic data for mineral geochronology.

4.2.1 Zircon and monazite U–Pb

The U–Pb decay system is one of the most widely used geochronometers in the study of tectonics, as well as within many other geological disciplines. This is, in part, because of the extremely robust decay constants evaluated for ^{238}U and ^{235}U, which are considered to be among the most accurate and precise in geochronology (e.g. Mattinson, 2010). Another benefit of the U–Pb system is the independent radioactive decay chains of the parent isotopes ^{238}U and ^{235}U, to the daughter isotopes ^{206}Pb and ^{207}Pb, respectively. The evaluation of both decay systems allows their comparison as an internal check for the reliability of evaluated dates, most commonly using concordia plots. Ideally, given optimal conditions within a given mineral, where the system is closed and there has been no external loss or addition of U or Pb, the results of isotope analysis should plot along a concordia curve, and the combination of multiple analyses can combine to give a concordia age. However, even in the situation when samples are discordant (that is, do not plot along the concordia), the distribution of data within the concordia plot can still be used to infer information about the timing of events, such as Pb loss, that contribute to the discordance.

In **Papers I & III**, laser ablation inductively coupled plasma mass spectrometry (LA-ICP-MS) was used to obtain U–Pb zircon ages, as the method allows the rapid in situ analysis of the large numbers of zircon grains needed for detrital zircon investigations (**Paper I**) and the formation of reliable concordia ages (**Paper III**). For **Paper III**, secondary ion mass spectrometry (SIMS) was used for samples with small numbers of zircon grains, and to confirm one LA-ICP-MS age. Zircon grains were imaged by cathodoluminescence (CL) prior to analysis, and monazite grains were imaged using back-scattered electron (BSE) imaging. For **Papers II & III**, SIMS was used to analyse U–Pb in monazite, due to the small sample sizes and small grain sizes, and the high precision and high spatial resolution of the method.

Monazite trace element chemistry was also analysed to investigate the Rare Earth Element (REE) partitioning between monazite and garnet to establish if they grew in equilibrium. Monazite and garnet directly compete for the heavy REEs during growth, and in general it has been found that the partitioning of these elements into these two minerals is consistent (e.g. Hermann and Rubatto, 2003; Rubatto et al., 2006; Warren et al., 2018). Thus, comparing the trace elements from these minerals within one sample can help determine if they grew together, and thus help to interpret the meaning of analysed ages (**Paper II**).

4.2.2 Garnet Lu–Hf and Sm–Nd

In **Papers II & III**, isotope dilution ICP-MS was used to obtain Lu–Hf and Sm–Nd garnet ages. Garnet Lu–Hf and Sm–Nd geochronology is one of the most useful geochronometers for medium- to high-grade metapelitic rocks, as the timing of garnet growth can often be tied to a specific event or events using microstructural observations and mineral geochemistry (Anczkiewicz et al., 2014; Konopásek et al., 2019; Pollington and Baxter, 2010). Furthermore, the Lu–Hf and Sm–Nd geochronometers can be coupled to constrain the entire timescale of garnet growth, and thus by inference the duration of prograde metamorphism (Lapen et al., 2003; Soldner et al., 2017; Soldner et al., 2020). Garnet is also a key mineral used when employing phase equilibria modelling (e.g. Gaidies et al., 2006), and thus the timing of garnet growth as determined by Lu–Hf and Sm–Nd geochronology can be directly linked to specific pressure and temperature conditions allowing the interpretations of specific tectonic events (Jung et al., 2019; Walczak et al., 2017).

Garnet Lu–Hf and Sm–Nd geochronology does not come without its complications, however. Among the most problematic obstacles are high-Hf/high-REE mineral inclusions. Common inclusions in garnet that can concentrate large amounts of the daughter Hf isotope include zircon and rutile. In the case of zircon, it is common for metasedimentary rocks to contain older inherited grains that did not grow in equilibrium with the matrix assemblage, and therefore do not preserve the same $^{176}Hf/^{177}Hf$ ratio. Because of the high Hf concentrations in zircon, even a small volume of inclusions can completely overwhelm the signal preserved in garnet and result in erroneous ages (Scherer et al., 2000). Similarly, common mineral phases that contain high concentrations of Sm and Nd include REE-bearing minerals such as monazite and apatite. Such minerals, particularly Nd-rich monazite, can overwhelm the Sm/Nd ratio of the garnet and result in an age that is too young and imprecise (Pollington and Baxter, 2010, 2011; Thöni, 2002).

To obtain accurate and precise ages, it is vital to attempt to remove as many of these inclusions from the garnet as possible prior to analysis. Most of the sample preparation for Lu–Hf and Sm–Nd isotope analysis, therefore, is taken up by removal of these inclusions, first by mechanical picking under the microscope to remove visible inclusions and then through dissolution (Anczkiewicz and Thirlwall, 2003; Lagos et al., 2007; Pollington and Baxter, 2011). The first stage of dissolution attempts to dissolve mineral inclusions out of the garnet (for example, monazite), and the second stage is the selective dissolution of the garnet leaving refractory inclusions behind (for example, zircon) which can then be removed mechanically. This final step also prepares the samples for element separation and final isotopic analysis. The methods for sample preparation used in **Papers II & III** follow that of Anczkiewicz et al. (2004).

In **Papers II & III**, trace elements were analysed across garnet grains using LA-ICP-MS to determine the distribution of the isotopes of interest, which are then used to interpret the meaning of the ages. Using the method as described above and in greater detail in **Papers II & III**, the resulting isochron ages will be an average age of the entire growth of the garnet as there is no discrimination between the collection different parts of the garnet during mechanical picking. However, due to the fractionation of Lu over Hf during garnet growth, following a profile predicted by Rayleigh fractionation, garnet tends to concentrate Lu in the cores resulting in much higher Lu to Hf ratios in garnet cores compared to its rims. The preferential Lu enrichment in the cores means that whole-grain garnet Lu–Hf ages tend to be biased towards early garnet growth (Lapen et al., 2003). In contrast, Rayleigh fraction of Sm and Nd suggests that Sm–Nd ages tend to be biased more towards later garnet growth, and thus the combination of Lu–Hf and Sm–Nd geochronology can give a minimum estimate of the duration of garnet growth (Lapen et al., 2003). The trace element profiles are used to determine the true distribution of Lu, Hf, Sm and Nd.

4.2.3 Mica Ar–Ar

In **Paper II**, Ar–Ar geochronology was used to date the cooling of biotite within the Brusque Complex during exhumation, and the recrystallisation of muscovite during late orogenic deformation along sub-vertical high-strain zones. Ar–Ar geochronology of micas is one of the few geochronometers that can be used to date events occurring at low metamorphic conditions and is particularly useful at constraining events along shear zones and faults where the growth and recrystallisation of mica is common. However, because the closure temperature of Ar–Ar within micas is relatively low (~300–400°C; Grove and Harrison, 1996; Harrison et al., 2009), the geochronometers are particularly susceptible to changes in temperature and partial or complete resetting. This is even more problematic in slowly cooling rocks, such as plutonic or metamorphic rocks, and so care needs to be taken when interpreting the meaning of these ages (Schaen et al., 2020).

4.3 Phase equilibria modelling

There are various methods available for estimating the pressure–temperature (P–T) conditions of metamorphic rocks, which all rely on the chemical equilibrium between or within minerals as a function of pressure and temperature. Classical thermobarometry allows the calculation of P or T using individual chemical reactions within or between minerals, and the combination of multiple techniques can result in adequate P–T estimates. Computational phase equilibrium modelling was used to estimate P–T conditions for the rocks in this study, however, as it allows for a broader and more developed understanding of the stable and metastable mineral assemblages and compositions formed during a rock's metamorphic history. Using this method, assemblage stability diagrams, or *pseudosections*, can be calculated by modelling the phase relations within a constrained bulk composition defined by a given rock, which then represent estimates of the equilibrium assemblages of that rock over P–T space. The mineral assemblage observed in a given rock can then be compared with the calculated pseudosection, defining a range of P–T values that can be used to constrain the conditions at which a rock was metamorphosed. This estimate can be further refined by calculating the compositional and/or modal proportional variation of individual minerals—such as garnet—as *isopleths* within the pseudosection and comparing these values with observed mineral compositions in the rock (Stüwe and Powell, 1995). Ultimately, phase equilibria modelling has the potential to produce reliable estimates of P–T through multiple stages of the metamorphic evolution of a rock, enabling the construction of P–T paths.

4.3.1 Modelling methods and assumptions

For **Papers II & III** I have used the Perplex (ver. 6.9.0) modelling software of Connolly (2005) in combination with the thermodynamic dataset DS6.22 of Holland and Powell (2011). Perplex is one of the leading thermodynamic modelling packages available for phase equilibria modelling and receives regular updates and fixes. The solution models we used were predominantly those from White et al. (2014), as they were calibrated with the dataset of Holland and Powell (2011) and made specifically for modelling of metapelitic rocks. Some exceptions are outlined in **Papers II & III**.

Bulk rock compositions were analysed using inductively coupled plasma emission spectroscopy (ICP-ES) and atomic absorption spectroscopy (AAS) (**Papers II & III**). One major assumption made when constraining the bulk rock composition in this way is that the analysed bulk rock accurately reflects the effective composition of the sample examined under thin section. Many metamorphic rocks show significant heterogeneity, which is particularly obvious in low- to medium-grade, layered schists such as those studied in **Paper II**. Using the mineral assemblage observed in a thin section that was cut from part of the sample that is not representative of the average bulk composition may result in an erroneous pseudosection and/or modal compositional isopleths that do not intersect. Attempts were made to avoid this by cutting multiple thin sections from different parts of the sample and analysing mineral compositions across each of these sections to get a broad overview of the mineral assemblage and chemistries within the rock.

The mineral assemblage observed in a metamorphic rock ideally represents the stable assemblage formed at the metamorphic climax, which typically occurs when a rock reaches a peak in temperature and is at its least hydrated state. However, unless the rock has very rapidly cooled from this peak temperature, or has somehow otherwise escaped further metamorphism, there will often be signs of retrograde metamorphic reactions as the rock attempts to maintain thermodynamic equilibrium with changing P–T conditions. This requires careful petrological study of the samples to determine what, if anything, remains of the relict peak mineral assemblage, and what represents retrograde or secondary overprint.

It is also possible that thin sections reveal small sub-domains within a sample that contain isolated mineral assemblages that are not in equilibrium with the matrix assemblage, which can potentially reveal the P–T conditions during earlier stages of metamorphism. One sample from this study (**Paper III**) showed such features, and in this case the effective bulk composition of the isolated domain was determined by thin section 2D volume estimation in combination with mineral compositional analysis.

Another assumption made for the modelling in this study is the conversion of all analysed iron into FeO (with the exception of one sample in **Paper II**), effectively ignoring Fe_2O_3 in the system. Iron analysed during whole rock compositional analysis is typically reported as Fe_2O_3 (Fe^{3+}) due to the oxidation of FeO (Fe^{2+}) during sample preparation. The conversion of Fe_2O_3 to FeO was done with samples containing no significant Fe_2O_3-bearing phases, as the absence of such minerals implies that the small amount of Fe_2O_3 present in the rock will have a negligible effect on the chemical equilibrium of the system. This assumption is supported by studies investigating the effect of Fe_2O_3 on modelling of metapelitic rocks (e.g. Diener and Powell, 2010; Forshaw and Pattison, 2021). For the one sample in this study containing a significant proportion of Fe_2O_3-bearing phases (**Paper II**), the concentrations of Fe_2O_3 and FeO were separately analysed by titration and used for pseudosection modelling. In this case, the relatively large proportion of Fe_2O_3-bearing phases (in particular, hematite and magnetite) indicated the importance of Fe^{3+} for the chemical system.

5 Summary of papers

Paper I

Percival, J. J., Konopásek, J., Eiesland, R., Sláma, J., Campos, R. S., Battisti, M. A., Bitencourt, M. F., 2021, **Pre-orogenic connection of the foreland domains of the Kaoko–Dom Feliciano–Gariep orogenic system**, *Precambrian Research*, vol. 354, pp. 106060, https://doi.org/10.1016/j.precamres.2020.106060

The supracrustal rocks of the Schist Belt in the Dom Feliciano Belt have long assumed to be a continuous unit with a shared pre-orogenic sedimentary history (Basei et al., 2000). More recently, studies have further proposed a pre-orogenic connection with rocks from the hinterland (Battisti et al., 2018), as well as with the foreland supracrustal rocks of the Kaoko Belt in Namibia (Konopásek et al., 2020). However, data from the central and southern parts of the Schist Belt has recently challenged this view, with the finding that parts of the Schist Belt record markedly different ages of sedimentation; age constraints from the central Schist Belt suggests predominantly Neoproterozoic sedimentation, whereas the southern Schist Belt records Mesoproterozoic sedimentation (Oriolo et al., 2019; Pertille et al., 2017; Saalmann et al., 2011). To investigate the potential correlation of these units across the southern SANOS, **Paper I** is focused on the pre-orogenic history of the Brusque Complex metasediments that comprise the foreland supracrustal sequences of the northern Dom Feliciano Belt. The Brusque Complex is the least studied of the Schist Belt sub-units, and available constraints on the timing and sources of sedimentation are imprecise or inconsistent (Basei et al., 2005; Basei et al., 2011a). Furthermore, the current position of the northern Dom Feliciano Belt implies close proximity to the Kaoko Belt prior to the opening of the Atlantic, and thus represents the best location to study a possible connection between the African and South American supracrustal sequences (Fig. 2b). The study is based on the interpretation of zircon U–Pb data from the Brusque Complex, including detrital and igneous zircon from metapelitic, metapsammitic and metavolcanic rocks.

A concordia age of 811 ± 6 Ma was obtained from igneous zircon within a deformed and metamorphosed felsic dyke intruding the sedimentary protolith of the Brusque Complex, which constrains the minimum timing of earliest sedimentation into the paleo-basin to sometime before ca. 811 Ma. This is close to estimates for the timing of rifting (i.e. basin formation) at ca. 835 Ma (Basei et al., 2008a), and is consistent with age constraints from the central Schist Belt (Porongos Complex) of ca. 810–780 Ma (Pertille et al., 2017; Saalmann et al., 2011). Furthermore, it matches the timing of igneous activity in the hinterland (Coastal–Punta del Este Terrane) between ca. 820–770 Ma (Konopásek et al., 2008; Konopásek et al., 2018; Lenz et al., 2011; Oyhantçabal et al., 2009).

Detrital zircon analysis reveals that the Brusque Complex metasedimentary rocks fall into two distinct groups based on age patterns: one group containing only Paleoproterozoic-aged zircon between 2.2–2.0 Ga, and another with both Paleo- to Mesoproterozoic age peaks of between ca. 2.1–1.8 and ca. 1.6–1.0 Ga. The detrital zircon ages from the Paleoproterozoic sample group are consistent with erosion of the adjacent Luis Alves Craton. This sedimentary source is unsurprising assuming that the current relative positions of the supracrustal rocks and the Luis Alves craton reflects their past positions during sedimentation, and it confirms interpretations that the Brusque Complex was deposited along the shoulder of the craton. The Mesoproterozoic ages from the second group of samples, however, are not known from basement rocks in southern South America, and instead are more consistent with the igneous provinces and/or sedimentary cover sequences of the African cratonic margins (the Congo and Kalahari cratons). This suggests a major sedimentary source of African affinity. The detrital zircon ages and patterns are nearly identical to those from the central Dom Feliciano Belt (Porongos Complex), indicating a shared sedimentary source. Similarities are also found when compared with the eastern foreland supracrustal rocks in the Kaoko Belt, and to a lesser extent in the Gariep Belt.

We interpret this data as indicating that sedimentation occurred in a shared system of basins at the onset of, and during, rifting between the African and South American Cratonic blocks during the Tonian. This implies that the cratons involved in late-Neoproterozoic orogenesis were in close proximity prior to rifting and intracontinental basin formation at ca. 810 Ma, which has major implications for pre-orogenic plate reconstructions.

Paper II

Percival, J. J., Konopásek, J., Anczkiewicz, R., Ganerød, M., Sláma, J., Campos, R. S., Battisti, M. A., Bitencourt, M. F., 2021, **Tectono-metamorphic evolution of the northern Dom Feliciano Belt foreland, Santa Catarina, Brazil: Implications for models of subduction-driven orogenesis**, in review at *Tectonics*

The metamorphosed supracrustal rocks within the foreland of the Dom Feliciano Belt (the Schist Belt) occupy a unique position along the western edge of the SANOS, potentially recording the structural and metamorphic evolution of Neoproterozoic orogenesis from its earliest stages. In particular, the Schist Belt should be an ideal candidate to test subduction–collision models of orogenesis, as it lies immediately to the west of the proposed suture (e.g. Basei et al., 2018). Thus, if the Adamastor subduction–collision model is accurate, the Schist Belt should record collision between the arc (the Granite Belt) with the South American passive margin (the Schist Belt). Although there are various studies describing deformation and metamorphism affecting the Schist Belt during Neoproterozoic orogenesis (e.g. Basei et al., 2011a; Saalmann et al., 2006; Sánchez Bettucci et al., 2001), there are currently no reliable constraints on the timing or conditions of these events, and detailed study of the tectono-metamorphic history of the foreland supracrustal rocks in the northern Dom Feliciano Belt (the Brusque Complex) is almost completely lacking. Unravelling orogenic events as recorded within the Brusque Complex can hopefully also shed light on the validity of alternative tectonic models.

Structural mapping of the Brusque Complex reveals that early deformation occurred during top-to-NW thrusting with tectonic transport near-perpendicular to the trend of the orogenic belt. This deformation was associated with prograde regional metamorphism along a geothermal gradient of ~25°C/km, reaching peak conditions of 540–570°C and 5.5–6.7 kbar. These observations suggest earliest deformation and metamorphism in the Schist Belt occurred during early orogenic crustal thickening driven by thrusting and tectonic burial. We used garnet–whole rock Lu–Hf geochronology to date the timing of earliest garnet growth in the highest-grade rocks of the Brusque Complex, which constrains prograde metamorphism, and by inference the timing of thrusting, to between ca. 660–650 Ma. A combination of garnet–whole rock Sm–Nd and monazite U–Pb geochronology constrains the end of this event to between ca. 650–645 Ma. Finally, a biotite Ar–Ar cooling age suggests that thrust-driven exhumation of the Brusque Complex resulted in cooling at ca. 635 Ma.

Structural mapping further reveals a second set of major deformation structures that are oriented parallel with the primary NE–SW trend of the belt. These consist of upright folds, crenulations, and axial planar cleavages showing association with retrograde overprint of the earlier fabric. This style of deformation contrasts with the dextral strike-slip dominated deformation recorded in the Major Gercino Shear zone at the south-eastern boundary with the Granite Belt. These observations are consistent with a transition from thrusting to partitioned transpression as reported by De Toni et al. (2020a), where the pure shear component of transpression is concentrated in the foreland and the simple shear strike-slip component is concentrated in the hinterland. Large granitic batholiths aged between ca. 615–585 Ma intrude the Brusque Complex parallel to the orientation of these structures (Hueck et al., 2019), indicating intrusion during or after deformation. P–T modelling and garnet dating from a metavolcanic rock adjacent to these intrusions shows that at least parts of the complex were at pressures of ~2.2–3.2 kbar by ca. 600 Ma. Muscovite Ar–Ar ages from shear zones within the complex indicate localised deformation continued until at least ca. 570 Ma.

Our results show that the foreland reached metamorphic conditions typical for orogenic crustal thickening ca. 20–30 million years prior to the onset of massive magmatic activity in the hinterland characterised by the intrusion of the Granite Belt. This unequivocally indicates that early deformation and peak metamorphism in the northern Schist Belt does not record collision with the Granite Belt, suggesting the absence of a large Adamastor Ocean between the hinterland and foreland domains prior to convergence. Instead, based on this data, we believe it is more likely that crustal thickening as the result of convergence between the Congo and Luis Alves Cratons began ca. 660–650 Ma with thrusting of a high-grade metamorphic hinterland over the foreland, and that granitic magmatism was the result of post-collisional melting processes and not arc magmatism (Bitencourt and Nardi, 1993, 2000; Florisbal et al., 2009; Florisbal et al., 2012a; Florisbal et al., 2012b; Florisbal et al., 2012c; Lara et al., 2017; Oyhantçabal et al., 2007). Such a delay of ca. 20–30 Myr between the timing of earliest recorded crustal thickening and large-scale melting is typical of hot, internal parts of orogens (England and Thompson, 1986; Jamieson et al., 2011; Jamieson and Beaumont, 2013). We suggest that orogenesis in the northern Dom Feliciano Belt was initiated by rift-basin inversion driven by far-field forces transmitted through the crust in an intracontinental or back-arc rift setting (e.g. De Toni et al., 2020b; Konopásek et al., 2018; Konopásek et al., 2020).

Paper III

Percival, J. J., Konopásek, J., Oyhantçabal, P., Sláma, J., Anczkiewicz, R. 2021, **Diachronous two-stage Neoproterozoic evolution of the southern Dom Feliciano Belt, Uruguay**, in preparation for submission to *Journal of Metamorphic Geology* or *Tectonics*

Like the Brusque Complex in the northern Dom Feliciano Belt, the southern part of the Schist Belt (the Lavalleja Complex) potentially records tectonic events from throughout the entire evolution of the orogen. Furthermore, the southern Dom Feliciano Belt contains the largest exposure of Tonian-aged rocks in the hinterland, which are preserved in the basement of the Punta del Este Terrane (the Cerro Olivo Complex). By studying and comparing the tectono-metamorphic histories of the hinterland and foreland domains of the southern Dom Feliciano Belt, we hope to see if the tectonic model presented in **Paper II** is applicable along the entire length of the belt, and if not, what this can tell us about the tectonic evolution of the southern SANOS in general. One noticeable difference in the southern foreland compared to the northern and central sections is the presence of a sliver of Paleoproterozoic basement thrust over the Schist Belt (Mallmann et al., 2007; Oyhantçabal et al., 2018; Rossini and Legrand, 2003), which already alludes to differing tectonic processes between the various parts of the belt. As such, the aim of **Paper III** is to determine the conditions and timing of metamorphism and deformation in 1) the Tonian-aged, high-grade hinterland rocks (Cerro Olivo Complex), 2) the foreland supracrustal rocks (Schist Belt), and 3) the foreland basement nappe (Campanero Unit). To do this, we use a combination of structural mapping, phase equilibria modelling, and geochronology.

Previous studies have shown that the Cerro Olivo Complex hinterland rocks experienced granulite-facies metamorphism associated with top-to-W thrusting (Masquelin et al., 2011). Our P–T modelling shows that the hinterland rocks experienced near-isothermal decompression from ~10 kbar and ~770°C, down to ~6 kbar, which we interpret to reflect rapid thrust-driven exhumation. Garnet Lu–Hf and zircon U–Pb geochronology constrains the timing of this event to between ca. 655–640 Ma, which is consistent with the timing of crustal thickening recorded in the northern foreland, as discussed in **Paper II**. After high-T metamorphism and associated thrust-dominated deformation in the hinterland at ca. 650 Ma, sub-vertical dextral strike-slip shear zones developed along the boundary between the hinterland and foreland, and the foreland and the Rio de le Plata Craton, such as is observed in the northern part of the belt (**Paper II**). Intrusion of the Granite Belt from ca. 630 Ma was focused along the Sierra Ballena Shear Zone between the hinterland and foreland (Lara et al., 2017; Oyhantçabal et al., 2007).

In contrast, P–T modelling of the Lavalleja Complex revealed that prograde metamorphism in the foreland supracrustal rocks reached up to only lower amphibolite facies conditions, between ~6–7kbar and ~550–570°C, similar to the schists in the Brusque Complex (**Paper II**). However, the timing of this event is dated by garnet Lu–Hf geochronology at 582 ± 23 Ma, which, although imprecise, indicates that garnet growth (and thus peak metamorphism) occurred much later in the southern foreland than in the hinterland and northern foreland. P–T modelling of the foreland basement nappe (the Campanero Unit) indicates similar pressures but higher temperature conditions of ~4–9 kbar and ~670–770°C, and monazite U–Pb dating shows that this high-T metamorphism and partial melting occurred close to timing of metamorphism in the Lavalleja Complex, at ca. 585–570 Ma. These observations support previous interpretations that the Campanero Unit represents a deep part of the foreland basement thrust over the more distal foreland supracrustal rocks. Deformation within the foreland at this time appears to have been dominated by NW-directed thrusting. We interpret this as reflecting a transpressional structure similar to a restraining bend contractional duplex, where the foreland is caught between two major sinistral shear zones at the boundaries with the Rio de la Plata Craton and the hinterland, developing thrusts with movement oblique to the trend of the orogen.

This metamorphic event from ca. 585 Ma is also coeval with the intrusion of large volumes of magmatic rocks into the southern foreland (Lara et al., 2017) and the sinistral reactivation of previously dextral major strike-slip shear zones bordering the foreland (Oriolo et al., 2016a; Oriolo et al., 2016c). Thus, unlike in the northern Dom Feliciano Belt, a significant amount of sinistral transpressional deformation in the southern section appears to have occurred from ca. 585 Ma, which is coeval with sinistral transpressional orogenesis in the Kaoko and Gariep belts (Frimmel, 2018; Goscombe et al., 2003a; Goscombe et al., 2003b; Goscombe et al., 2005a; Goscombe et al., 2005b; Goscombe and Gray, 2008). This diachronous two-stage orogenic history, marked by 1) early thrusting and crustal thickening transitioning into dextral transpression, followed by 2) sinistral transpression, suggests a major tectonic shift within the southern SANOS, which appears to be recorded heterogeneously along the length of the orogen. We suggest that this tectonic shift was driven by the convergence and incorporation of the Kalahari Craton into orogenesis (e.g. Oriolo et al., 2016a).

6 Concluding remarks and future research

Prior to the completion of this thesis, there were no significant detrital zircon data from the Brusque Complex to allow a comparison and correlation between the central and northern Schist Belts, or to demonstrate a clear pre-orogenic connection between the western and eastern foreland supracrustal rocks. **Paper I** provides a contribution for further research into the evolution of the southern SANOS, as well as for Neoproterozoic plate tectonic reconstructions of the transition from Rodinia to Gondwana. This work also provides the first geochronological constraints for the timing of sedimentation (**Paper I**) and metamorphism (**Paper II**) in the Brusque Complex of the northern Dom Feliciano Belt foreland, as well as metamorphism in the southern foreland (**Paper III**) (summarised in Fig. 6). With these data, it is possible to further correlate records of pre-orogenic rifting in the foreland with that seen in the hinterland, as well as to correlate crustal thickening in the northern foreland with high temperature, decompressive metamorphism and thrusting in the hinterland (**Papers II & III**). Metamorphism in the southern foreland, in contrast, shows a stronger temporal connection with later transpressive orogenesis

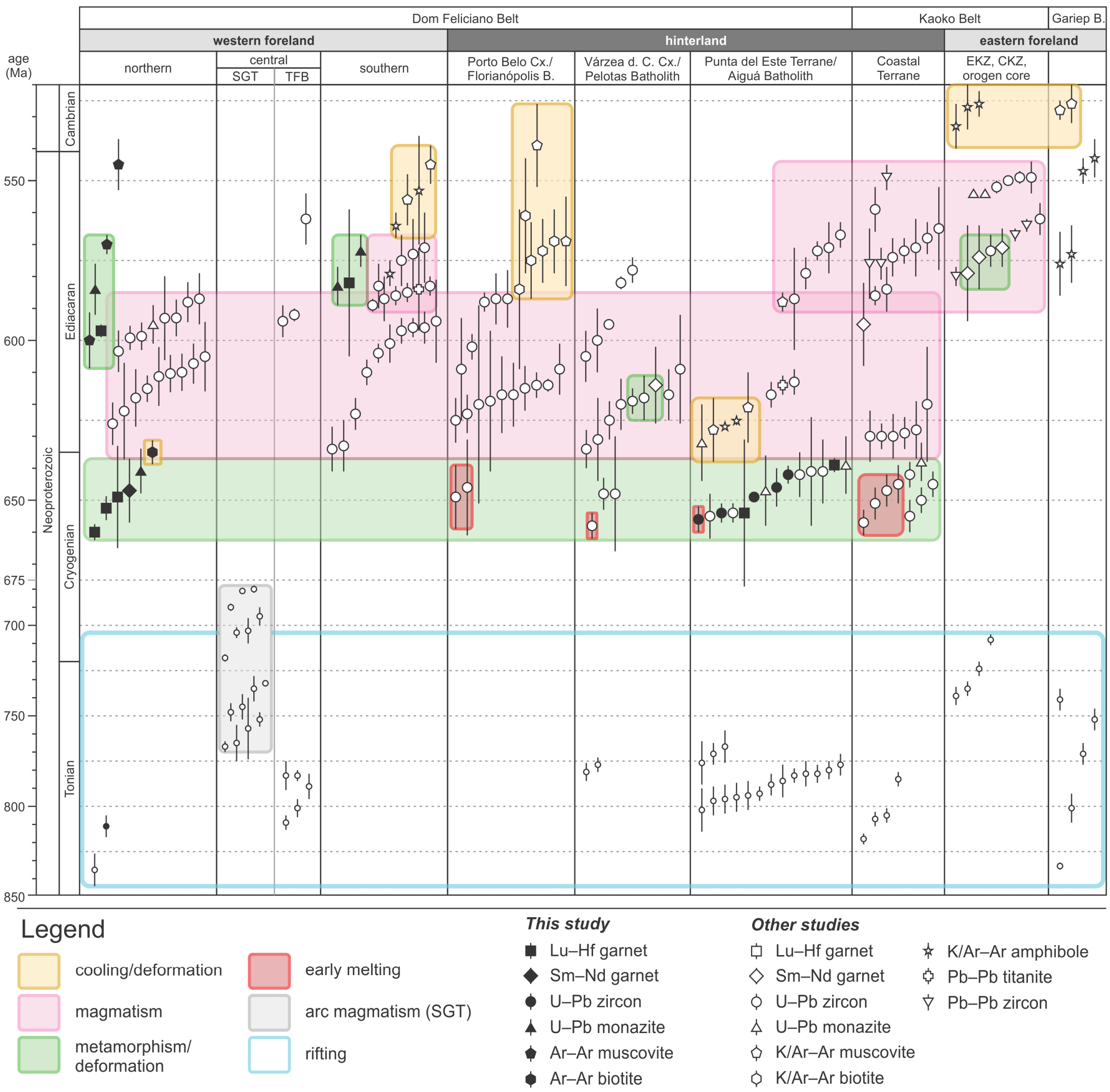

Figure 6. *(previous page)* Summary of major tectonic events using available geochronological data from the southern SANOS. Data from this work (**Papers I, II & III**) are represented by filled shapes, and data from other works are represented by unfilled shapes. Data are grouped by location from the western to eastern forelands (left to right), and within these domains they are grouped from north to south (left to right). SGT = São Gabriel Terrane; TFB = Tijucas Fold Belt; EKZ = Eastern Kaoko Zone; CKZ = Central Kaoko Zone. Sources for data: **northern foreland** – Basei et al. (2008a); Basei et al. (2011a); Campos et al. (2012); Florisbal et al. (2012c); Hueck et al. (2019); Silva et al. (2003); Silva et al. (2005b); Vlach et al. (2009), **central foreland** – Cerva-Alves et al. (2021); Chemale (2000); Gubert et al. (2016); Hartmann et al. (2011); Pertille et al. (2017); Remus et al. (1999); Remus et al. (2000a); Remus et al. (2000b); Saalmann et al. (2011); Silva et al. (2005a); Siviero et al. (2021), **southern foreland** – Gaucher et al. (2008); Hartmann et al. (2002); Lara et al. (2017); Lara et al. (2020); Oriolo et al. (2016c); Oyhantçabal et al. (2007); Oyhantçabal et al. (2009); Oyhantçabal et al. (2012); Rapalini et al. (2015), **northern hinterland** – Chemale et al. (2012); Florisbal et al. (2012c); Passarelli et al. (2010), **central hinterland** – Babinski et al. (1997); Frantz et al. (2003); Gross et al. (2006); Gruber et al. (2016); Koester et al. (2016); Martil (2016); Oliveira et al. (2015); Philipp et al. (2016); Silva et al. (1999); Völz et al. (2020), **southern hinterland** – Basei et al. (2000); Hartmann et al. (2002); Lara et al. (2020); Lenz et al. (2011); Masquelin et al. (2011); Oyhantçabal et al. (2007); Oyhantçabal et al. (2009); Will et al. (2019), **Coastal Terrane and Kaoko Belt** – (Franz et al., 1999); Goscombe et al. (2003b); Goscombe et al. (2005a); Konopásek et al. (2008); Konopásek et al. (2016); Konopásek et al. (2018); Kröner et al. (2004); Seth et al. (1998), **Gariep Belt** – Frimmel and Frank (1998).

in the eastern foreland, where the hinterland is thrust over the foreland in the Kaoko Belt and a small amount of oceanic crust is thrust over the foreland in the Gariep Belt (Fig. 6). The results presented in this thesis highlight the importance of the development and integration of robust geochronological and structural datasets, and thermodynamic modelling, for the study of orogenic belts.

6.1 Future work

6.1.1 Further fieldwork and detailed structural analysis in the southern foreland

The direction of thrusting of the Campanero Unit is difficult to ascertain given the presence of two lineations in the high-T S1 foliation, and detailed structural analysis is hindered by poor outcrop exposure. Although it is not possible to rule out that L2 is the result of pure shear stretching orthogonal to the shear direction, assuming consistent transport-parallel stretching lineations there are two possible scenarios supported by the combined geochronological and structural data: 1) S1 and L1 were produced by an early (ca. 640─630 Ma) low-angle shear event, possibly correlated with west-directed thrusting seen in the Cerro Olivo Complex, and this was followed much later by NNE-directed low-angle thrusting during transpression and sinistral reactivation of the Sierra Ballena Shear Zone, producing L2 by overprinting S1, and developing E─W-trending S2; 2) both lineations developed during the period ca. 585─570 Ma, where L1 and NW-directed thrusting immediately preceded L2 and NNE-directed thrusting, with the direction of tectonic transport rotating during the transpressional episode at ca. 585─570 Ma. Whichever scenario is considered, orogen-parallel stretching contributed significantly to the Neoproterozoic tectono-metamorphic evolution of the Nico Perez Terrane. Such a scenario could be explained through lateral extrusion of the foreland between the restrictive Sarandí del Yí and Sierra Ballena shear zones during oblique transpression, like what is described in the Kaoko Belt (Goscombe et al., 2005b). Further complicating the model are the undeformed, ca. 630 Ma granites that appear to be intruding the Zanja del Tigre Complex (Oyhantçabal et al., 2009). Exactly how these granitic bodies escaped the ca. 580 Ma transpressional event without being deformed together with the schists is currently unexplained by our model, although possibly they represent underlying rocks exposed as basement inliers beneath another thrust sheet comprised of the Zanja del Tigre Complex supracrustal rocks, and deformation of the overlying schists simply reflects thin skinned tectonics. Ultimately, further detailed strain analysis of the Campanero Unit and adjacent rocks is needed to develop a more robust model.

6.1.2 Intracontinental or back-arc rifting?

One of the primary findings put forth in this study is the high likelihood that orogenic crustal thickening (i.e., continental convergence between the Luis Alves–Nico Perez and the Congo–Kalahari) was already underway by ca. 660–650 Ma, and the low likelihood that subduction arc magmatism was responsible for formation of large volumes of magmatic rocks intruding the orogenic hinterland (the Granite Belt) between ca. 630–580 Ma. This implies the absence of a large Adamastor Ocean, and probably the tectonic setting at the onset of convergence was more similar to an extended rift basin with little to no oceanic crust. However, what cannot be fully answered by the data collected in this study is whether this rift basin was the result of intracontinental or back-arc rifting. Many recent studies in the northern SANOS advocate for intracontinental rifting, which greatly simplifies the geological evolution of the orogen and explains many contradictions and data unexplained by the various subduction–collision models (Cavalcante et al., 2019; Fossen et al., 2020; Konopásek et al., 2020; Meira et al., 2015; Meira et al., 2019b). In contrast, the predominant alternative model in the southern SANOS is that the pre-orogenic tectonic setting for the Dom Feliciano Belt was an arc or back-arc active between ca. 900 and 700 Ma (De Toni et al., 2020b; Koester et al., 2016; Lenz et al., 2013; Martil et al., 2017). These interpretations are supported by the presence of the Sao Gabriel Terrane in the central Dom Feliciano Belt preserving arc magmatism between ca. 900 and 700 Ma (Philipp et al., 2018), as well as the reported arc-like geochemistry of igneous rocks in the hinterland of the belt. However, some studies propose that these latter rocks could well be entirely rift-related, and simply inheriting arc-like geochemistry from the melting of their source rocks (Konopásek et al., 2020). This would place the evolution of the southern SANOS more in line with recently proposed intracontinental orogenic models for the northern sections. In any case, further work is needed to integrate the existing data into a fully realised model, or to find further evidence supporting those that currently exist.

7 References

Abre P., Blanco G., Gaucher C., Frei D. & Frei R., 2020. Provenance of the Late Ediacaran Rocha Formation, Cuchilla Dionisio Terrane, Uruguay: Tectonic implications on the assembly of Gondwana. Precambrian Res., vol. 342, p. 105704. https://doi.org/10.1016/j.precamres.2020.105704.

Alkmim F. F., Kuchenbecker M., Reis H. L. S. & Pedrosa-Soares A. C., 2017. The Araçuaí Belt. In Heilbron M., Cordani U. G. & Alkmim F. F. eds. São Francisco Craton, Eastern Brazil: Tectonic Genealogy of a Miniature Continent. pp. 255-276. Cham: Springer International Publishing https://doi.org/10.1007/978-3-319-01715-0_14.

Amaral L., Caxito F. d. A., Pedrosa-Soares A. C., Queiroga G., Babinski M., Trindade R., Lana C. & Chemale F., 2020. The Ribeirão da Folha ophiolite-bearing accretionary wedge (Araçuaí orogen, SE Brazil): New data for Cryogenian plagiogranite and metasedimentary rocks. Precambrian Res., vol. 336, p. 105522. https://doi.org/10.1016/j.precamres.2019.105522.

Anczkiewicz R. & Thirlwall M. F., 2003. Improving precision of Sm-Nd garnet dating by H2SO4 leaching: a simple solution to the phosphate inclusion problem. Geological Society, London, Special Publications, vol. 220, no. 1, pp. 83–91. https://10.1144/GSL.SP.2003.220.01.05.

Anczkiewicz R., Platt J. P., Thirlwall M. F. & Wakabayashi J., 2004. Franciscan subduction off to a slow start: evidence from high-precision Lu–Hf garnet ages on high grade-blocks. Earth Planet. Sci. Lett., vol. 225, no. 1, pp. 147–161. https://doi.org/10.1016/j.epsl.2004.06.003.

Anczkiewicz R., Chakraborty S., Dasgupta S., Mukhopadhyay D. & Kołtonik K., 2014. Timing, duration and inversion of prograde Barrovian metamorphism constrained by high resolution Lu–Hf garnet dating: A case study from the Sikkim Himalaya, NE India. Earth Planet. Sci. Lett., vol. 407, pp. 70–81. http://dx.doi.org/10.1016/j.epsl.2014.09.035.

Arena K. R., Hartmann L. A. & Lana C., 2018. U–Pb–Hf isotopes and trace elements of metasomatic zircon delimit the evolution of neoproterozoic Capané ophiolite in the southern Brasiliano Orogen. Int. Geol. Rev., pp. 1-18. https://doi.org/10.1080/00206814.2017.1355269.

Babinski M., Chemale F., Van Schmus W. R., Hartmann L. A. & Da Silva L. C., 1997. U-Pb and Sm-Nd geochronology of the neoproterozoic granitic-gneissic Dom Feliciano belt, Southern Brazil. J. S. Am. Earth Sci., vol. 10, no. 3, pp. 263-274. https://doi.org/10.1016/S0895-9811(97)00021-7.

Basei M. A. S., Siga Jr O., Masquelin H., Harara O. M., Reis Neto J. M. & Preciozzi F., 2000. The Dom Feliciano Belt of Brazil and Uruguay and its Foreland Domain, the Rio de la Plata Craton: framework, tectonic evolution and correlation with similar provinces of Southwestern Africa. In Cordani U. G., et al. eds. Tectonic Evolution of South America. pp. 311─334. Rio de Janeiro, Brazil: Geological Society http://10.13140/RG.2.1.5109.4567.

Basei M. A. S., Frimmel H. E., Nutman A. P., Preciozzi F. & Jacob J., 2005. A connection between the Neoproterozoic Dom Feliciano (Brazil/Uruguay) and Gariep (Namibia/South Africa) orogenic belts - Evidence from a reconnaissance provenance study. Precambrian Res., vol. 139, no. 3-4, pp. 195-221. https://www.doi.org/10.1016/j.precamres.2005.06.005.

Basei M. A. S., Grasso C. B., Vlach S. R. F., Nutman A., Siga Jr. O. & Osaki L. S., 2008a. A-type rift-related granite and the lower cryogenian age for the beginning of the Brusque Belt basin. Proceedings of South American Symposium on Isotope Geology. San Carlos de Bariloche, Argentina.

Basei M. A. S., Frimmel H. E., Nutman A. P. & Preciozzi F., 2008b. West Gondwana amalgamation based on detrital zircon ages from Neoproterozoic Ribeira and Dom Feliciano belts of South America and comparison with coeval sequences from SW Africa. Geol. Soc. Spec. Publ., vol. 294, no. 1, pp. 239-256. https://www.doi.org/10.1144/SP294.13.

Basei M. A. S., Campos Neto M. C., Castro N. A., Nutman A. P., Wemmer K., Yamamoto M. T., Hueck M., Osako L., Siga Jr O. & Passarelli C. R., 2011a. Tectonic evolution of the Brusque Group, Dom Feliciano belt, Santa Catarina, Southern Brazil. J. S. Am. Earth Sci., vol. 32, no. 4, p. 324─350. https://doi.org/10.1016/j.jsames.2011.03.016.

Basei M. A. S., Peel E., Sánchez Bettucci L., Preciozzi F. & Nutman A. P., 2011b. The basement of the Punta del Este Terrane (Uruguay): an African Mesoproterozoic fragment at the eastern border of the South American Río de La Plata craton. Int. J. Earth Sci., vol. 100, pp. 289-304. https://www.doi.org/10.1007/s00531-010-0623-1.

Basei M. A. S., Campos Neto M. d. C., Lopes A. P., Nutman A. P., Liu D. & Sato K., 2013. Polycyclic evolution of Camboriú Complex migmatites, Santa Catarina, Southern Brazil: integrated Hf isotopic and U-Pb age zircon evidence of episodic reworking of a Mesoarchean juvenile crust. Brazilian Journal of Geology, vol. 43, no. 3, pp. 427-443. https://doi.org/10.5327/Z2317-48892013000300002.

Basei M. A. S., Frimmel H. E., Campos Neto M. d. C., de Araujo C. E. G., de Castro N. A. & Passarelli C. R., 2018. The Tectonic History of the Southern Adamastor Ocean Based on a Correlation of the Kaoko and Dom Feliciano Belts. In Siegesmund S., et al. eds. Geology of Southwest Gondwana. pp. 63─85. 1st ed. Cham: Springer International Publishing https://doi.org/10.1007/978-3-319-68920-3_3.

Battisti M. A., Bitencourt M. F., De Toni G. B., Nardi L. V. S. & Konopásek J., 2018. Metavolcanic rocks and orthogneisses from Porongos and Várzea do Capivarita complexes: A case for identification of tectonic interleaving at different crustal levels from structural and geochemical data in southernmost Brazil. J. S. Am. Earth Sci., vol. 88, p. 253─274. https://doi.org/10.1016/j.jsames.2018.08.009.

Bento dos Santos T. M., Munhá J. M., Tassinari C. C. G., Fonseca P. E. & Neto C. D., 2011. Metamorphic P-T evolution of granulites in the central Ribeira Fold Belt, SE Brazil. Geosciences Journal, vol. 15, no. 1, pp. 27-51. https://doi.org/10.1007/s12303-011-0004-1.

Bitencourt M. F. & Nardi L. V. S., 1993. Late- to Post-collisional Brasiliano Magmatism in Southernmost Brazil. Anais da Academia Brasileira de Ciências, vol. 65, p. 3─16. https://10.25249/0375-7536.2000301186189.

Bitencourt M. F. & Nardi L. V. S., 2000. Tectonic setting and sources of magmatism related to the southern Brazilian shear belt. Revista Brasileira de Geociencias, vol. 30, no. 1, p. 186─189.

Bossi J. & Gaucher C., 2004. The Cuchilla Dionisio Terrane, Uruguay: An Allochthonous Block Accreted in the Cambrian to SW-Gondwana. Gondwana Res., vol. 7, no. 3, pp. 661-674. https://doi.org/10.1016/S1342-937X(05)71054-6.

Campos R. S., Philipp R. P., Massonne H.-J., Chemale Jr F. & Theye T., 2011. Petrology and isotope geology of mafic to ultramafic metavolcanic rocks of the Brusque Metamorphic Complex, southern Brazil. Int. Geol. Rev., vol. 54, no. 6, p. 686─713. https://doi.org/10.1080/00206814.2011.569393.

Campos R. S., Philipp R. P., Massonne H.-J. & Chemale Jr F., 2012. Early post-collisional Brasiliano magmatism in Botuverá region, Santa Catarina, southern Brazil: Evidence from petrology, geochemistry, isotope geology and geochronology of the diabase and lamprophyre dikes. J. S. Am. Earth Sci., vol. 37, p. 266─278. https://doi.org/10.1016/j.jsames.2012.02.005.

Cavalcante C., Hollanda M. H., Vauchez A. & Kawata M., 2018. How long can the middle crust remain partially molten during orogeny? Geology, vol. 46, no. 10, pp. 839–842. https://doi.org/10.1130/g45126.1.

Cavalcante C., Fossen H., de Almeida R. P., Hollanda M. H. B. M. & Egydio-Silva M., 2019. Reviewing the puzzling intracontinental termination of the Araçuaí-West Congo orogenic belt and its implications for orogenic development. Precambrian Res., vol. 322, pp. 85–98. https://doi.org/10.1016/j.precamres.2018.12.025.

Cawood P. A., Kröner A., Collins W. J., Kusky T. M., Mooney W. D. & Windley B. F., 2009. Accretionary orogens through Earth history. Geological Society, London, Special Publications, vol. 318, no. 1, pp. 1–36. https://doi.org/10.1144/SP318.1.

Cerva-Alves T., Hartmann L. A., Lana C., Queiroga G. N., Maciel L. A. C., Leandro C. G. & Savian J. F., 2021. Rutile and zircon age and geochemistry in the evolution of the juvenile São Gabriel Terrane early in the Brasiliano Orogeny. J. S. Am. Earth Sci., vol. 112, p. 103505. https://doi.org/10.1016/j.jsames.2021.103505.

Chemale F., Jr, 2000. Evolução geológica do Escudo Sul-rio-grandense. Geologia e Estratigrafia do Rio Grande do Sul, pp. 3-44.

Chemale F., Jr, Mallmann G., Bitencourt M. F. & Kawashita K., 2012. Time constraints on magmatism along the Major Gercino Shear Zone, southern Brazil: Implications for West Gondwana

reconstruction. Gondwana Res., vol. 22, no. 1, pp. 184–199. https://doi.org/10.1016/j.gr.2011.08.018.
Connolly J. A. D., 2005. Computation of phase equilibria by linear programming: A tool for geodynamic modeling and its application to subduction zone decarbonation. Earth Planet. Sci. Lett., vol. 236, no. 1–2, pp. 524–541. https://doi.org/10.1016/j.epsl.2005.04.033.
Costa E. O. d., Gomes E. M., Bitencourt M. d. F., De Toni G. B. & Nardi L. V. S., 2020. Reassessing the PT conditions of Neoproterozoic collisional metamorphism and partial melting in southernmost Brazil. J. S. Am. Earth Sci., vol. 100, p. 102584. https://doi.org/10.1016/j.jsames.2020.102584.
De Toni G. B., Bitencourt M. F., Konopásek J., Martini A., Andrade P. H. S., Florisbal L. M. & Campos R. S., 2020a. Transpressive strain partitioning between the Major Gercino Shear Zone and the Tijucas Fold Belt, Dom Feliciano Belt, Santa Catarina, southern Brazil. J. Struct. Geol., vol. 136, p. 104058. https://doi.org/10.1016/j.jsg.2020.104058.
De Toni G. B., Bitencourt M. F., Nardi L. V. S., Florisbal L. M., Almeida B. S. & Geraldes M., 2020b. Dom Feliciano Belt orogenic cycle tracked by its pre-collisional magmatism: The Tonian (ca. 800 Ma) Porto Belo Complex and its correlations in southern Brazil and Uruguay. Precambrian Res., vol. 342, p. 105702. https://doi.org/10.1016/j.precamres.2020.105702.
De Toni G. B., Bitencourt M. F., Konopásek J., Battisti M. A., Oliveira da Costa E. & Savian J. F., 2021. Autochtonous origin of the Encruzilhada Block, Dom Feliciano Belt, southern Brazil, based on aerogeophysics, image analysis and PT-paths. JGeo, vol. 144, p. 101825. https://doi.org/10.1016/j.jog.2021.101825.
Diener J. F. A. & Powell R., 2010. Influence of ferric iron on the stability of mineral assemblages. Journal of Metamorphic Geology, vol. 28, no. 6, pp. 599-613. https://doi.org/10.1111/j.1525-1314.2010.00880.x.
Diener J. F. A., Thomas R. J. & Macey P. H., 2017. Pan-African accretionary metamorphism in the Sperrgebiet Domain, Gariep Belt, SW Namibia. Precambrian Res., vol. 292, pp. 152-162. https://doi.org/10.1016/j.precamres.2017.02.006.
Dürr S. B. & Dingeldey D. P., 1996. The Kaoko belt (Namibia): Part of a late Neoproterozoic continental-scale strike-slip system. Geology, vol. 24, no. 6, pp. 503-506. https://doi.org/10.1130/0091-7613(1996)024<0503:Tkbnpo>2.3.Co;2.
Egydio-Silva M., Vauchez A., Fossen H., Gonçalves Cavalcante G. C. & Xavier B. C., 2018. Connecting the Araçuaí and Ribeira belts (SE – Brazil): Progressive transition from contractional to transpressive strain regime during the Brasiliano orogeny. J. S. Am. Earth Sci., vol. 86, pp. 127-139. https://doi.org/10.1016/j.jsames.2018.06.005.
England P. C. & Thompson A., 1986. Some thermal and tectonic models for crustal melting in continental collision zones. Geological Society, London, Special Publications, vol. 19, no. 1, p. 83. https://doi.org/10.1144/GSL.SP.1986.019.01.05.
Florisbal L. M., Bitencourt M. F., Nardi L. V. S. & Conceição R. V., 2009. Early post-collisional granitic and coeval mafic magmatism of medium- to high-K tholeiitic affinity within the Neoproterozoic Southern Brazilian Shear Belt. Precambrian Res., vol. 175, no. 1–4, pp. 135–148. https://doi.org/10.1016/j.precamres.2009.09.003.
Florisbal L. M., Janasi V. A., Bitencourt M. F., Nardi L. V. S. & Heaman L. M., 2012a. Contrasted crustal sources as defined by whole-rock and Sr–Nd–Pb isotope geochemistry of neoproterozoic early post-collisional granitic magmatism within the Southern Brazilian Shear Belt, Camboriú, Brazil. J. S. Am. Earth Sci., vol. 39, pp. 24–43. https://doi.org/10.1016/j.jsames.2012.06.013.
Florisbal L. M., Bitencourt M. F., Janasi V. A., Nardi L. V. S. & Heaman L. M., 2012b. Petrogenesis of syntectonic granites emplaced at the transition from thrusting to transcurrent tectonics in post-collisional setting: Whole-rock and Sr–Nd–Pb isotope geochemistry in the Neoproterozoic Quatro Ilhas and Mariscal Granites, Southern Brazil. Lithos, vol. 153, pp. 53–71. https://doi.org/10.1016/j.lithos.2012.04.031.
Florisbal L. M., Janasi V. A., Bitencourt M. F. & Heaman L. M., 2012c. Space–time relation of post-collisional granitic magmatism in Santa Catarina, southern Brazil: U–Pb LA-MC-ICP-MS zircon geochronology of coeval mafic–felsic magmatism related to the Major Gercino Shear Zone. Precambrian Res., vol. 216–219, pp. 132–151. https://doi.org/10.1016/j.precamres.2012.06.015.

Forshaw J. B. & Pattison D. R. M., 2021. Ferrous/ferric (Fe2+/Fe3+) partitioning among silicates in metapelites. Contributions to Mineralogy and Petrology, vol. 176, no. 9, p. 63. https://doi.org/10.1007/s00410-021-01814-4.

Fossen H., Cavalcante C., Konopásek J., Tieppo Meira V., Almeida R., Hollanda M. & Trompette R., 2020. A critical discussion of the subduction-collision model for the Neoproterozoic Araçuaí-West Congo orogen. Precambrian Res., p. 105715. https://doi.org/10.1016/j.precamres.2020.105715.

Fragoso-Cesar A. R. S., 1980. O craton do Rio de la Plata eo cinturao Dom Feliciano no escudo Uruguaio-Sul-Riograndense. Congresso Brasileiro de Geologia. pp. 2879-2882. Anais Camboriú.

Frantz J., McNaughton N. J., Marques J., Hartmann L. A., Botelho N. & Caravaca G., 2003. Shrimp U-Pb zircon ages of granitoids from southernmost Brazil: constraints on the temporal evolution on the Dorsal do Canguçu transcurrent shear zone and the eastern Dom Feliciano Belt. IV South American Symposium on Isotope Geology, pp. 174-177.

Franz L., Romer R. L. & Dingeldey D. P., 1999. Diachronous Pan-African granulite-facies metamorphism (650 Ma and 550 Ma) in the Kaoko Belt, NW Namibia. European Journal of Mineralogy, vol. 11, no. 1, pp. 167-180. https://doi.org/10.1127/ejm/11/1/0167.

Frimmel H. E., Hartnady C. J. H. & Koller F., 1996. Geochemistry and tectonic setting of magmatic units in the Pan-African Gariep Belt, Namibia. Chem. Geol., vol. 130, no. 1-2, pp. 101-121. https://doi.org/10.1016/0009-2541(95)00188-3.

Frimmel H. E. & Frank W., 1998. Neoproterozoic tectono-thermal evolution of the Gariep Belt and its basement, Namibia and South Africa. Precambrian Res., vol. 90, no. 1, pp. 1-28. https://doi.org/10.1016/S0301-9268(98)00029-1.

Frimmel H. E., 2018. The Gariep Belt. In Siegesmund S., et al. eds. Geology of Southwest Gondwana. pp. 353-386. 1st ed. Cham: Springer International Publishing https://www.doi.org/10.1007/978-3-319-68920-3_13.

Gaidies F., Abart R., De Capitani C., Schuster R., Connolly J. A. D. & Reusser E., 2006. Characterization of polymetamorphism in the Austroalpine basement east of the Tauern Window using garnet isopleth thermobarometry. Journal of Metamorphic Geology, vol. 24, no. 6, pp. 451-475. https://doi.org/10.1111/j.1525-1314.2006.00648.x.

Gaucher C., Finney S. C., Poiré D. G., Valencia V. A., Grove M., Blanco G., Pamoukaghlián K. & Peral L. G., 2008. Detrital zircon ages of Neoproterozoic sedimentary successions in Uruguay and Argentina: Insights into the geological evolution of the Río de la Plata Craton. Precambrian Res., vol. 167, no. 1, pp. 150-170. https://doi.org/10.1016/j.precamres.2008.07.006.

Germs G. J. B., 1995. The Neoproterozoic of southwestern Africa, with emphasis on platform stratigraphy and paleontology. Precambrian Res., vol. 73, no. 1, pp. 137-151. https://doi.org/10.1016/0301-9268(94)00075-3.

Goscombe B., Hand M. & Gray D., 2003a. Structure of the Kaoko Belt, Namibia: progressive evolution of a classic transpressional orogen. J. Struct. Geol., vol. 25, no. 7, pp. 1049-1081. https://www.doi.org/10.1016/S0191-8141(02)00150-5.

Goscombe B., Hand M., Gray D. & Mawby J. O., 2003b. The Metamorphic Architecture of a Transpressional Orogen: the Kaoko Belt, Namibia. J. Petrol., vol. 44, no. 4, pp. 679-711. https://www.doi.org/10.1093/petrology/44.4.679.

Goscombe B., Gray D., Armstrong R., Foster D. A. & Vogl J., 2005a. Event geochronology of the Pan-African Kaoko Belt, Namibia. Precambrian Res., vol. 140, no. 3–4, pp. 103.e1–103.e41. https://doi.org/10.1016/j.precamres.2005.07.003.

Goscombe B., Gray D. & Hand M., 2005b. Extrusional Tectonics in the Core of a Transpressional Orogen; the Kaoko Belt, Namibia. J. Petrol., vol. 46, no. 6, pp. 1203-1241. https://www.doi.org/10.1093/petrology/egi014.

Goscombe B. & Gray D., 2007. The Coastal Terrane of the Kaoko Belt, Namibia: Outboard arc-terrane and tectonic significance. Precambrian Res., vol. 155, no. 1, pp. 139-158. https://doi.org/10.1016/j.precamres.2007.01.008.

Goscombe B. & Gray D., 2008. Structure and strain variation at mid-crustal levels in a transpressional orogen: A review of Kaoko Belt structure and the character of West Gondwana amalgamation and dispersal. Gondwana Res., vol. 13, no. 1, pp. 45–85. https://doi.org/10.1016/j.gr.2007.07.002.

Gross A. O. M. S., Porcher C. C., Fernandes L. A. D. & Koester E., 2006. Neoproterozoic low-pressure/high-temperature collisional metamorphic evolution in the Varzea do Capivarita Metamorphic Suite, SE Brazil: Thermobarometric and Sm/Nd evidence. Precambrian Res., vol. 147, no. 1, pp. 41-64. https://doi.org/10.1016/j.precamres.2006.02.001.

Gross A. O. M. S., Droop G. T. R., Porcher C. C. & Fernandes L. A. D., 2009. Petrology and thermobarometry of mafic granulites and migmatites from the Chafalote Metamorphic Suite: New insights into the Neoproterozoic P–T evolution of the Uruguayan—Sul-Rio-Grandense shield. Precambrian Res., vol. 170, no. 3–4, pp. 157–174. https://doi.org/10.1016/j.precamres.2009.01.011.

Grove M. & Harrison T. M., 1996. 40Ar* diffusion in Fe-rich biotite. Am. Mineral., vol. 81, no. 7–8, pp. 940–951. https://doi.org/10.2138/am-1996-7-816.

Gruber L., Porcher C. C., Koester E., Bertotti A. L., Lenz C., Fernandes L. A. D. & Remus M. V. D., 2016. Isotope geochemistry and geochronology of syn-depositional volcanism in Porongos Metamorphic Complex, Santana da Boa Vista Antiform, Dom Feliciano Belt, Brazil: Onset of an 800 Ma continental arc. J. Sediment. Environ., vol. 1, no. 2, pp. 196-215. https://www.doi.org/10.12957/jse.2016.22722.

Guadagnin F., Chemale Jr F., Dussin I. A., Jelinek A. R., dos Santos M. N., Borba M. L., Justino D., Bertotti A. L. & Alessandretti L., 2010. Depositional age and provenance of the Itajaí Basin, Santa Catarina State, Brazil: Implications for SW Gondwana correlation. Precambrian Res., vol. 180, no. 3–4, pp. 156–182. https://doi.org/10.1016/j.precamres.2010.04.002.

Gubert M. L., Philipp R. P. & Stipp Basei M. A., 2016. The Bossoroca Complex, São Gabriel Terrane, Dom Feliciano Belt, southernmost Brazil: UPb geochronology and tectonic implications for the neoproterozoic São Gabriel Arc. J. S. Am. Earth Sci., vol. 70, pp. 1-17. https://doi.org/10.1016/j.jsames.2016.04.006.

Harrison T. M., Célérier J., Aikman A. B., Hermann J. & Heizler M. T., 2009. Diffusion of 40Ar in muscovite. Geochimica et Cosmochimica Acta, vol. 73, no. 4, pp. 1039–1051. https://doi.org/10.1016/j.gca.2008.09.038.

Hartmann L. A., Santos J. O. S., Bossi J., Campal N., Schipilov A. & McNaughton N. J., 2002. Zircon and titanite U–Pb SHRIMP geochronology of Neoproterozoic felsic magmatism on the eastern border of the Rio de la Plata Craton, Uruguay. J. S. Am. Earth Sci., vol. 15, no. 2, pp. 229-236. https://doi.org/10.1016/S0895-9811(02)00030-5.

Hartmann L. A., Philipp R. P., Santos J. O. S. & McNaughton N. J., 2011. Time frame of 753–680 Ma juvenile accretion during the São Gabriel orogeny, southern Brazilian Shield. Gondwana Res., vol. 19, no. 1, pp. 84-99. https://doi.org/10.1016/j.gr.2010.05.001.

Hartnady C., Joubert P. & Stowe C., 1985. Proterozoic Crustal Evolution in Southwestern Africa. International Union of Geological Sciences, vol. 8, no. 4, pp. 236–244. https://doi.org/10.18814/epiiugs/1985/v8i4/003.

Hasui Y., Carneiro C. D. R. & Coimbra A. M., 1975. The Ribeira Folded Belt. Revista Brasileira de Geociências, vol. 5, no. 4, pp. 257-266.

Heilbron M. & Machado N., 2003. Timing of terrane accretion in the Neoproterozoic–Eopaleozoic Ribeira orogen (se Brazil). Precambrian Res., vol. 125, no. 1, pp. 87–112. https://doi.org/10.1016/S0301-9268(03)00082-2.

Heilbron M., Valeriano C. M., Tassinari C. C. G., Almeida J., Tupinambá M., Siga O. & Trouw R., 2008. Correlation of Neoproterozoic terranes between the Ribeira Belt, SE Brazil and its African counterpart: comparative tectonic evolution and open questions. Geological Society, London, Special Publications, vol. 294, no. 1, p. 211. https://doi.org/10.1144/SP294.12.

Heilbron M., de Morisson Valeriano C., Peixoto C., Tupinambá M., Neubauer F., Dussin I., Corrales F., Bruno H., Lobato M., Horta de Almeida J. C. & Guilherme do Eirado Silva L., 2020. Neoproterozoic magmatic arc systems of the central Ribeira belt, SE-Brazil, in the context of the West-Gondwana pre-collisional history: A review. J. S. Am. Earth Sci., vol. 103, p. 102710. https://doi.org/10.1016/j.jsames.2020.102710.

Heine C., Zoethout J. & Müller R. D., 2013. Kinematics of the South Atlantic rift. Solid Earth, vol. 4, no. 2, pp. 215–253. https://doi.org/10.5194/se-4-215-2013.

Hermann J. & Rubatto D., 2003. Relating zircon and monazite domains to garnet growth zones: age and duration of granulite facies metamorphism in the Val Malenco lower crust. Journal of Metamorphic Geology, vol. 21, no. 9, pp. 833–852. https://doi.org/10.1046/j.1525-1314.2003.00484.x.

Hoffman P. F. & Halverson G. P., 2008. Otavi Group of the western Northern Platform, the Eastern Kaoko Zone and the western Northern Margin Zone. In Miller R. M. ed. The Geology of Namibia. pp. 69-136. Namibia: Geological Survey Namibia.

Höfig D. F., Marques J. C., Basei M. A. S., Giusti R. O., Kohlrausch C. & Frantz J. C., 2018. Detrital zircon geochronology (U-Pb LA-ICP-MS) of syn-orogenic basins in SW Gondwana: New insights into the Cryogenian-Ediacaran of Porongos Complex, Dom Feliciano Belt, southern Brazil. Precambrian Res., vol. 306, pp. 189–208. https://doi.org/10.1016/j.precamres.2017.12.031.

Holland T. J. B. & Powell R., 2011. An improved and extended internally consistent thermodynamic dataset for phases of petrological interest, involving a new equation of state for solids. Journal of Metamorphic Geology, vol. 29, no. 3, pp. 333–383. https://doi.org/10.1111/j.1525-1314.2010.00923.x.

Hueck M., Oyhantçabal P., Basei M. & Siegesmund S., 2018. The Dom Feliciano Belt in Southern Brazil and Uruquay. In Siegesmund S., et al. eds. Geology of Southwest Gondwana. pp. 267–302. 1st ed. Cham: Springer International Publishing https://doi.org/10.1007/978-3-319-68920-3_11.

Hueck M., Basei M. A. S. & Castro N. A. d., 2019. Tracking the sources and the evolution of the late Neoproterozoic granitic intrusions in the Brusque Group, Dom Feliciano Belt, South Brazil: LA-ICP-MS and SHRIMP geochronology coupled to Hf isotopic analysis. Precambrian Res., vol. 338, p. 105566. https://doi.org/10.1016/j.precamres.2019.105566.

Jamieson R. A., Unsworth M. J., Harris N. B. W., Rosenberg C. L. & Schulmann K., 2011. Crustal Melting and the Flow of Mountains. Elements, vol. 7, no. 4, pp. 253–260. https://doi.org/10.2113/gselements.7.4.253.

Jamieson R. A. & Beaumont C., 2013. On the origin of orogens. Geological Society of America Bulletin, vol. 125, no. 11–12, pp. 1671–1702. https://doi.org/10.1130/b30855.1.

Juliani C., Hackspacher P., Dantas E. L. & Fetter A. H., 2000. The mesoproterozoic volcano-sedimentary Serra do Itaberaba Group of the Central Ribeira Belt, São Paulo State, Brazil: implications for the age of the overlying São Roque Group. Revista brasileira de geociências, vol. 30, no. 1, pp. 82-86. https://doi.org/10.25249/0375-7536.2000301082086.

Jung S., Brandt S., Bast R., Scherer E. E. & Berndt J., 2019. Metamorphic petrology of a high-T/low-P granulite terrane (Damara belt, Namibia) – Constraints from pseudosection modelling and high-precision Lu–Hf garnet-whole rock dating. Journal of Metamorphic Geology, vol. 37, no. 1, pp. 41-69. https://doi.org/10.1111/jmg.12448.

Koester E., Porcher C. C., Pimentel M. M., Fernandes L. A. D., Vignol-Lelarge M. L., Oliveira L. D. & Ramos R. C., 2016. Further evidence of 777 Ma subduction-related continental arc magmatism in Eastern Dom Feliciano Belt, southern Brazil: The Chácara das Pedras Orthogneiss. J. S. Am. Earth Sci., vol. 68, pp. 155–166. https://doi.org/10.1016/j.jsames.2015.12.006.

Konopásek J., Kosler J., Tajčmanová L., Ulrich S. & Kitt S., 2008. Neoproterozoic igneous complex emplaced along major tectonic boundary in the Kaoko Belt (NW Namibia): ion probe and LA-ICP-MS dating of magmatic and metamorphic zircons. J. Geol. Soc. Lond., vol. 165, no. 1, pp. 153–165. https://doi.org/10.1144/0016-76492006-192.

Konopásek J., Košler J., Sláma J. & Janoušek V., 2014. Timing and sources of pre-collisional Neoproterozoic sedimentation along the SW margin of the Congo Craton (Kaoko Belt, NW Namibia). Gondwana Res., vol. 26, no. 1, pp. 386–401. https://doi.org/10.1016/j.gr.2013.06.021.

Konopásek J., Sláma J. & Košler J., 2016. Linking the basement geology along the Africa-South America coasts in the South Atlantic. Precambrian Res., vol. 280, pp. 221–230. https://doi.org/10.1016/j.precamres.2016.05.011.

Konopásek J., Hoffmann K.-H., Sláma J. & Košler J., 2017. The onset of flysch sedimentation in the Kaoko Belt (NW Namibia) – Implications for the pre-collisional evolution of the Kaoko–Dom

Feliciano–Gariep orogen. Precambrian Res., vol. 298, pp. 220–234. http://dx.doi.org/10.1016/j.precamres.2017.06.017.
Konopásek J., Janoušek V., Oyhantçabal P., Sláma J. & Ulrich S., 2018. Did the circum-Rodinia subduction trigger the Neoproterozoic rifting along the Congo–Kalahari Craton margin? Int. J. Earth Sci., vol. 107, no. 5, pp. 1859–1894. https://doi.org/10.1007/s00531-017-1576-4.
Konopásek J., Anczkiewicz R., Jeřábek P., Corfu F. & Žáčková E., 2019. Chronology of the Saxothuringian subduction in the West Sudetes (Bohemian Massif, Czech Republic and Poland). Journal of the Geological Society, vol. 176, no. 3, pp. 492-504. https://doi.org/10.1144/jgs2018-173.
Konopásek J., Cavalcante C., Fossen H. & Janoušek V., 2020. Adamastor – an ocean that never existed? Earth-Sci. Rev., vol. 205, p. 103201. https://doi.org/10.1016/j.earscirev.2020.103201.
Kröner A., 1975. Late Precambrian formations in the western Richtersveld, northern Cape Province. Transactions of the Royal Society of South Africa, vol. 41, no. 4, pp. 375-433. https://doi.org/10.1080/00359197509519451.
Kröner A., 1977. Precambrian mobile belts of southern and eastern Africa — ancient sutures or sites of ensialic mobility? A case for crustal evolution towards plate tectonics, vol. 40, pp. 101-136.
Kröner S., Konopásek J., Kröner A., Passchier C. W., Poller U., Wingate M. T. D. & Hofmann K. H., 2004. U-Pb and Pb-Pb zircon ages for metamorphic rocks in the Kaoko Belt of Northwestern Namibia: A Palaeo- to Mesoproterozoic basement reworked during the Pan-African orogeny. S. Afr. J. Geol., vol. 107, no. 3, pp. 455-476. https://www.doi.org/10.2113/107.3.455.
Lagos M., Scherer E. E., Tomaschek F., Münker C., Keiter M., Berndt J. & Ballhaus C., 2007. High precision Lu–Hf geochronology of Eocene eclogite-facies rocks from Syros, Cyclades, Greece. Chem. Geol., vol. 243, no. 1, pp. 16-35. https://doi.org/10.1016/j.chemgeo.2007.04.008.
Lapen T. J., Johnson C. M., Baumgartner L. P., Mahlen N. J., Beard B. L. & Amato J. M., 2003. Burial rates during prograde metamorphism of an ultra-high-pressure terrane: an example from Lago di Cignana, western Alps, Italy. Earth Planet. Sci. Lett., vol. 215, no. 1, pp. 57–72. https://doi.org/10.1016/S0012-821X(03)00455-2.
Lara P., Oyhantçabal P. & Dadd K., 2017. Post-collisional, Late Neoproterozoic, high-Ba-Sr granitic magmatism from the Dom Feliciano Belt and its cratonic foreland, Uruguay: Petrography, geochemistry, geochronology, and tectonic implications. Lithos, vol. 277, pp. 178-198. https://doi.org/10.1016/j.lithos.2016.11.026.
Lara P., Oyhantçabal P. & Belousova E., 2020. Two distinct crustal sources for Late Neoproterozoic granitic magmatism across the Sierra Ballena Shear Zone, Dom Feliciano Belt, Uruguay: Whole-rock geochemistry, zircon geochronology and Sr-Nd-Hf isotope evidence. Precambrian Res., vol. 341, p. 105625. https://doi.org/10.1016/j.precamres.2020.105625.
Lenz C., 2006. Evolução metamórfica dos metapelitos da antiforme Serra dos Pedrosas: condições e idades do metamorfismo. Instituto de Geociências. Universidade Federal do Rio Grande do Sul.
Lenz C., Fernandes L. A. D., McNaughton N. J., Porcher C. C. & Masquelin H., 2011. U–Pb SHRIMP ages for the Cerro Bori Orthogneisses, Dom Feliciano Belt in Uruguay: Evidences of a ~800Ma magmatic and ~650Ma metamorphic event. Precambrian Res., vol. 185, no. 3, pp. 149–163. https://doi.org/10.1016/j.precamres.2011.01.007.
Lenz C., Porcher C., Fernandes L., Masquelin H., Koester E. & Conceição R., 2013. Geochemistry of the Neoproterozoic (800–767 Ma) Cerro Bori orthogneisses, Dom Feliciano Belt in Uruguay: tectonic evolution of an ancient continental arc. Mineral. Petrol., vol. 107, pp. 785–806. https://doi.org/10.1007/s00710-012-0244-4.
Mallmann G., Chemale Jr F., Ávila J. N., Kawashita K. & Armstrong R. A., 2007. Isotope geochemistry and geochronology of the Nico Pérez Terrane, Rio de la Plata Craton, Uruguay. Gondwana Res., vol. 12, no. 4, pp. 489-508. https://doi.org/10.1016/j.gr.2007.01.002.
Martil M. M. D., 2016. O Magmatismo De Arco Continental Pré-colisional (790 Ma) E a Reconstituição Espaço-temporal Do Regime Transpressivo (650 Ma) No Complexo Várzea Do Capivarita, Sul Da Província Mantiqueira. Universidade Federal do Rio Grande do Sul, Available at: https://www.lume.ufrgs.br/handle/10183/149194.
Martil M. M. D., Bitencourt M. F., Nardi L. V. S., Koester E. & Pimentel M. M., 2017. Pre-collisional, Tonian (ca. 790 Ma) continental arc magmatism in southern Mantiqueira Province, Brazil:

Geochemical and isotopic constraints from the Várzea do Capivarita Complex. Lithos, vol. 274–275, pp. 39–52. https://doi.org/10.1016/j.lithos.2016.11.011.

Martin H. & Porada H., 1977. The intracratonic branch of the Damara Orogen in South West Africa I. Discussion of geodynamic models. Precambrian Res., vol. 5, no. 4, pp. 311-338. https://doi.org/10.1016/0301-9268(77)90039-0.

Masquelin H., Fernandes L., Lenz C., Porcher C. C. & McNaughton N. J., 2011. The Cerro Olivo Complex: A pre-collisional Neoproterozoic magmatic arc in Eastern Uruguay. Int. Geol. Rev., vol. 54, pp. 1161-1183. https://www.doi.org/10.1080/00206814.2011.626597.

Mattinson J. M., 2010. Analysis of the relative decay constants of 235U and 238U by multi-step CA-TIMS measurements of closed-system natural zircon samples. Chem. Geol., vol. 275, no. 3, pp. 186-198. https://doi.org/10.1016/j.chemgeo.2010.05.007.

McCourt S., Armstrong R., Jelsma H. & Mapeo R., 2013. New U-Pb SHRIMP ages from the Lubango region, SW Angola: Insights into the Palaeoproterozoic evolution of the Angolan Shield, southern Congo Craton, Africa. Geol. Soc. Spec. Publ., vol. 170, no. 2, pp. 353–363. https://doi.org/10.1144/jgs2012-059.

Meira V. T., García-Casco A., Juliani C., Almeida R. P. & Schorscher J. H. D., 2015. The role of intracontinental deformation in supercontinent assembly: insights from the Ribeira Belt, Southeastern Brazil (Neoproterozoic West Gondwana). Terra Nova, vol. 27, no. 3, pp. 206-217. https://doi.org/10.1111/ter.12149.

Meira V. T., Garcia-Casco A., Juliani C. & Schorscher J. H. D., 2019a. Late Tonian within-plate mafic magmatism and Ediacaran partial melting and magmatism in the Costeiro Domain, Central Ribeira Belt, Brazil. Precambrian Res., vol. 334, p. 105440. https://doi.org/10.1016/j.precamres.2019.105440.

Meira V. T., Garcia-Casco A., Hyppolito T., Juliani C. & Schorscher J. H. D., 2019b. Tectono-Metamorphic Evolution of the Central Ribeira Belt, Brazil: A Case of Late Neoproterozoic Intracontinental Orogeny and Flow of Partially Molten Deep Crust During the Assembly of West Gondwana. Tectonics, vol. 38, no. 8, pp. 3182–3209. https://doi.org/10.1029/2018tc004959.

Oliveira D. S. d., Sommer C. A., Philipp R. P., Lima E. F. d. & Basei M. Â. S., 2015. Post-collisional subvolcanic rhyolites associated with the Neoproterozoic Pelotas Batholith, southern Brazil. J. S. Am. Earth Sci., vol. 63, pp. 84-100. https://doi.org/10.1016/j.jsames.2015.05.009.

Oriolo S., Oyhantçabal P., Wemmer K., Heidelbach F., Pfänder J., Basei M. A. S., Hueck M., Hannich F., Sperner B. & Siegesmund S., 2016a. Shear zone evolution and timing of deformation in the Neoproterozoic transpressional Dom Feliciano Belt, Uruguay. J. Struct. Geol., vol. 92, pp. 59-78. https://doi.org/10.1016/j.jsg.2016.09.010.

Oriolo S., Oyhantçabal P., Basei M. A. S., Wemmer K. & Siegesmund S., 2016b. The Nico Pérez Terrane (Uruguay): From Archean crustal growth and connections with the Congo Craton to late Neoproterozoic accretion to the Río de la Plata Craton. Precambrian Res., vol. 280, pp. 147–160. https://doi.org/10.1016/j.precamres.2016.04.014.

Oriolo S., Oyhantçabal P., Wemmer K., Basei M. A. S., Benowitz J., Pfänder J., Hannich F. & Siegesmund S., 2016c. Timing of deformation in the Sarandí del Yí Shear Zone, Uruguay: Implications for the amalgamation of western Gondwana during the Neoproterozoic Brasiliano-Pan-African Orogeny. Tectonics, vol. 35, no. 3, pp. 754–771. https://doi.org/10.1002/2015tc004052.

Oriolo S., Oyhantçabal P., Konopásek J., Basei M. A. S., Frei R., Sláma J., Wemmer K. & Siegesmund S., 2019. Late Paleoproterozoic and Mesoproterozoic magmatism of the Nico Pérez Terrane (Uruguay): Tightening up correlations in southwestern Gondwana. Precambrian Res., vol. 327, pp. 296-313. https://doi.org/10.1016/j.precamres.2019.04.012.

Oyhantçabal P., Siegesmund S., Wemmer K., Frei R. & Layer P., 2007. Post-collisional transition from calc-alkaline to alkaline magmatism during transcurrent deformation in the southernmost Dom Feliciano Belt (Braziliano–Pan-African, Uruguay). Lithos, vol. 98, no. 1–4, p. 141─159. https://doi.org/10.1016/j.lithos.2007.03.001.

Oyhantçabal P., Siegesmund S., Wemmer K., Presnyakov S. & Layer P., 2009. Geochronological constraints on the evolution of the southern Dom Feliciano Belt (Uruguay). Journal of the

Geological Society, vol. 166, no. 6, p. 1075–1084. https://doi.org/10.1144/0016-76492008-122.
Oyhantçabal P., Siegesmund S. & Wemmer K., 2011a. The Río de la Plata Craton: a review of units, boundaries, ages and isotopic signature. Int. J. Earth Sci., vol. 100, no. 2, p. 201–220. https://doi.org/10.1007/s00531-010-0580-8.
Oyhantçabal P., Siegesmund S., Wemmer K. & Passchier C. W., 2011b. The transpressional connection between Dom Feliciano and Kaoko Belts at 580–550 Ma. Int. J. Earth Sci., vol. 100, p. 379–390. https://doi.org/10.1007/s00531-010-0577-3.
Oyhantçabal P., Wagner-Eimer M., Wemmer K., Schulz B., Frei R. & Siegesmund S., 2012. Paleo- and Neoproterozoic magmatic and tectonometamorphic evolution of the Isla Cristalina de Rivera (Nico Pérez Terrane, Uruguay). Int. J. Earth Sci., vol. 101, no. 7, pp. 1745-1762. https://doi.org/10.1007/s00531-012-0757-4.
Oyhantçabal P., Oriolo S., Philipp R. P., Wemmer K. & Siegesmund S., 2018. The Nico Pérez Terrane of Uruguay and Southeastern Brazil. In Siegesmund S., et al. eds. Geology of Southwest Gondwana. pp. 161-188. Cham: Springer International Publishing https://doi.org/10.1007/978-3-319-68920-3_7.
Oyhantçabal P., Oriolo S., Wemmer K., Basei M. A. S., Frei D. & Siegesmund S., 2021. Provenance of metasedimentary rocks of the western Dom Feliciano Belt in Uruguay: Insights from U–Pb detrital zircon geochronology, Hf and Nd model ages, and geochemical data. J. S. Am. Earth Sci., vol. 108, p. 103139. https://doi.org/10.1016/j.jsames.2020.103139.
Passarelli C. R., Basei M. A. S., Siga O., Reath I. M. & Campos Neto M. d. C., 2010. Deformation and geochronology of syntectonic granitoids emplaced in the Major Gercino Shear Zone, southeastern South America. Gondwana Res., vol. 17, no. 4, p. 688–703. https://doi.org/10.1016/j.gr.2009.09.013.
Passarelli C. R., Basei M. A. S., Siga O. & Harara O. M. M., 2018. The Luis Alves and Curitiba Terranes: Continental Fragments in the Adamastor Ocean. In Siegesmund S., et al. eds. Geology of Southwest Gondwana. pp. 189-215. Cham: Springer International Publishing https://www.doi.org/10.1007/978-3-319-68920-3_8.
Passarelli C. R., Verma S. K., McReath I., Basei M. A. S. & Siga O., 2019. Tracing the history from Rodinia break-up to the Gondwana amalgamation in the Embu Terrane, southern Ribeira Belt, Brazil. Lithos, vol. 342-343, pp. 1-17. https://doi.org/10.1016/j.lithos.2019.05.024.
Passchier C. W., Trouw R. A. J., Ribeiro A. & Paciullo F. V. P., 2002. Tectonic evolution of the southern Kaoko belt, Namibia. J. Afr. Earth Sci., vol. 35, no. 1, pp. 61-75. https://doi.org/10.1016/S0899-5362(02)00030-1.
Pecoits E., Aubet N. R., Heaman L. M., Philippot P., Rosière C. A., Veroslavsky G. & Konhauser K. O., 2016. UPb detrital zircon ages from some Neoproterozoic successions of Uruguay: Provenance, stratigraphy and tectonic evolution. J. S. Am. Earth Sci., vol. 71, pp. 108-130. https://doi.org/10.1016/j.jsames.2016.07.003.
Pedrosa-Soares A. C., Noce C. M., Wiedemann C. M. & Pinto C. P., 2001. The Araçuaí-West-Congo Orogen in Brazil: an overview of a confined orogen formed during Gondwanaland assembly. Precambrian Res., vol. 110, no. 1, p. 307–323. https://doi.org/10.1016/S0301-9268(01)00174-7.
Pedrosa-Soares A. C., De Campos C. P., Noce C., Silva L. C., Novo T., Roncato J., Medeiros S., Castañeda C., Queiroga G., Dantas E., Dussin I. & Alkmim F., 2011. Late Neoproterozoic-Cambrian granitic magmatism in the Araçuaí orogen (Brazil), the Eastern Brazilian Pegmatite Province and related mineral resources. Geological Society, London, Special Publications, vol. 350, no. 1, p. 25. https://doi.org/10.1144/SP350.3.
Pedrosa-Soares A. n. C., Vidal P., Leonardos O. H. & de Brito Neves B. B., 1998. Neoproterozoic oceanic remnants in eastern Brazil: Further evidence and refutation of an exclusively ensialic evolution for the Araçuaí–West Congo orogen. Geology, vol. 26, no. 6, pp. 519-522. https://doi.org/10.1130/0091-7613(1998)026<0519:Norieb>2.3.Co;2.
Pertille J., Hartmann L. A., Philipp R. P., Petry T. S. & de Carvalho Lana C., 2015a. Origin of the Ediacaran Porongos Group, Dom Feliciano Belt, southern Brazilian Shield, with emphasis on whole rock and detrital zircon geochemistry and U–Pb, Lu–Hf isotopes. J. S. Am. Earth Sci., vol. 64, pp. 69-93. https://www.doi.org/10.1016/j.jsames.2015.09.001.

Pertille J., Hartmann L. A. & Philipp R. P., 2015b. Zircon U–Pb age constraints on the Paleoproterozoic sedimentary basement of the Ediacaran Porongos Group, Sul-Riograndense Shield, southern Brazil. J. S. Am. Earth Sci., vol. 63, pp. 334-345. https://doi.org/10.1016/j.jsames.2015.08.005.

Pertille J., Hartmann L. A., Santos J. O. S., McNaughton N. J. & Armstrong R., 2017. Reconstructing the Cryogenian–Ediacaran evolution of the Porongos fold and thrust belt, Southern Brasiliano Orogen, based on Zircon U–Pb–Hf–O isotopes. Int. Geol. Rev., vol. 59, no. 12, p. 1532─1560. https://doi.org/10.1080/00206814.2017.1285257.

Philipp R. P., Mallmann G., Bitencourt M. F., Souza E. R., Liz J. D., Wild F., Arendt S., Oliveira A. S., Duarte L. C., Rivera C. B. & Prado M., 2004. Caracterização Litológica e Evolução Metamórfica da Porção Leste do Complexo Metamórfico Brusque, Santa Catarina. Revista Brasileira de Geociências, vol. 34, p. 21─34. https://doi.org/10.25249/0375-7536.20043412134.

Philipp R. P. & Machado R., 2005. The Late Neoproterozoic granitoid magmatism of the Pelotas Batholith, southern Brazil. J. S. Am. Earth Sci., vol. 19, no. 4, p. 461─478. https://doi.org/10.1016/j.jsames.2005.06.010.

Philipp R. P., Bom F. M., Pimentel M. M., Junges S. L. & Zvirtes G., 2016. SHRIMP U-Pb age and high temperature conditions of the collisional metamorphism in the Várzea do Capivarita Complex: Implications for the origin of Pelotas Batholith, Dom Feliciano Belt, southern Brazil. J. S. Am. Earth Sci., vol. 66, pp. 196-207. https://doi.org/10.1016/j.jsames.2015.11.008.

Philipp R. P., Pimentel M. M. & Basei M. A. S., 2018. The Tectonic Evolution of the São Gabriel Terrane, Dom Feliciano Belt, Southern Brazil: The Closure of the Charrua Ocean. In Siegesmund S., et al. eds. Geology of Southwest Gondwana. pp. 243─265. Cham: Springer International Publishing https://doi.org/10.1007/978-3-319-68920-3_10.

Pollington A. D. & Baxter E. F., 2010. High resolution Sm–Nd garnet geochronology reveals the uneven pace of tectonometamorphic processes. Earth Planet. Sci. Lett., vol. 293, no. 1, p. 63─71. https://doi.org/10.1016/j.epsl.2010.02.019.

Pollington A. D. & Baxter E. F., 2011. High precision microsampling and preparation of zoned garnet porphyroblasts for Sm–Nd geochronology. Chem. Geol., vol. 281, no. 3, pp. 270-282. https://doi.org/10.1016/j.chemgeo.2010.12.014.

Porada H., 1979. The Damara-Ribeira orogen of the Pan-African─Brasiliano cycle in Namibia (Southwest Africa) and Brazil as interpreted in terms of continental collision. Tectonophysics, vol. 57, no. 2, p. 237─265. https://doi.org/10.1016/0040-1951(79)90150-1.

Porada H., 1989. Pan-African rifting and orogenesis in southern to equatorial Africa and eastern Brazil. Precambrian Res., vol. 44, no. 2, p. 103─136. https://doi.org/10.1016/0301-9268(89)90078-8.

Preciozzi F., Masquelin H. & Basei M., 1999. The namaqua/grenville terrane of eastern Uruguay: 2nd South American symposium on isotope geology. Argentina, pp. 338-340.

Raimondo T., Hand M. & Collins W. J., 2014. Compressional intracontinental orogens: Ancient and modern perspectives. Earth-Sci. Rev., vol. 130, p. 128─153. https://doi.org/10.1016/j.earscirev.2013.11.009.

Rapalini A. E., Tohver E., Bettucci L. S., Lossada A. C., Barcelona H. & Pérez C., 2015. The late Neoproterozoic Sierra de las Ánimas Magmatic Complex and Playa Hermosa Formation, southern Uruguay, revisited: Paleogeographic implications of new paleomagnetic and precise geochronologic data. Precambrian Res., vol. 259, pp. 143-155. https://doi.org/10.1016/j.precamres.2014.11.021.

Remus M. V. D., McNaughton N. J., Hartmann L. A., Koppe J. C., Fletcher I. R., Groves D. I. & Pinto V. M., 1999. Gold in the Neoproterozoic juvenile Bossoroca Volcanic Arc of southernmost Brazil: isotopic constraints on timing and sources. J. S. Am. Earth Sci., vol. 12, no. 4, pp. 349-366. https://doi.org/10.1016/S0895-9811(99)00026-7.

Remus M. V. D., Hartmann L. A., McNaughton N. J., Groves D. I. & Reischl J. L., 2000a. Distal Magmatic-Hydrothermal Origin for the Camaquã Cu (Au-Ag) and Santa Maria Pb, Zn (Cu-Ag) Deposits, Southern Brazil. Gondwana Res., vol. 3, no. 2, pp. 155-174. https://doi.org/10.1016/S1342-937X(05)70094-0.

Remus M. V. D., Hartmann L. A., McNaughton N. J., Groves D. I. & Fletcher I. R., 2000b. The link between hydrothermal epigenetic copper mineralization and the Caçapava Granite of the

Brasiliano Cycle in southern Brazil. J. S. Am. Earth Sci., vol. 13, no. 3, pp. 191-216. https://doi.org/10.1016/S0895-9811(00)00017-1.
Rossini C. A. & Legrand J. M., 2003. Tecto-metamorphic events in the Carapé group: a model for its Neoproterozoic evolution. Revista de la Sociedad Uruguaya de Geología, vol. 1, p. 49–67.
Rubatto D., Hermann J. & Buick I. S., 2006. Temperature and Bulk Composition Control on the Growth of Monazite and Zircon During Low-pressure Anatexis (Mount Stafford, Central Australia). J. Petrol., vol. 47, no. 10, p. 1973–1996. https://doi.org/10.1093/petrology/egl033.
Saalmann K., Remus M. V. D. & Hartmann L. A., 2006. Structural evolution and tectonic setting of the Porongos belt, southern Brazil. Geological Magazine, vol. 143, no. 1, p. 59–88. https://doi.org/10.1017/S0016756805001433.
Saalmann K., Gerdes A., Lahaye Y., Hartmann L., Remus M. & Läufer A., 2011. Multiple accretion at the eastern margin of the Rio de la Plata craton: the prolonged Brasiliano orogeny in southernmost Brazil. Int. J. Earth Sci., vol. 100, p. 355–378. https://doi.org/10.1007/s00531-010-0564-8.
Sánchez Bettucci L., Cosarinsky M. & Ramos V. A., 2001. Tectonic Setting of the Late Proterozoic Lavalleja Group (Dom Feliciano Belt), Uruguay. Gondwana Res., vol. 4, no. 3, pp. 395-407. https://doi.org/10.1016/S1342-937X(05)70339-7.
Schaen A. J., Jicha B. R., Hodges K. V., Vermeesch P., Stelten M. E., Mercer C. M., Phillips D., Rivera T. A., Jourdan F., Matchan E. L., Hemming S. R., Morgan L. E., Kelley S. P., Cassata W. S., Heizler M. T., Vasconcelos P. M., Benowitz J. A., Koppers A. A. P., Mark D. F., Niespolo E. M., Sprain C. J., Hames W. E., Kuiper K. F., Turrin B. D., Renne P. R., Ross J., Nomade S., Guillou H., Webb L. E., Cohen B. A., Calvert A. T., Joyce N., Ganerød M., Wijbrans J., Ishizuka O., He H., Ramirez A., Pfänder J. A., Lopez-Martínez M., Qiu H. & Singer B. S., 2020. Interpreting and reporting 40Ar/39Ar geochronologic data. Geological Society of America Bulletin, vol. 133, no. 3–4, pp. 461–487. https://doi.org/10.1130/B35560.1.
Scherer E. E., Cameron K. L. & Blichert-Toft J., 2000. Lu–Hf garnet geochronology: closure temperature relative to the Sm–Nd system and the effects of trace mineral inclusions. Geochimica et Cosmochimica Acta, vol. 64, no. 19, pp. 3413–3432. https://doi.org/10.1016/S0016-7037(00)00440-3.
Seth B., Kröner A., Mezger K., Nemchin A. A., Pidgeon R. T. & Okrusch M., 1998. Archaean to Neoproterozoic magmatic events in the Kaoko belt of NW Namibia and their geodynamic significance. Precambrian Res., vol. 92, no. 4, pp. 341-363. https://doi.org/10.1016/S0301-9268(98)00086-2.
Silva Lara H., Siegesmund S., Wemmer K., Hueck M., Basei M. A. S. & Oyhantçabal P., 2021. The Sierra de Aguirre Formation, Uruguay: Post-collisional Ediacaran volcanism in the southernmost Dom Feliciano Belt. J. S. Am. Earth Sci., vol. 107, p. 103118. https://doi.org/10.1016/j.jsames.2020.103118.
Silva L. C., Hartmann L. A., McNaughton N. J. & Fletcher I. R., 1999. SHRIMP U/Pb Zircon Dating of Neoproterozoic Granitic Magmatism and Collision in the Pelotas Batholith, Southernmost Brazil. Int. Geol. Rev., vol. 41, no. 6, pp. 531-551. https://doi.org/10.1080/00206819909465156.
Silva L. C., Armstrong R., Pimentel M. M., Scandolara J., Ramgrab G., Wildner W., Angelim L. A. d. A., Vasconcelos A. M., Rizzoto G., Quadros M. L. d. E. S., Sander A. & de Rosa A. L. Z., 2002. Reavaliacao da evolucao geologica em terrenos pre-cambrianos brasileiros com base em novos dados U/Pb SHRIMP Parte III, Provincias Borborema, Mantiqueira meridional e Rio Negro-Juruena. Revista Brasileira de Geociencias, vol. 32, no. 4, pp. 529-544. https://doi.org/10.25249/0375-7536.2002324529544.
Silva L. C., McNaughton N. J., Hartmann L. & Fletcher I. R., 2003. Contrasting Zircon Growth Patterns in Neoproterozoic Granites of Southern Brazil Revealed by Shrimp U-Pb Analyses and SEM Imaging: Consequences for the Discrimination of Emplacement and Inheritance Ages. Short Papers - IV South American Symposium on Isotope Geology. pp. 689-690.
Silva L. C., McNaughton N. J., Armstrong R., Hartmann L. A. & Fletcher I. R., 2005a. The neoproterozoic Mantiqueira Province and its African connections: a zircon-based U–Pb geochronologic subdivision for the Brasiliano/Pan-African systems of orogens. Precambrian Res., vol. 136, no. 3, pp. 203-240. https://doi.org/10.1016/j.precamres.2004.10.004.

Silva L. C., McNaughton N. J. & Fletcher I. R., 2005b. SHRIMP U–Pb zircon geochronology of Neoproterozoic crustal granitoids (Southern Brazil): A case for discrimination of emplacement and inherited ages. Lithos, vol. 82, no. 3–4, pp. 503–525. https://doi.org/10.1016/j.lithos.2004.09.029.

Siviero R. S., Bruguier O., D'ávila Fernandes L. A., Koester E., Porcher C. C. & Kraemer G., 2021. Age and geochemistry of Cambaí Complex, São Gabriel Terrane, Brazil: Arc-related TTG-like rocks. J. S. Am. Earth Sci., vol. 108, p. 103165. https://doi.org/10.1016/j.jsames.2021.103165.

Soldner J., Oliot E., Schulmann K., Štípská P., Kusbach V. & Anczkiewicz R., 2017. Metamorphic P–T–t–d evolution of (U)HP metabasites from the South Tianshan accretionary complex (NW China) — Implications for rock deformation during exhumation in a subduction channel. Gondwana Res., vol. 47, pp. 161-187. https://doi.org/10.1016/j.gr.2016.07.007.

Soldner J., Štípská P., Schulmann K., Yuan C., Anczkiewicz R., Sala D., Jiang Y., Zhang Y. & Wang X., 2020. Coupling of P–T–t–D histories of eclogite and metagreywacke—Insights to late Ordovician–Silurian crustal folding events recorded in the Beishan Orogen (NW China). Journal of Metamorphic Geology, vol. 38, no. 6, pp. 555-591. https://doi.org/10.1111/jmg.12531.

Stüwe K. & Powell R., 1995. PT Paths from modal proportions: application to the Koralm Complex, Eastern Alps. Contributions to Mineralogy and Petrology, vol. 119, no. 1, pp. 83-93. https://doi.org/10.1007/BF00310719.

Tack L., Wingate M. T. D., Liégeois J. P., Fernandez-Alonso M. & Deblond A., 2001. Early Neoproterozoic magmatism (1000–910 Ma) of the Zadinian and Mayumbian Groups (Bas-Congo): onset of Rodinia rifting at the western edge of the Congo craton. Precambrian Res., vol. 110, no. 1, pp. 277-306. https://doi.org/10.1016/S0301-9268(01)00192-9.

Tedeschi M., Novo T., Pedrosa-Soares A., Dussin I., Tassinari C., Silva L. C., Gonçalves L., Alkmim F., Lana C., Figueiredo C., Dantas E., Medeiros S., De Campos C., Corrales F. & Heilbron M., 2016. The Ediacaran Rio Doce magmatic arc revisited (Araçuaí-Ribeira orogenic system, SE Brazil). J. S. Am. Earth Sci., vol. 68, pp. 167–186. https://doi.org/10.1016/j.jsames.2015.11.011.

Thomas R. J., Macey P. H., Spencer C., Dhansay T., Diener J. F. A., Lambert C. W., Frei D. & Nguno A., 2016. The Sperrgebiet Domain, Aurus Mountains, SW Namibia: A ~2020–850Ma window within the Pan-African Gariep Orogen. Precambrian Res., vol. 286, pp. 35-58. https://doi.org/10.1016/j.precamres.2016.09.023.

Thöni M., 2002. Sm–Nd isotope systematics in garnet from different lithologies (Eastern Alps): age results, and an evaluation of potential problems for garnet Sm–Nd chronometry. Chem. Geol., vol. 185, no. 3, pp. 255-281. https://doi.org/10.1016/S0009-2541(01)00410-7.

Trompette R., 1994. Geology of Western Gondwana (2000 - 500 Ma): Pan-African-Brasiliano Aggregation of South America and Africa (translated by A. V. Carozzi, Univ. of Illinois, USA). Milton: Taylor & Francis Group, Milton.

Trompette R., 1997. Neoproterozoic (~600 Ma) aggregation of Western Gondwana: a tentative scenario. Precambrian Res., vol. 82, no. 1, pp. 101-112. https://doi.org/10.1016/S0301-9268(96)00045-9.

Vlach S., Basei M. & Castro N. A., 2009. Idade U-Th-Pb de monazita por microssonda eletrônica do Granito Nova Trento, Grupo Brusque, SC. Simpósio 45 anos de Geocronologia no Brasil, Boletim de Resumos Expandidos. São Paulo, Brasil, pp. 325-327.

Völz W. M., Koester E., Pinto V. M., Debruyne D., Cardozo E., Vieira D. T., Dal Olmo-Barbosa L. & Bastos V. A., 2020. Geochemistry and U–Pb (SHRIMP) geochronology of Grupelli Granite: New constraints on the cessation of felsic magmatism in the Pelotas Batholith, Dom Feliciano Belt. J. S. Am. Earth Sci., vol. 103, p. 102746. https://doi.org/10.1016/j.jsames.2020.102746.

Walczak K., Anczkiewicz R., Szczepański J., Rubatto D. & Košler J., 2017. Combined garnet and zircon geochronology of the ultra-high temperature metamorphism: Constraints on the rise of the Orlica-Śnieżnik Dome, NE Bohemian Massif, SW Poland. Lithos, vol. 292-293, pp. 388-400. https://doi.org/10.1016/j.lithos.2017.09.013.

Warren C. J., Greenwood L. V., Argles T. W., Roberts N. M. W., Parrish R. R. & Harris N. B. W., 2018. Garnet-monazite rare earth element relationships in sub-solidus Metapelites: A case study from Bhutan. Geol. Soc. Spec. Publ., vol. 478, no. 1, pp. 145–166. https://doi.org/10.1144/SP478.1.

White R. W., Powell R., Holland T. J. B., Johnson T. E. & Green E. C. R., 2014. New mineral activity–composition relations for thermodynamic calculations in metapelitic systems. Journal of Metamorphic Geology, vol. 32, no. 3, pp. 261–286. https://doi.org/10.1111/jmg.12071.

Will T. M., Gaucher C., Ling X. X., Li X. H., Li Q. L. & Frimmel H. E., 2019. Neoproterozoic magmatic and metamorphic events in the Cuchilla Dionisio Terrane, Uruguay, and possible correlations across the South Atlantic. Precambrian Res., vol. 320, pp. 303–322. https://doi.org/10.1016/j.precamres.2018.11.004.

SECTION II Research papers

Paper I

Precambrian Research 354 (2021) 106060

Contents lists available at ScienceDirect

Precambrian Research

journal homepage: www.elsevier.com/locate/precamres

Pre-orogenic connection of the foreland domains of the Kaoko–Dom Feliciano–Gariep orogenic system

Jack James Percival [a,*], Jiří Konopásek [a,b], Ragnhild Eiesland [a], Jiří Sláma [c], Roberto Sacks de Campos [d], Matheus Ariel Battisti [e], Maria de Fátima Bitencourt [e]

[a] Department of Geosciences, UiT–The Arctic University of Norway, Dramsveien 201, 9037 Tromsø, Norway
[b] Czech Geological Survey, Klárov 3, 118 21 Prague 1, Czech Republic
[c] Institute of Geology of the Czech Academy of Sciences, Rozvojová 269, 165 00 Prague 6, Czech Republic
[d] Programa de Pós-graduação em Geologia (PPGGeologia), Universidade Federal de Santa Catarina (UFSC), Florianópolis, SC, Brazil
[e] Programa de Pós-graduação em Geociências, Instituto de Geociências, Universidade Federal do Rio Grande do Sul, Porto Alegre, Brazil

ARTICLE INFO

Keywords:
Gondwana
Rodinia
Dom Feliciano Belt
Kaoko Belt
Neoproterozoic
Rifting

ABSTRACT

Neoproterozoic metasedimentary rocks in the foreland domains of the Kaoko–Dom Feliciano–Gariep orogenic system record sedimentation from the breakup of Rodinia to the amalgamation of Gondwana, and thus provide ideal subjects for investigation of the mutual pre-orogenic positions of rifted margins of the African and South American cratonic blocks. U–Pb isotopic dating of zircon in the Brusque Complex of the northern Dom Feliciano Belt, Brazil, provides new constraints on the timing and sources of Neoproterozoic sedimentation along the eastern margin of the Luis Alves Craton. The minimum age of sedimentation is constrained by a U–Pb zircon age of 811 ± 6 Ma from a dyke cross-cutting the Brusque Complex. U–Pb detrital zircon analysis reveals two distinct groups: one with ages ca. 2.2–2.0 Ga consistent with erosion of the adjacent Luis Alves Craton, and another with ages ca. 2.1–1.8 and 1.6–1.0 Ga consistent with erosion of Paleoproterozoic to Mesoproterozoic igneous provinces and/or supracrustal sequences at the edge of the Congo Craton. The age distributions match with analogous rocks of the central Dom Feliciano Belt and the Kaoko Belt, and show similarities with the Gariep Belt, suggesting deposition in a system of coeval and spatially related paleobasins around the time of Rodinia breakup. The absence of Neoproterozoic detrital zircon close to the age of sedimentation suggests deposition in an intracontinental rift or passive margin. A third group contains a significant proportion of Neoproterozoic ca. 670–560 Ma zircon, suggesting similarities with the adjacent Itajaí Basin syn-orogenic foreland sedimentary rocks. This indicates that foreland basin sediments were partly tectonically interleaved with the pre-orogenic metasediments of the Brusque Complex during late-stage orogenic deformation. The findings support an intracontinental rifting model for the formation of the Kaoko–Dom Feliciano–Gariep basin system. The data further indicate that the Luis Alves Craton was in close proximity to the Congo Craton, and likely with the Nico Pérez Terrane and the Kalahari Craton, at the onset of Tonian rifting and the breakup of Rodinia.

1. Introduction

The period between the breakup of Rodinia and the amalgamation of Gondwana during the Neoproterozoic (ca. 800 to 500 Ma) is interpreted to involve the reconfiguration of many of Earth's major cratonic blocks (Johansson, 2014; Li et al., 2008; Merdith et al., 2017a, 2017b). Paleogeographic reconstructions at the time of Rodinia breakup vary significantly in the placement of continental blocks that now belong to the African and South American continents. Some models place the African and South American cratons as close neighbours (Johansson, 2014; Li et al., 2008, 2013), and in other models they are far apart with a large oceanic domain between them (Evans, 2009; Gray et al., 2008; Merdith et al., 2017a). The latter models contrast with tectonic reconstructions of the orogenic belts exposed today along the South Atlantic coastlines, in which authors assume that there was no major reconfiguration of continental blocks and instead suggest that pairs of previously rifted continental margins came back together during their convergent evolution (Basei et al., 2018; Frimmel et al., 2011;

* Corresponding author at: Department of Geosciences, UiT – The Arctic University of Norway, Dramsveien 201, 9037 Tromsø, Norway.
E-mail address: jack.j.percival@uit.no (J.J. Percival).

https://doi.org/10.1016/j.precamres.2020.106060
Received 18 August 2020; Received in revised form 7 December 2020; Accepted 7 December 2020
Available online 30 December 2020

Konopásek et al., 2018, 2020; Oriolo et al., 2016; Porada, 1989).

The breakup of Rodinia and the transition into what would become Western Gondwana began with extensive early-Neoproterozoic rifting at ca. 840–800 Ma (Basei et al., 2008b; Frimmel et al., 2001, 2011; Hueck et al., 2018a; Konopásek et al., 2014, 2018; Porada, 1989), which developed by way of convergence into orogenesis active between ca. 650–550 Ma (Hueck et al., 2018b; Konopásek et al., 2008; Lenz et al., 2011; Oyhantçabal et al., 2009), leaving behind a ca. 3000 km long orogen recently named the South Atlantic Neoproterozoic Orogenic System (SANOS) (Konopásek et al., 2020). The southern part of this system (Fig. 1) is an orogenic triple junction comprised of multiple orogenic belts: the Kaoko, Dom Feliciano and Gariep belts forming a North–South oriented belt continuous with the rest of the SANOS, and the Damara Belt forming an offshoot junction on the African side of the orogen. In the Kaoko–Dom Feliciano–Gariep part of this system, orogenesis was the result of convergence between the Congo and Kalahari cratons on the African side, and the Rio de la Plata craton and other smaller crustal blocks such as the Luis Alves Craton and Nico Pérez and Curitiba terranes on the South American side (Basei et al., 2000, 2009; Frimmel et al., 2011; Frimmel, 2018; Goscombe et al., 2003b; Hueck et al., 2018b; Oriolo et al., 2016). The pre-convergent evolution of this orogenic system is an extensively discussed topic, as it provides context in linking through time the breakup of Rodinia and the amalgamation of Western Gondwana. Central to these discussions is whether early-Neoproterozoic rifting culminated in breakup of the crust and the development of a large ocean known as the Adamastor Ocean (see Fig. 2 in Konopásek et al., 2020; and references therein), and thus the exact pre-orogenic connections between the African and South American parts of the Kaoko–Dom Feliciano–Gariep orogen remains an important line of research (e.g. Basei et al., 2005, 2011c; Oyhantçabal et al., 2018). Recent works have correlated the convergent history of rocks of the orogenic hinterland across both the Kaoko and Dom Feliciano Belts (Gross et al., 2009; Konopásek et al., 2016; Oyhantçabal et al., 2009, 2011a); however, connecting the pre-convergence histories of the two belts so far remains problematic.

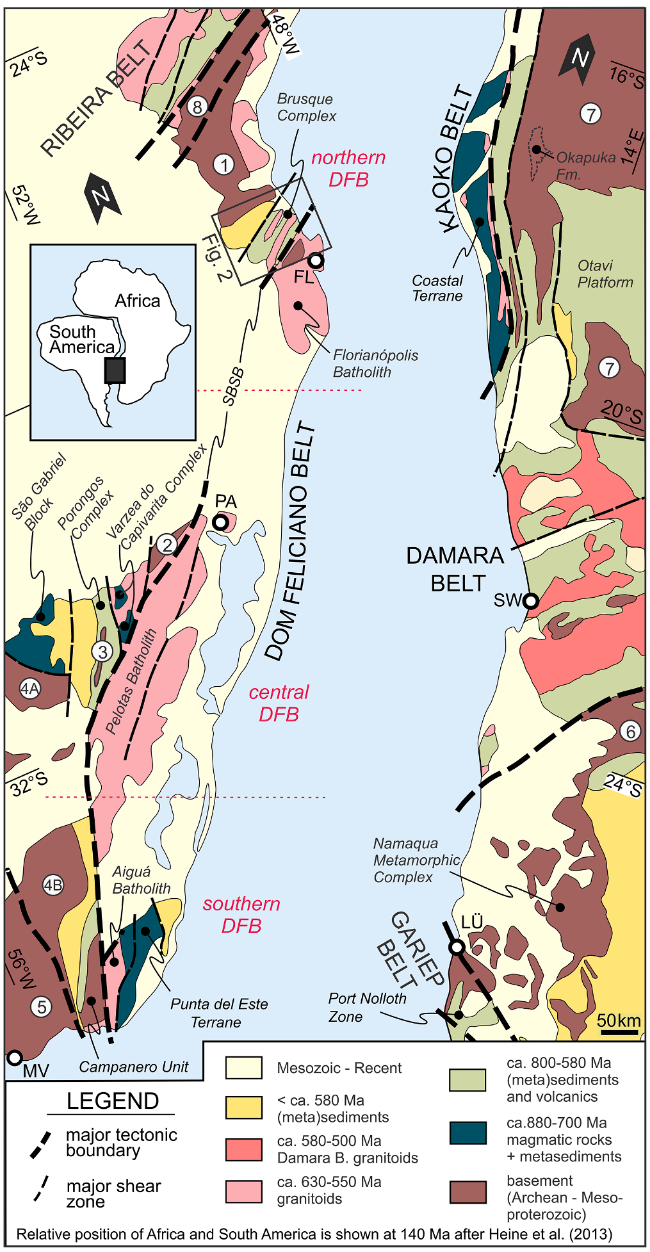

Fig. 1. Overview geological sketch of the Kaoko–Dom Feliciano–Gariep orogenic system (modified after Konopásek et al., 2017). 1—Luis Alves Craton, 2—Arroio dos Ratos Complex, 3—Encantadas Complex, 4A—Nico Pérez Terrane (Taquarembó Block), 4B—Nico Pérez Terrane, 5—Rio de la Plata Craton, 6—Kalahari Craton, 7—Congo Craton, 8—Curitiba Terrane. SBSB—Southern Brazilian Shear Belt, FL—Florianópolis, PA—Porto Alegre, MV—Montevideo, LÜ—Lüderitz, SW—Swakopmund.

Some of the most promising targets for investigation of the early history of the orogen are the supracrustal schist belts that run the length of the orogen, and that outcrop on both sides of the Atlantic Ocean. These units are interpreted as rifting-related basin deposits (Basei et al., 2008b; Campos et al., 2011; Frimmel and Fölling, 2004; Frimmel, 2018; Konopásek et al., 2014; Saalmann et al., 2006) that were later deformed and metamorphosed in the foreland positions of the orogen (Basei et al., 2011b; Frimmel et al., 2011; Frimmel, 2018; Goscombe et al., 2003b; Saalmann et al., 2006). As such, they should contain a record of the pre-convergence history from rifting to the onset of orogenesis.

The aim of this work is to discuss the mutual pre-orogenic positions of rifted margins of the Congo and Luis Alves cratons by studying the depositional history and potential source regions of the supracrustal rocks of the northern Dom Feliciano Belt using U–Pb detrital zircon geochronology. If the African and South American cratons represented one coherent crustal block at the beginning of rifting, the provenance record of metamorphosed rifting-related sediments on top of them should correlate. Studies with large datasets have been published investigating the timing of sedimentation and potential sources for these supracrustal rocks in the African counterpart of the belt (the Kaoko and Gariep orogenic belts) (Andersen et al., 2018a; Hofmann et al., 2014; Konopásek et al., 2014, 2017). Similarly, the central parts of the Dom Feliciano Belt are well studied (Gruber et al., 2011, 2016; Höfig et al., 2018; Pertille et al., 2015a, 2015b, 2017) (for a current review of the relevant provenance record in Western Gondwana, see Zimmermann, 2018). However, there is little data for the northern part of the belt (Basei et al., 2008a; Hartmann et al., 2003), which represents the direct counterpart to the Kaoko Belt in a pre-Atlantic setting (Fig. 1). We present a robust dataset of detrital zircon ages from metamorphosed clastic sedimentary and igneous rocks of the northern Dom Feliciano foreland that enables comparison and possible correlation of syn-rifting evolution with the Kaoko Belt in Africa, as well as with the central and southern Dom Feliciano Belt.

2. Geological setting

2.1. The Kaoko–Dom Feliciano–Gariep orogenic system

The Kaoko, Dom Feliciano and Gariep belts (Fig. 1) are three geographically separate orogenic belts that, prior to the opening of the Atlantic Ocean, represented a continuous orogenic system formed during the Neoproterozoic Brasiliano/Pan African orogenic cycle (Porada, 1989). The system crops out along the South Atlantic coastlines of South

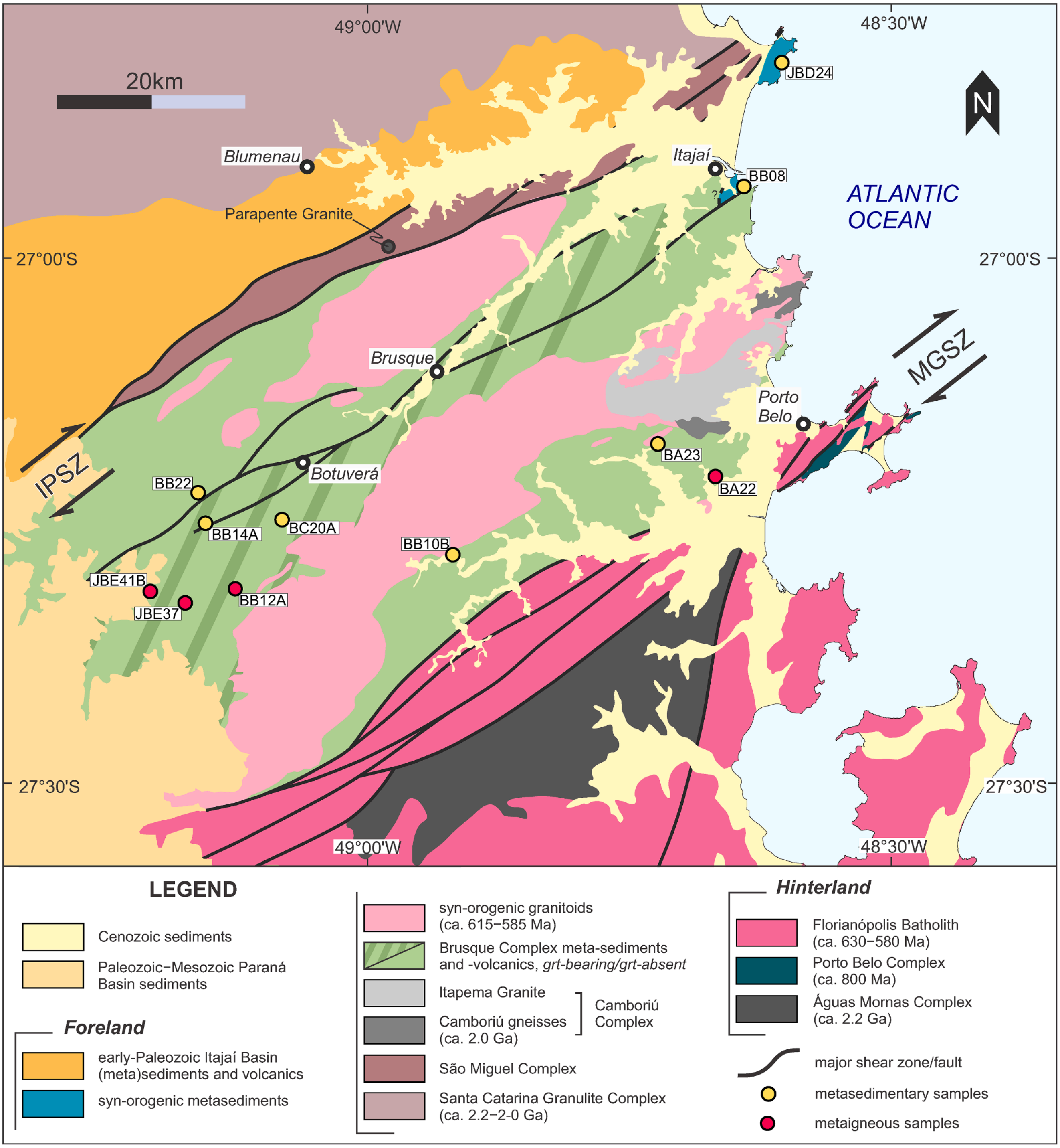

Fig. 2. Geological map of the northern Dom Feliciano Belt foreland. MGSZ = Major Gercino Shear Zone, IPSZ = Itajaí–Perimbó Shear Zone. Modified after Basei et al. (2006); Campos et al. (2011); De Toni et al. (2020a); Florisbal et al. (2012b); Hueck et al. (2018b). See text for geochronological references.

America and Africa, and forms the southern part of the larger South Atlantic Neoproterozoic Orogenic System (*sensu* Konopásek et al., 2020). The Kaoko–Dom Feliciano–Gariep orogenic system is structurally symmetric, with an eastern and western foreland domain lying either side of an internal orogenic hinterland (Fig. 1). Both foreland domains contain fold-and-thrust belts incorporating early- to middle-Neoproterozoic rift-related volcano-sedimentary rocks and associated basement, overlain by syn-orogenic flysch and molasse deposits (Frimmel, 2018; Goscombe et al., 2003b; Hueck et al., 2018b).

The basement of the eastern foreland consists of the Archean–Paleoproterozoic Congo and Kalahari cratons, and associated Mesoproterozoic crust exposed along the cratons' western edges (Kröner and Rojas-Agramonte, 2017; Kröner et al., 2004; Macey et al., 2018; Seth et al., 1998) (Fig. 1). In the Kaoko Belt, the eastern-most part of the foreland consists of autochthonous early- to middle-Neoproterozoic sedimentary successions lying directly on the Congo Craton basement, named the Otavi Carbonate Platform (Hoffman and Halverson, 2008). The low-grade Otavi Carbonate Platform is overridden by an imbricated fold-and-thrust belt, the Central Kaoko Zone, which consists of deformed and metamorphosed early- to middle-Neoproterozoic sedimentary successions interlayered with slices of the basement, and overlain by late-Neoproterozoic syn-orogenic sedimentary rocks (Konopásek et al., 2014, 2017). The equivalent unit in the Gariep Belt is the para-utochthonous Port Nolloth Zone, which comprises all Neoproterozoic sedimentary rocks within the fold-and-thrust belt including rift-related basin deposits overlain by foredeep sediments (Frimmel et al., 1996; Frimmel, 2018 and references therein). The Port Nolloth Zone is overridden by the allochthonous Marmora Terrane, consisting of post-rift oceanic metabasalts overlain by late-Neoproterozoic siliciclastic and carbonate sedimentary rocks (Frimmel and Fölling, 2004; Frimmel, 2018).

The orogenic hinterland outcrops on both sides of the Atlantic Ocean, and consists of tectonically interleaved orthogneisses, paragneisses and migmatites intruded by numerous late-Neoproterozoic plutons. It is represented by the Coastal Terrane in the Kaoko Belt (Goscombe et al., 2005b), and the Cerro Olivo Complex of the Punta del Este Terrane, the Várzea do Capivarita Complex, and the Porto Belo and Águas Mornas Complexes in the southern, central and northern Dom Feliciano Belt respectively (Fig. 1) (Battisti et al., 2018; De Toni et al., 2020a; Gross et al., 2009; Oyhantçabal et al., 2009; Silva et al., 2000). The protoliths of the metamorphic hinterland consist of Paleoproterozoic cratonic basement intruded by early-Neoproterozoic bimodal magmatic rocks that are interpreted as remnants of arc-related (De Toni et al., 2020a; Koester et al., 2016; Lenz et al., 2013; Martil et al., 2017; Philipp et al., 2016) or rift-related (Konopásek et al., 2018; Oyhantçabal et al., 2009; Will et al., 2019) magmatism, and associated sedimentary cover. The episodic crustal stretching, melting and basin sedimentation that formed the early-Neoproterozoic parts of the hinterland rocks occurred from ca. 840 Ma to at least ca. 710 Ma (Basei et al., 2011c; De Toni et al., 2020a; Konopásek et al., 2014; Lenz et al., 2011; Martil et al., 2017; Oyhantçabal et al., 2009), and likely up to ca. 660–650 Ma ending shortly before the onset of orogenesis (Konopásek et al., 2017, 2018; Kröner et al., 2004). Orogenesis coincides with a strong metamorphic overprint in the hinterland rocks at ca. 670–640 Ma (Chemale et al., 2012; Masquelin et al., 2012; Oyhantçabal et al., 2009).

Along the western edge of the hinterland, in the Dom Feliciano Belt, is the Granite Belt: an extensive belt of late-Neoproterozoic, syn- and post-collisional granitoid batholiths (Fig. 1) (Bitencourt and Nardi, 1993, 2000; Florisbal et al., 2009, 2012a, 2012b; Hueck et al., 2018b; Oyhantçabal et al., 2007; Philipp and Machado, 2005; Philipp et al., 2013), that intrude the Paleoproterozoic to early-Neoproterozoic units of the high-grade hinterland (De Toni et al., 2020a; Koester et al., 2016; Lenz et al., 2013; Martil et al., 2017; Masquelin et al., 2012). The granitoids predominantly intruded between ca. 630–580 Ma (Florisbal et al., 2012b; Lara et al., 2020; Philipp and Machado, 2005), with scattered evidence of early magmatism at ca. 660–650 Ma (Chemale et al., 2012; Frantz et al., 2003).

The Granite Belt is in tectonic contact with the western foreland, separated by a large strike-slip dominated shear zone system running the entire length of the Dom Feliciano Belt, known as the Southern Brazilian Shear Belt (Fig. 1) (Bitencourt and Nardi, 2000). The foreland consists of a fold-and-thrust belt comprised of pre-orogenic rift-related sedimentary successions – known as the Schist Belt – and their associated basement rocks (Basei et al., 2011b; Bettucci et al., 2001; Saalmann et al., 2006), and a system of foreland basins (Fig. 1) (Almeida et al., 2010; Basei et al., 2011a; Guadagnin et al., 2010; Hueck et al., 2018b). The Schist Belt is comprised of the Brusque, Porongos and Lavalleja complexes in the Northern, Central and Southern Dom Feliciano Belt respectively. The Schist Belt and foreland basins lie on Archean–Paleoproterozoic basement units (Fig. 1). In Uruguay, the basement of the Dom Feliciano Belt foreland is the Nico Pérez Terrane (Oriolo et al., 2016; Oyhantçabal et al., 2011b). In the Central Dom Feliciano Belt, the basement of the foreland is exposed as tectonic windows in the Schist Belt (Saalmann et al., 2006).

2.2. The northern Dom Feliciano Belt

The foreland basement of the northern Dom Feliciano Belt is the Luis Alves Craton, which is predominantly comprised of Paleoproterozoic granulitic gneisses of the Santa Catarina Granulite Complex (Fig. 2) (Basei et al., 2009; Hartmann et al., 2015; Passarelli et al., 2018). The complex is made up of ca. 2.2–2.0 Ga orthogneisses, interspersed with mafic–ultramafic enclaves and subordinate paragneisses (Basei et al., 1998a, 2009; Hartmann et al., 1999, 2000). The southern margin of the Luis Alves Craton is covered by the Itajaí Basin (Fig. 2) (Basei et al., 2009; Passarelli et al., 2018), which consists of volcano-sedimentary successions deposited in an orogenic foreland environment (Basei et al., 2011a) with a maximum age of deposition constrained by U–Pb zircon dating of interlayered volcanics at ca. 560–550 Ma (Guadagnin et al., 2010). The Itajaí Basin is weakly deformed, with deformation increasing south-eastwards towards the Itajaí–Perimbó Shear Zone where it is in contact with the foreland fold-and-thrust belt (Fig. 2) (Basei et al., 2011a).

The fold-and-thrust belt is predominantly comprised of metamorphosed volcano-sedimentary sequences of the Brusque Complex intruded by a series of Neoproterozoic granitoids between ca. 630–585 Ma (Fig. 2) (Florisbal et al., 2012b; Hueck et al., 2019). A narrow sliver of crystalline basement of unknown age and origin, known as the São Miguel Complex, is exposed at the north-western contact with the Itajaí Basin (Fig. 2) (Basei et al., 2011b). Syenogranites intruding this foreland basement have been dated at 835 ± 9 Ma and 843 ± 12 Ma (U–Pb zircon), and are interpreted as A-type granitoids marking the beginning of rifting that lead to the formation of the Brusque Complex paleobasin (Parapente Granite, see Fig. 2) (Basei et al., 2008b). This is within error of a 833 ± 3 Ma (U–Pb zircon) age found in granitic to syenitic rocks of the Richtersveld Igneous Complex in the Gariep Belt, which is similarly interpreted as evidence of the earliest crustal thinning in the region marking the beginning of continental breakup (Frimmel et al., 2001).

A basement inlier—the Camboriú Complex—outcrops along the coast in central part of the Brusque Complex (Fig. 2). The Camboriú Complex is predominantly comprised of migmatitic felsic orthogneisses interleaved with amphibolites (Martini et al., 2019), which predominantly show U–Pb zircon ages of 2.2–2.0 Ga comparable with the Luis Alves Craton (Hartmann et al., 2003; Silva et al., 2000, 2005).

The southern border of the Brusque Complex is in tectonic contact with the Florianópolis Batholith, and the two units are separated by the large-scale Major Gercino Shear Zone (Fig. 2). The Florianópolis Batholith is the northern exposure of the Granite Belt (Fig. 1), and is comprised of a vast series of Neoproterozoic granitoids that intruded the western edge of the hinterland represented by the ca. 800 Ma migmatitic orthogneisses of the Porto Belo Complex (De Toni et al., 2020a) and the Paleoproterozoic Águas Mornas Complex (Fig. 2) (Silva et al., 2005). The granitoids were emplaced predominantly between ca. 630–590 Ma (Chemale et al., 2012; Florisbal et al., 2012b).

2.3. Early evolution of the Brusque Complex

The rocks in this study belong to the metamorphosed volcano-sedimentary successions of the Brusque Complex, which forms a NE–SW oriented belt of predominantly pelitic schists divided into a northern and southern section by an elongate syn-orogenic granitic batholith (Fig. 2) (Valsungana Batholith). Metamorphism in the Brusque Complex is characterised by a general increase in metamorphic grade from NW–SE (Basei et al., 2011b; Campos et al., 2011, 2012). In the NW, the Brusque Complex metapelites are dominated by lower-greenschist facies chlorite – mica schists and phyllites, and a narrow garnet zone in the centre and southern parts of the belt suggests metamorphic conditions reached maximum lowermost amphibolite facies (Fig. 2). The Brusque Complex rocks are intensely deformed, showing evidence of multiple deformation structures associated with its prolonged contractional history (Basei et al., 2011b; Campos et al., 2011).

There is little published work available concerning the early evolution of the Brusque Complex, as poor exposure and the intensity of deformation makes any stratigraphic subdivision difficult. Despite this, three sequences are generally described based on the presence or absence of volcanic sub-units (e.g. Basei et al., 2006, 2011b). The lower-most and upper-most formations—the Rio do Oliveira and Rio da Areia sequences respectively—are described as being dominated by meta-sedimentary rocks, with some mafic and rare felsic metavolcanics interlayered within (Basei et al., 2011b; Campos et al., 2011). The upper sequence is described as containing a large proportion of metacarbonate rocks, and the lower sequence frequently containing calc-silicate lenses of volcanogenic origin (Basei et al., 2011b; Campos et al., 2011). The middle formation—the Botuverá sequence—is described as entirely clastic, varying in composition between metapelitic and metapsammitic and containing no metavolcanic or metacarbonate rocks (Basei et al., 2011b).

There is also little published data to constrain the timing of sedimentation of the Brusque Complex protolith. The upper limit is loosely placed at ca. 840 Ma at the start of basin formation (Basei et al., 2008b), but within the Brusque Complex itself there are currently no reliable constraints on the upper limit of sedimentation. Basei et al. (2008a) reported a minimum age at ca. 570–540 Ma based on the two youngest detrital zircon grains from pelitic schists of the Brusque Complex. However, this age is contradicted by the well-constrained age of intrusion of granitic plutons and dykes into the Brusque Complex metasediments between ca. 620 and 580 Ma (Campos et al., 2012; Hueck et al., 2019). Currently, these post-metamorphic magmatic rocks remain the only robust constraint on the minimum age of sedimentation into the Brusque Complex paleobasin.

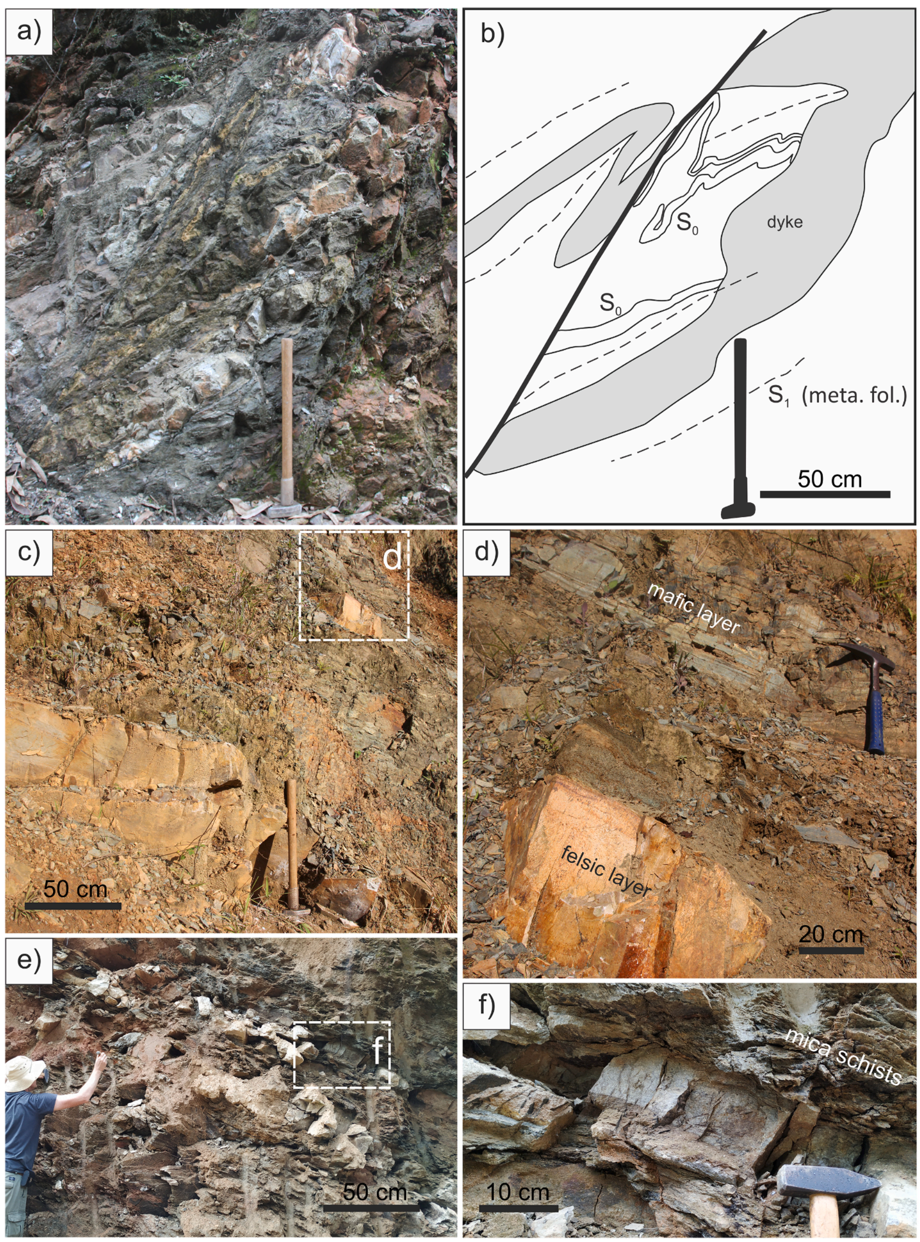

Fig. 3. Outcrops of metaigneous rocks: a) photo of the metamorphosed and deformed felsic dyke BB12A, b) an accompanying sketch of the same road-cut outcrop outlining the cross-cutting nature of the dyke relative to remnant S_0, c) road-cut outcrop BA22, d) detail of outcrop BA22 showing bimodal volcanics, e) outcrop JBE37, f) detail of outcrop JBE37 showing foliation-parallel nature of felsic rock.

3. Geochronology

3.1. Materials and methods

Zircon U–Pb ages were determined at the Institute of Geology of the Czech Academy of Sciences, Prague, Czech Republic, using laser ablation inductively coupled plasma mass spectrometry (LA-ICP-MS), and the complete isotopic dataset is presented in Electronic Appendix A. For detrital zircon data, U–Pb age spectra are presented as cumulative distribution curves with 95% confidence intervals after Andersen et al. (2016) and using the visualisation package (*detzrcr*) of Andersen et al. (2018b), and as frequency histograms with 30 Ma binwidths and adaptive kernel density estimate (KDE) curves as described in Vermeesch et al. (2016) using the software package (*densityplotter* version 8.4) of Vermeesch (2012). Only concordant dates with calculated discordance within ± 10%, are included. Concordance is calculated from ages, using ($^{206}Pb/^{238}U$) / ($^{207}Pb/^{206}Pb$) for $^{207}Pb/^{206}Pb$, and using ($^{206}Pb/^{238}U$) / ($^{207}Pb/^{235}U$) for $^{206}Pb/^{238}U$. $^{207}Pb/^{206}Pb$ dates are reported for data > 1.0 Ga, and $^{206}Pb/^{238}U$ dates for data < 1.0 Ga. Description of zircon separation and analytical methods is provided in Electronic Appendix B. Locations of analysed samples are plotted in Fig. 2.

3.2. Description of metaigneous samples and results of U–Pb zircon dating

3.2.1. Sample BB12A

Sample BB12A (Fig. 2) (27° 18.940′ S, 49° 07.682′ W) was collected from a felsic dyke intrusive in metapelitic schists. The dyke is approximately 30 cm thick, and is folded and metamorphosed together with the schists indicating intrusion prior to deformation and metamorphism of the host rock (Fig. 3a and b). The metamorphic mineral assemblage is dominated by quartz, plagioclase and K-feldspar, with minor white mica, chlorite and biotite, and accessory opaque minerals. Chlorite pseudomorphs after garnet completely replace poikiloblastic garnet, suggesting overprint at lower metamorphic conditions. The original magmatic texture has been almost completely overprinted by metamorphism and deformation, although K-feldspar crystals much larger than those in the matrix remain as inclusions in garnet pseudomorphs suggesting that the magmatic fabric is locally preserved.

From 42 spot analyses in oscillatory-zoned parts of the zircon grains, 25 concordant dates combine in a concordia U–Pb age of 811 ± 6 Ma (Fig. 4a and b), interpreted as the age of intrusion and crystallisation of the dyke. Zircon grains range from ca. 60 to 150 μm in length, and most are idiomorphic and show oscillatory zoning in cathodoluminescence (CL) images (Fig. 4c). Some grains show truncated zoning at the edges, which are likely fractured and abraded inherited zircons. Of the remaining 17 analyses, three are discordant likely due to lead loss at an unspecified time, and the rest are older than the major cluster of dates and likely represent inherited grains.

3.2.2. Sample BA22

Sample BA22 (27° 12.195′ S, 48° 39.853′ W) is a fine-grained metarhyolite, consisting of quartz, plagioclase, K-feldspar, minor amounts of muscovite, and with accessory garnet and opaque minerals. The outcrop consists of a series of metamorphosed, interlayered mafic and felsic volcanic rocks interspersed with metapelitic schists (Fig. 3c and d). The outcrop shows a penetrative metamorphic foliation, overprinting any previous magmatic texture. However, due to layering of the mafic, felsic and pelitic layers, and the presence of abundant K-feldspar, we interpret the sample as a metamorphosed felsic volcanic rock.

Only a small number of zircon grains were recovered from the sample, varying between 70 and 190 μm in length and 60 and 130 μm in width. The grains predominantly show sector zoning, with minor oscillatory zoning, and are strongly fractured and rounded. Of 22 grains analysed, 19 yielded concordant dates. Four grains were analysed twice, and repeated dates were not plotted. The data are plotted in Fig. 5a, and show that the dates mainly cluster at ca. 2.05 Ga. Due to similarities with the surrounding samples (see below), we interpret all zircon grains as inherited.

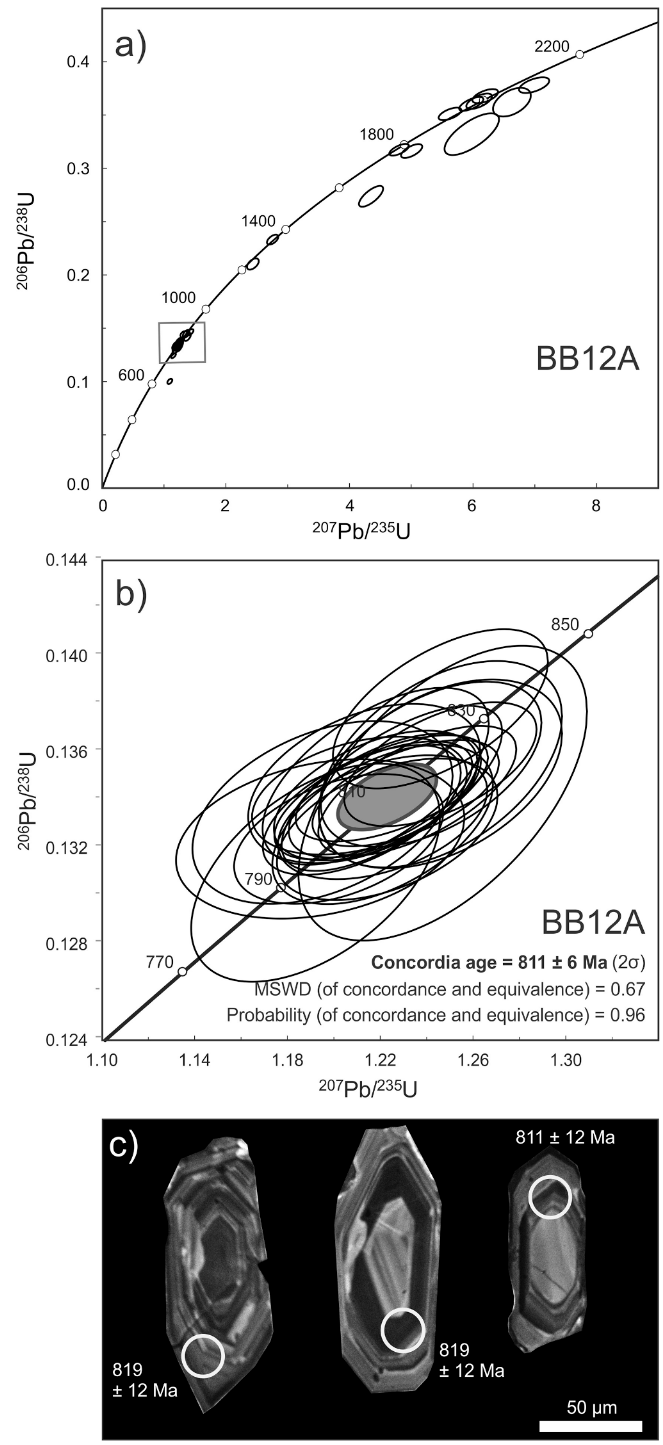

Fig. 4. Results of U–Pb zircon dating of sample BB12A: a) zircon U–Pb concordia plot for sample BB12A (analysed by LA–ICP–MS), b) detail of inset showing combined 25 data points used for calculation of the concordia age (data point error ellipses are plotted at 2σ level, MSWD = mean square weighted deviation), and c) cathodoluminescence images and individual dates of example zircon grains.

3.2.3. Sample JBE41B and JBE37

Samples JBE41B (27° 19.083′ S, 49° 12.516′ W) and JBE37 (27°

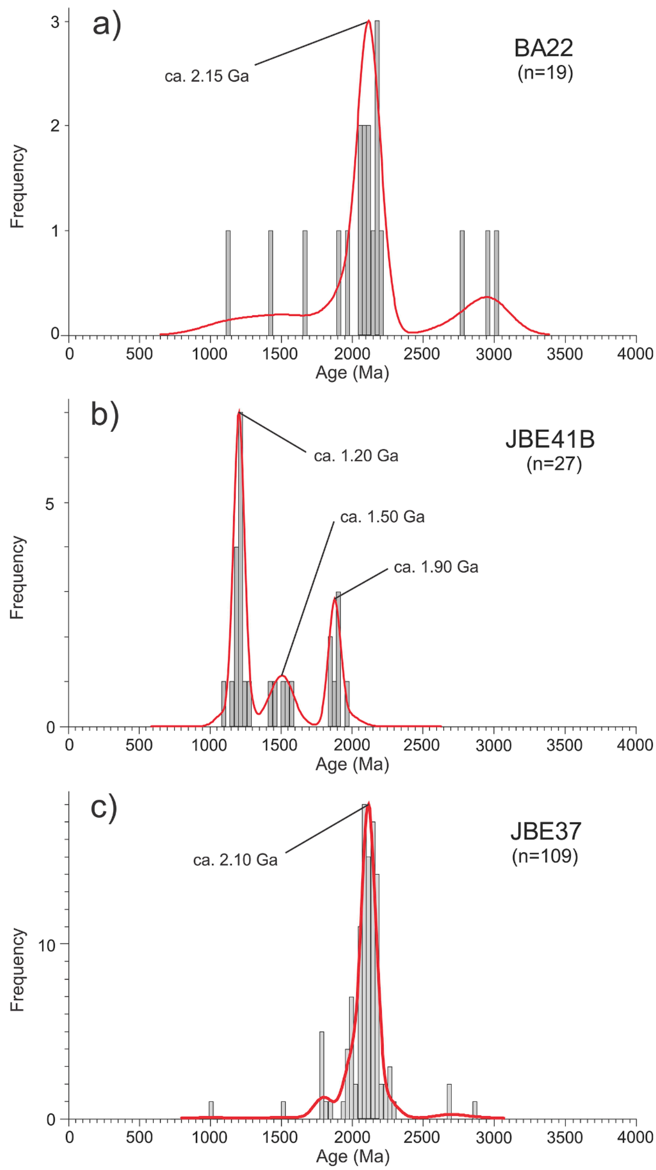

Fig. 5. U-Pb zircon age data for analysed metaigneous samples, presented as frequency histograms and KDEs. n = number of data.

20.192′ S, 49° 10.536′ W) were collected from approximately foliation-parallel felsic layers within the garnet-schists of the Brusque Complex. Both outcrops consist of a series of felsic layers approximately 10–30 cm thick, interlayered with garnet-bearing schists. The samples contain the mineral assemblage quartz, plagioclase and K-feldspar, with subordinate biotite, white mica, chlorite and opaque minerals. Chlorite pseudomorphs after garnet in sample JBE37 contain K-feldspar inclusions similar to sample BB12A. Based on field observations and the presence of blastoporphyritic K-feldspar, we interpret the protoliths of the samples as metamorphosed felsic volcanic rocks. However, due to metamorphic overprint it remains difficult to conclusively differentiate them from a meta-arkose.

For sample JBE41B, 28 zircon grains were analysed and 27 yielded concordant dates with 2σ uncertainty ≤ 10%. The data are plotted in Fig. 5b, and the resulting spectrum shows age peaks at ca. 1.90, 1.50 and 1.20 Ga. All of the zircon grains are interpreted as inherited/detrital.

For sample JBE37, analysis of 112 zircon grains produced 109 concordant dates with 2σ uncertainty ≤ 10%. The data are plotted in Fig. 5c, and the resulting spectrum shows a single dominant age peak centred at ca. 2.10 Ga, with a much smaller peak at ca. 1.80 Ga, and some individual data between ca. 3.00–1.00 Ga. All of the zircon grains are also interpreted as inherited/detrital.

3.3. Description of metasedimentary samples and results of U–Pb detrital zircon dating

3.3.1. Sample JBD24

Sample JBD24 (26° 48.324′ S, 48° 35.838′ W) is a micaceous quartzite collected from within the Itajaí–Perimbó Shear Zone, close to the northern contact with the underlying basement (Basei et al., 2011b) (Fig. 2). The rock is intensely folded and deformed, though weakly metamorphosed, containing quartz, muscovite, biotite, chlorite and plagioclase, with accessory opaque minerals. Zircon grains are mostly ca. 50 to 120 μm in length, and show varying degrees of fragmentation from whole, prismatic crystals to small, abraded fragments. The majority show oscillatory zoning, and often with truncated edges likely due to transport and abrasion. No grains appear to have metamorphic overgrowth rims, and few show sector zoning or no zoning at all.

Analysis of 140 grains yielded 118 concordant dates. The spectrum of dates (Fig. 6a) shows distinct peaks at ca. 2.20 Ga and 660 Ma, with individual data in the intervals between ca. 2.10–0.80 Ga, and ca. 3.60–2.30 Ga.

3.3.2. Sample BB08

Sample BB08 (26° 55.544′ S, 48° 38.055′ W) is a carbonate-bearing phyllitic metarhythmite collected from a coastal outcrop within the southern part of the Itajaí–Perimbó Shear Zone (Fig. 2). The rock is strongly deformed, with a primary metamorphic foliation containing intrafolial folding that is overprinted by a steep, pervasive crenulation cleavage parallel to the Itajaí–Perimbó Shear Zone. The style of deformation at this outcrop is consistent with other high-strain parts of the Brusque Complex (Basei et al., 2011b).

The rock contains quartz, muscovite, biotite, chlorite, plagioclase and calcite, with accessory opaque minerals. Zircon grains vary between ca. 60 and 200 μm in length. Most of the grains show oscillatory zoning, with some showing sector zoning and other more complex internal structures. The majority of grains are abraded and fragmented, and some show thin CL-bright overgrowth rims.

101 analysed zircon grains yielded 82 concordant dates. The data show a similar bimodal distribution to sample JBD24, with distinct peaks at ca. 2.15 Ga and 670 Ma, and minor peaks at ca. 625 and 560 Ma (Fig. 6b). Individual data appear over the intervals between ca. 2.95–1.75 Ga and ca. 750–500 Ma. The two youngest individual zircon grains are ca. 84 Ma and 375 Ma, which are significant outliers. These two grains are likely from contamination, either from beach sediment cemented onto the rock by dissolution and precipitation of calcite, or otherwise introduced during the separation process.

3.3.3. Sample BA23

Sample BA23 (27° 10.511′ S, 48° 43.054′ W) was collected in the southeast section of the Brusque Complex from a large, loose block at the foot of an isolated steep slope (not in situ, but inferred to be close to its original position on the hill above). The sample is a weakly foliated micaceous quartzite containing quartz, muscovite, biotite, chlorite and garnet, with accessory opaque minerals. Zircon grains range between ca. 80 and 150 μm in length, and are mostly fragmented and abraded. Most grains have oscillatory or sector zoning, and many show featureless overgrowth rims. A smaller number show complex zoning patterns or no zoning at all.

Isotopic dating yielded 136 concordant dates from 140 analysed zircon grains. The age spectrum (Fig. 6c) shows the majority of dates cluster at a single peak ca. 2.00 Ga. A minor, long-wavelength peak centred at 2.70 Ga encompasses a series of individual dates between ca. 3.15–2.30 Ga.

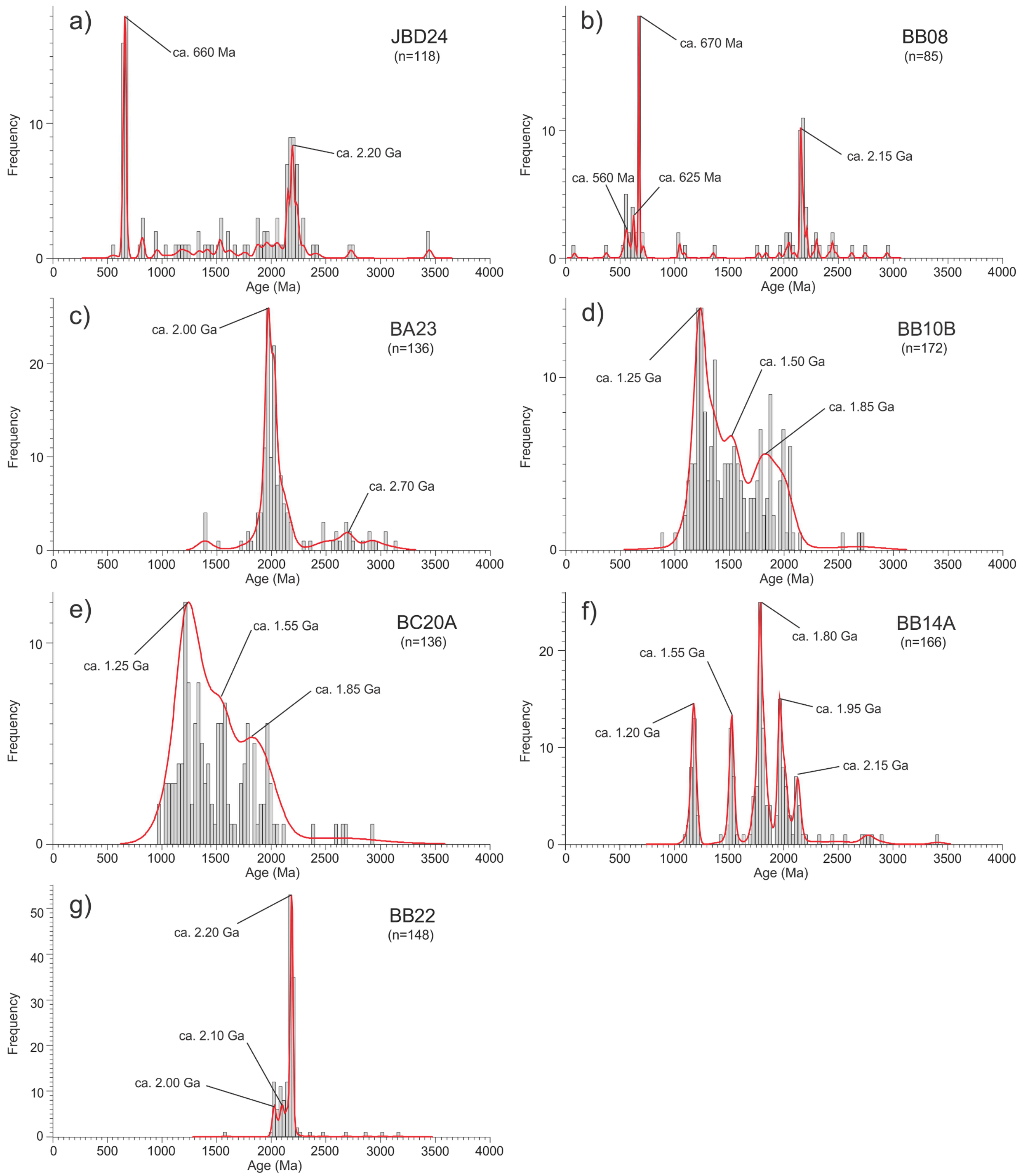

Fig. 6. U-Pb detrital zircon data for analysed metasedimentary samples, presented as frequency histograms and KDEs. n = number of data.

3.3.4. *Sample BB10B*

Sample BB10B (27° 16.964′ S, 48° 55.006′ W) was collected from the southern-central part of the Brusque Complex, from a strongly foliated quartz-rich schist containing quartz, muscovite, biotite, and chlorite, with accessory opaque minerals. Zircon grains range from ca. 50 to 120 µm in length, and ca. 30 to 50 µm in width. Many grains are elongate and euhedral, showing sector or oscillatory zoning. Thin, CL-bright overgrowth rims are common.

Analysis of 182 zircon grains yielded 172 concordant dates. The spectrum of ages (Fig. 6d) shows a broad distribution of dates from ca. 2.20–1.00 Ga, with the highest proportion centred at a peak at ca. 1.25 Ga. The remaining data are distributed between ca. 2.20–1.30 Ga with minor peaks at ca. 2.00, 1.80, 1.50 and 1.35 Ga.

3.3.5. Sample BC20A

Sample BC20A (27° 14.919′ S, 49° 04.959′ W) was collected from a strongly deformed garnet-bearing schist in the south-western part of the Brusque Complex. The sample contains quartz, garnet, muscovite, biotite, chlorite and plagioclase, with accessory tourmaline and opaque minerals. Zircon grains range from ca. 50 to 200 μm in length. Grains vary in shape and structure: some are euhedral with oscillatory zoning, while others have abraded edges, are often fractured, and with complex internal structures.

Isotopic analysis of 140 zircon grains produced 136 concordant dates. The data (Fig. 6e) show a broad distribution of dates between ca. 2.10 Ga and 900 Ma, with a major peak at ca. 1.25 Ga and minor peaks at ca. 1.95, 1.80, 1.55 and 1.35 Ga.

3.3.6. Sample BB14A

Sample BB14A (27° 15.128′ S, 49° 09.412′ W) is a quartzite collected from the western part of the Brusque Complex. The sample contains quartz, muscovite and biotite, with accessory rutile and opaque minerals. Zircon grains range from ca. 80 to 200 μm in length, and are predominantly elongate and rounded. Most grains show oscillatory zoning, with only a few showing sector or complex zoning patterns. The grains are mostly fragmented and abraded

From 168 zircon grains analysed, 166 produced concordant U–Pb dates. The resulting age spectrum (Fig. 6f) shows distinct peaks at ca. 2.15, 1.95, 1.80, 1.55 and 1.15 Ga.

3.3.7. Sample BB22

Sample BB22 (27° 13.358′ S, 49° 09.847′ W) is a quartzite collected from the low-grade section of the Brusque Complex in the north-west. The sample contains quartz and muscovite, with accessory titanite and opaque minerals. Zircon grains range from 70 to 250 μm in length, and are predominantly elongate and rounded. Most grains show oscillatory zoning, and are mostly fragmented and abraded. Some grains show more complex zoning patterns.

Isotopic analysis of 154 zircon grains produced 148 concordant U–Pb dates. The corresponding age spectrum (Fig. 6g) shows the majority of dates centred at a large peak at ca. 2.20 Ga, with two minor peaks at ca. 2.10 and 2.05 Ga.

4. Discussion

4.1. Constraining the age of sedimentation

The concordia U–Pb zircon age of 811 ± 6 Ma from sample BB12A represents the youngest cluster of data in the sample, and likely the crystallisation age of the dyke. Because the youngest detrital zircon grains from neighbouring samples (e.g. BB10B and BC20A; Fig. 2) are ca. 1.00 Ga, it is not likely that the ca. 800 Ma zircons in sample BB12A represent xenocrystic grains. Furthermore, considering that the rock is deformed and metamorphosed together with the host schists, we interpret that the dyke intruded the Brusque Complex protolith prior to the onset of orogenic evolution at ca. 650 Ma. Due to issues with stratigraphy, there is no constraint on what level of the Brusque Complex basin is represented by these metasediments, though it suggests that at least part of the Brusque Complex protolith was deposited prior to ca. 811 Ma.

This age is close to estimates of earliest sedimentation in the Porongos Complex of the central Dom Feliciano Belt foreland, which has been constrained to ca. 810–770 Ma by dating of syn-depositional volcanics (Pertille et al., 2017; Saalmann et al., 2011). These ages also correlate well with ca. 820–785 Ma syn-sedimentary magmatism in the Coastal Terrane of the Kaoko Belt hinterland (Konopásek et al., 2008, 2018), ca. 800 Ma magmatism in the Porto Belo Complex of the northern Dom Feliciano Belt hinterland (De Toni et al., 2020a), and ca. 790 Ma magmatism in the Várzea do Capivarita Complex of the central Dom Feliciano Belt hinterland (Martil et al., 2017), suggesting a genetic relationship between the early Neoproterozoic rocks of the foreland and hinterland domains (e.g. Battisti et al., 2018). Importantly, the dyke post-dates estimates for the beginning of continental rifting, and thus basin formation, in the Kaoko–Dom Feliciano–Gariep orogenic system at ca. 840 Ma (Basei et al., 2008b; Frimmel et al., 2001). All these data constrain the beginning of sedimentation in the Brusque Complex to between ca. 840–811 Ma.

None of the other potential metaigneous samples (BA22, JBE41B and JBE37) produced a cluster of dates that could be interpreted as a magmatic age. Thus, the ca. 811 Ma age obtained from sample BB12A provides the current best constraint for the minimum age of sedimentation of the Brusque Complex protolith.

4.2. Detrital zircon age patterns

Three distinct detrital zircon age patterns are identified within the studied samples (Fig. 7a). Sample BA22 contained too few zircons to confidently assign to a group, and so is not included in any further analysis.

The first pattern shows a polymodal age distribution, as seen in samples BB10B, BC20A, BB14A and JBE41B (Fig. 7b). These samples have age peaks predominantly within a range from ca. 2.10 to 1.00 Ga (Fig. 7b), with major Paleoproterozoic peaks at ca. 2.10, 1.95 and 1.80 Ga, and a series of peaks in the Mesoproterozoic at ca. 1.55, 1.35 and 1.20 Ga. Using the *1-O* parameter of Andersen et al. (2016) to statistically determine likeness between samples, samples BC20A, BB10B and JBE41B all show a perfect match within the sample confidence intervals (*1-O* = 0.00 for each comparison), and sample BB14A matches poorly with each (*1-O* = 0.11 for each comparison).

The next is a unimodal distribution pattern seen in samples BA23, BB22 and JBE37. The data show detrital zircon ages almost entirely within the Paleoproterozoic, and the pooled KDE (Fig. 7c) is dominated by a large, narrow peak at 2.20 Ga, with a series of smaller peaks between ca. 2.15–2.00 Ga. Sample JBE37 shows a good match with samples BA23 and BB22 (*1-O* = 0.03 and 0.02 respectively), and sample BA23 matches well with BB22 (*1-O* = 0.05). The pooled data do not show a strictly unimodal distribution pattern, but individually the samples show generally unimodal distributions (Fig. 5-c, 6-c, -g). The most noticeable difference when comparing the polymodal and the unimodal sample groups is the complete absence of Mesoproterozoic zircon age peaks in the latter, and the absence of a 2.20 Ga peak in the former.

Finally, an approximately bimodal distribution pattern is seen in samples JBD24 and BB08, and when these samples are pooled (Fig. 7d) the data show significant peaks at ca. 665 Ma and ca. 2.20 Ga, a minor peak at ca. 560 Ma, and individual dates distributed between ca. 2.10–0.80 Ga and between ca. 3.50–2.30 Ga. These two samples match perfectly within their confidence intervals (*1-O* = 0.00).

4.3. Polymodal detrital zircon pattern and its possible sources

When pooled, the major peaks in the polymodal pattern at ca. 2.10, 1.95, 1.80, 1.55, 1.35 and 1.20 Ga are distinct (Fig. 7b). Notably, there is no peak at 2.20 Ga, which is the dominant Paleoproterozoic age peak seen in the unimodal and bimodal pooled relative frequency plots (Fig. 7c and d). The oldest peaks in the pooled polymodal plot are at ca. 2.10 and 2.00 Ga, which correlate with magmatic ages of ca. 2.05–1.95 Ga from the Congo Craton basement of the Kaoko Belt (Kröner et al., 2004), as well as with similar ages reported from basement rocks of the Luis Alves Craton (Basei et al., 1999, 2009) and the Camboriú Complex (Silva et al., 2000). As the most proximal cratonic basement rocks to the Brusque Complex, the Luis Alves Craton would be the most likely candidate for protosource material for the Brusque Complex sediments. However, the absence of a ca. 2.20 Ga age peak suggests a closer affinity to the Congo Craton basement, which, unlike the Luis Alves Craton, does not contain a record of ca. 2.20 Ga activity.

The presence of Mesoproterozoic zircon grains in the polymodal

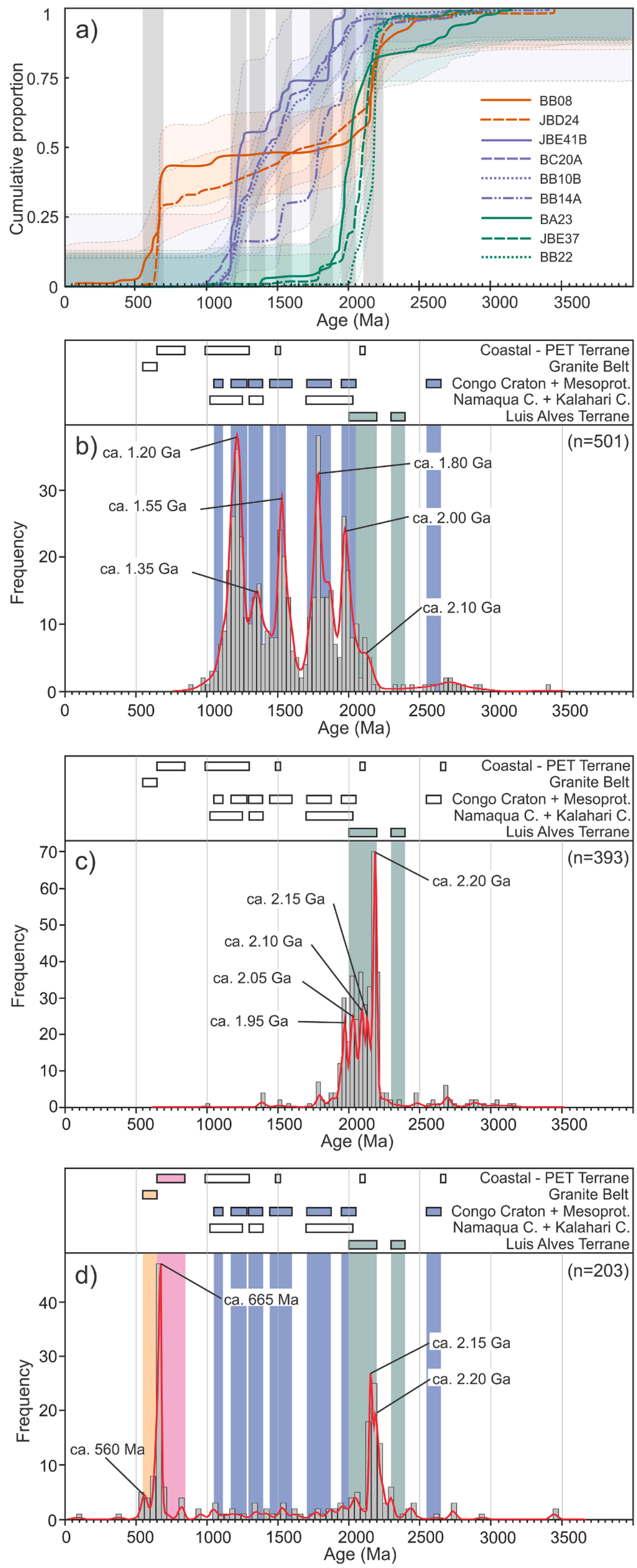

(caption on next column)

Fig. 7. Brusque Complex U–Pb detrital zircon data grouped into three patterns: a) cumulative proportion curves of each sample with 95% confidence intervals (shaded columns delineate major common age fractions), b) pooled polymodal group (samples BC20A, BB10B, BB14A and JBE41B), c) unimodal group (samples BA23, BB22 and JBE37), and d) bimodal group (samples BB08 and JBD24). Bars at the top of figures b, c and d show age ranges of relevant protosources, and the coloured columns behind the data show the best fit protosources for each group that correlate to major age fractions. Data for reference bars: Congo Craton + Mesoprot. from Kröner et al. (2015, 2004); Kröner and Rojas-Agramonte (2017); Seth et al. (1998, 2003), Namaqua Metamorphic Complex from Becker et al. (2006); Bial et al. (2015); Clifford et al. (2004), Luis Alves Craton from Basei et al. (2009); (Hartmann et al., 1999); Hartmann et al. (2000), Coastal–PET Terrane from Basei et al. (2011c); Goscombe et al. (2005a); Konopásek et al. (2008); Lenz et al. (2011); Oyhantçabal et al. (2009), Granite Belt from Florisbal et al. (2012b); Lara et al. (2020); Philipp and Machado (2005).

sample group indicates a significant contribution from Mesoproterozoic-aged protosource rocks, which were otherwise almost entirely absent during sedimentation of the protoliths of the unimodal sample group. However, rocks of this age are so far unknown from the basement rocks exposed in the northern Dom Feliciano Belt. In the southern Dom Feliciano Belt (Fig. 1), rocks with ages corresponding to the Mesoproterozoic peaks in the polymodal pattern, at ca. 1.50 and 1.40 Ga, are known only from the Nico Pérez Terrane in Uruguay (Gaucher et al., 2011; Mallmann et al., 2007; Oriolo et al., 2019; Oyhantçabal et al., 2018; Sánchez-Bettucci et al., 2004). A ca. 1.55 Ga crystallisation age is also recorded within the Capivarita Anorthosite in the exposed basement of the Granite Belt in the central part of the Dom Feliciano Belt in Rio Grande do Sul (Chemale et al., 2011). Given their distal nature to the northern Dom Feliciano Belt, though, it is unlikely that these rocks directly contributed to sedimentation into the Brusque Complex paleobasin.

The 1.55–1.40 Ga ages are common, however, in Mesoproterozoic magmatic rocks intruding the Congo Craton of Namibia and SW Angola (e.g. Bybee et al., 2019; Lehmann et al., 2020; Luft et al., 2011; Seth et al., 1998), providing possible protosources for the Brusque Complex sediment. The best-fit source rocks for the observed ages in the polymodal group come from metamorphosed supracrustal rocks of the Okapuka Formation and the underlying Epupa Metamorphic Complex in the Kaoko Belt (Fig. 7b). Part of the Congo Craton, the Epupa Metamorphic Complex is dated at ca. 1.85–1.75 Ga (Kröner et al., 2010, 2015), and is intruded by granitoid rocks with ages primarily clustered at ca. 1.50, 1.35 and 1.20 Ga (Drüppel et al., 2007; Kröner et al., 2015; Kröner and Rojas-Agramonte, 2017; Seth et al., 2003). These basement rocks are overlain by the ca. 1.35 Ga volcano-sedimentary Okapuka Formation (Fig. 1), which contains detrital zircon spanning ca. 2.05–1.40 Ga that was likely sourced from the nearby basement. The formation is intruded by magmatic rocks with ages between ca. 1.20–1.05 Ga (Kröner and Rojas-Agramonte, 2017).

The underlying Paleoproterozoic basement may represent part of the source for the Brusque Complex sediments, however it is equally likely that these rocks represent the protosource and that the Brusque Complex sediment is sourced directly from the Mesoproterozoic sedimentary cover (Okapuka Fm.) and associated intrusive rocks. Recycling of older sedimentary successions has been proposed by Andersen et al. (2018a) to explain the detrital zircon record in equivalent rocks in the Gariep Belt, and they point to preserved fragments of Meso- and Paleoproterozoic sedimentary cover on the surrounding cratonic basement as evidence of this recycling system. Similarly, Konopásek et al. (2017) and Konopásek et al. (2018) inferred an extensive Mesoproterozoic sedimentary cover sequence as the source for the Neoproterozoic successions of the Kaoko Belt foreland. Given the presumed pre-Atlantic proximity of the Kaoko Belt to the northern Dom Feliciano Belt (Konopásek et al., 2017; Porada, 1989), we judge this inferred extensive Mesoproterozoic cover sequence as the most likely candidate for the

Mesoproterozoic zircon populations in the Brusque Complex rocks.

4.4. Unimodal detrital zircon pattern and its possible sources

Zircon ages at ca. 2.20 Ga, corresponding to the largest peak in the unimodal pooled zircon age distribution pattern (Fig. 7c), are known from local basement rocks of the Luis Alves Craton, the Camboriú Complex and the Águas Mornas Complex (Basei et al., 2009; Hartmann et al., 1999, 2000; Silva et al., 2000, 2005). The closest basement unit of the Luis Alves Craton is the Santa Catarina Granulite Complex, which outcrops immediately to the north of the Itajaí Basin (Fig. 1). Zircon grains from granulitic gneisses of this complex mostly preserve U–Pb ages of ca. 2.20–2.10 Ga, with less common ca. 2.40–2.30 Ga ages and minor occurrences of ca. 2.00 Ga zircon (Basei et al., 2009; Hartmann et al., 1999, 2000). Ages corresponding to the smaller peaks at ca. 2.10 and 2.00 Ga are also known from the Camboriú Complex (Silva et al., 2000, 2005), as well as from exposed Congo Craton basement in the Kaoko Belt (Kröner et al., 2004). As the samples from the unimodal group contain only single zircon age peaks, which correspond to ages in the local basement, we interpret the unimodal group as reflecting first generation detrital zircon and thus direct erosion of the basement.

The Brusque Complex contains both local basement-derived sediment and recycled sediment, however the absence of a 2.20 Ga age peak in the polymodal group suggests that these two sources did not mix. This indicates that the inferred Mesoproterozoic sedimentary cover source was completely eroded before any of the local basement was exposed. Inferring from this that the sediment was sourced locally implies also that the Mesoproterozoic sedimentary sequences covered the Luis Alves basement prior to erosion into the Brusque Complex paleobasin, and thus that the Congo and Luis Alves cratons were in close proximity prior to Neoproterozoic rifting.

Both the unimodal and polymodal sample groups do not contain zircon age peaks younger than 1.20 Ga, and even the youngest individual zircons are no older than ca. 0.9–1.0 Ga (Fig. 7b and c). Considering the minimum age of sedimentation at ca. 810 Ma, the Brusque Complex metasediments therefore contain no zircon grains sourced from syn-sedimentary igneous rocks. This is typical of rift basin or passive margin environments, where the influx of material into the basin is dominated by older grains sourced from the surrounding craton (Cawood et al., 2012).

4.5. Bimodal detrital zircon pattern and its possible sources

The two samples with bimodal age distribution contain the youngest zircon grains of all the studied samples, with between one third and one half of the total analysed grains dated in the Neoproterozoic. Using the youngest zircon age peak as a conservative estimate of the timing of sedimentation (Dickinson and Gehrels, 2009), the maximum age of sedimentation of the protolith is ca. 560 Ma (Fig. 7d). However, the much more robust peak at ca. 665 Ma is a safer benchmark for the maximum sedimentation age, considering the possibility of lead loss in the small number of younger grains during late-stage orogenic deformation or modern weathering. This post-dates the ca. 811 Ma minimum age of sedimentation constrained in this study by at least ca. 150 million years, implying the presence of two temporally distinct sedimentary protoliths. This observation remains difficult to confirm in the field, as the younger rocks appear to be metamorphosed at similar greenschist facies conditions as the low-grade Brusque Complex rocks, and they exhibit a deformation style indistinguishable from the high-strain zones of the Brusque Complex further inland (see Basei et al., 2011b). Indeed, it is possible that ancient lead loss could account for the Neoproterozoic zircon peaks by skewing Mesoproterozoic ages along the concordia towards younger values (e.g. Andersen et al., 2019). However, the large Neoproterozoic fraction (up to ca. 45%), the low-grade metamorphic conditions, and the remarkable similarity of the detrital signature to that of the adjacent Itajaí Basin (see section 4.6) favours the former interpretation. Further, two distinct depositional episodes have also recently been identified in the Porongos Complex of the central Dom Feliciano Belt foreland (Battisti et al., 2018; Höfig et al., 2018).

The ca. 2.20 Ga age peak and the spread of individual Mesoproterozoic and Paleoproterozoic dates between ca. 2.10–1.00 Ga (Fig. 7d) show similarities with the unimodal and polymodal groups respectively (Fig. 7b and c). The ca. 665 Ma age fits well with earliest estimates of the timing of orogenesis in the Dom Feliciano Belt (De Toni et al., 2020b), and thus the most likely protosource for the ca. 665 peak is the orogenic hinterland. The hinterland rocks record ca. 650–645 Ma zircon ages (Chemale et al., 2012) associated with orogenesis in the northern Dom Feliciano Belt, and up to ca. 665–660 Ma (Frantz et al., 2003; Masquelin et al., 2012) in the southern Dom Feliciano Belt. The number of grains between ca. 640–600 Ma fit with known ages from the Granite Belt, which intruded the orogenic hinterland between ca. 640–580 Ma (Chemale et al., 2012; Florisbal et al., 2012b).

Considering this possible protosource, the distribution pattern shown in Fig. 7d can thus be explained by a combination of recycled (meta) sedimentary rocks with a detrital zircon content matching the unimodal and polymodal sample groups of the Brusque Complex, and syn-orogenic rocks sourced directly from the orogenic hinterland.

4.6. Comparison with the Itajaí basin

The data suggest that the sedimentary protoliths of the bimodal sample group were sourced from erosion of the rising orogen, and thus they possibly represent syn-orogenic flysch- or molasse-type sediments similar to the Itajaí Basin. In support of this, the data from the Itajaí Basin show remarkably similar detrital zircon patterns, with the same primary age fractions with major peaks at ca. 650–550 Ma and

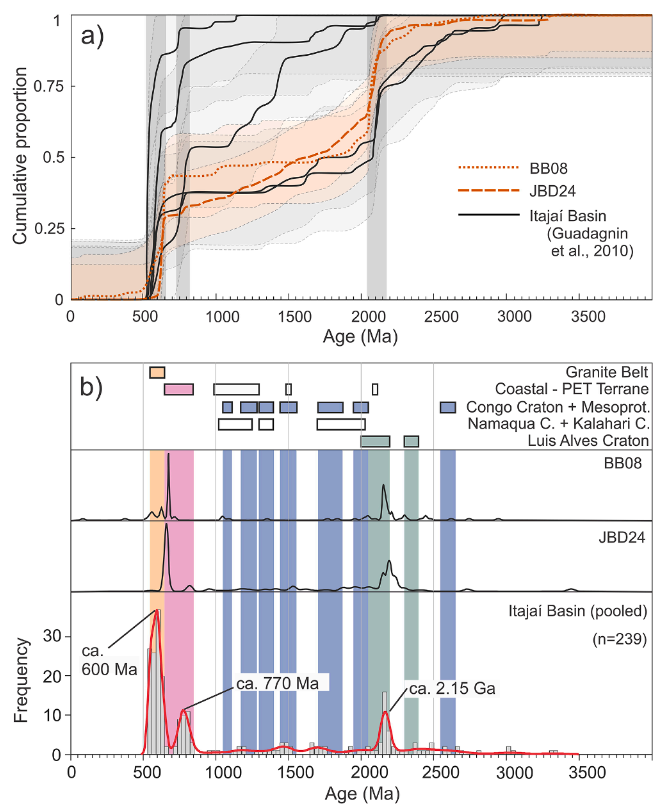

Fig. 8. Comparison between detrital zircon signatures of samples BB08, JBD24, and the Itajaí Basin: a) individual cumulative distribution curves with 95% confidence intervals (shaded columns delineate major common age fractions) b) KDEs and frequency histograms, with pooled Itajaí Basin data. Data for Itajaí Basin from Guadagnin et al. (2010). See Fig. 7 for age range references.

2.20–2.05 Ga, and a distribution of individual ages between ca. 2.00–1.00 Ga (Fig. 8a and b). Further, the ages corresponding to the small peak at ca. 560 Ma in the KDE curve are known from syn-sedimentary volcanism in the Itajaí Basin (Guadagnin et al., 2010), although the small number of grains younger than 600 Ma (8 grains) make this correlation only speculative.

The Itajaí Basin shows a typical orogenic foreland deformation style (e.g. Condie, 2016), with the margin closest to the foreland fold and thrust belt (i.e. the Schist Belt) showing stronger deformation than the opposite margin (Basei et al., 1998b; Guadagnin et al., 2010). Given the proposed source rocks and similarities with the Itajaí Basin sediments, we interpret samples JBD24 and BB08 as belonging to syn-orogenic sediments deposited in a foreland basin setting similar to the Itajaí Basin, or possibly part of the Itajaí Basin itself. The proximity and structural correlation of these rocks to the Itajaí–Perimbó Shear Zone (Fig. 2) lends support to this interpretation, as parts of the foreland basin closest to the leading edge of the fold-and-thrust belt would likely become tectonically interleaved with the Brusque Complex, making the deformation history between the two distinct protoliths indistinguishable.

4.7. Comparing the Kaoko–Dom Feliciano–Gariep Neoproterozoic foreland units

The Brusque Complex zircon distribution shares many similarities with the foreland fold-and-thrust belt cover sequences of the central Dom Feliciano Belt (Porongos Complex), the Kaoko Belt and the Gariep Belt. Fig. 9 compares detrital zircon data from these four regions, showing pooled data from various published detrital zircon studies (Andersen et al., 2018a; Gruber et al., 2011; Höfig et al., 2018; Hofmann et al., 2014; Konopásek et al., 2014, 2017; Pertille et al., 2015a, 2017), with samples grouped together based on the patterns as recognized in this study. The same two detrital zircon age distribution patterns as seen in the Brusque Complex are recorded in each of the other regions, with only minor differences (Fig. 9a and b). The Lavalleja Complex in Uruguay is often interpreted as the continuation of the Schist Belt in the southern Dom Feliciano Belt (Basei et al., 2008a). However, due to the small number of published detrital zircon datasets and poor age constraints (see Hueck et al., 2018b), the potential correlation of the Lavalleja Complex with the rest of the Schist Belt will not be further discussed.

The pooled polymodal group of the Porongos Complex samples matches well with the Brusque Complex rocks of this study (Fig. 9a and c). Using the *1-O* parameter of Andersen et al. (2016), they show a perfect pairwise overlap within 95% confidence intervals (*1-O* = 0.00). Like the Brusque Complex, the pooled data of the Porongos Complex is missing a 2.20 Ga peak, suggesting a majority African affinity for the sedimentary protosources (Fig. 9c). The similarities between the units imply that they shared the same source, which supports the interpretation that the Schist Belt of the Dom Feliciano Belt represents sediment deposited into a coeval and spatially related system of paleobasins.

The Porongos Complex unimodal group also shows a good match with the equivalent Brusque Complex rocks (Fig. 9b) (pairwise overlap *1-O* = 0.04). The Paleoproterozoic peaks between ca. 2.20–2.00 Ga in the samples with unimodal distribution have been linked with local basement rocks of the Encantadas Complex (Pertille et al., 2015a, 2017), and can also be correlated with ca. 2.50–2.00 Ga basement rocks of the Taquarembó Block, part of the Nico Pérez Terrane (Fig. 9d) (Oyhantçabal et al., 2011b, 2018 and references therein). The similarities in age between the Brazilian Nico Pérez Terrane (Taquarembó Block) and the Luis Alves Craton, most notably the presence of ca. 2.20 Ga rocks which are absent on the African side of the orogen, suggests that these cratonic blocks may represent a continuous basement unit.

For the Kaoko Belt, the two sample groups are pooled based on the patterns as recognised in this study and as constrained by the local stratigraphy (Fig. 9b and c) (Konopásek et al., 2014, 2017). Konopásek et al. (2017) showed that the pre-orogenic stratigraphic position of the Kaoko Belt metasedimentary rocks can be distinguished based on their detrital zircon signatures, with the lower sequences containing both Paleoproterozoic and Mesoproterozoic ages, and the upper sequences dominated by Paleoproterozoic ages only. The Kaoko Belt polymodal group shows strong similarities to the Brusque and Porongos Complexes (Fig. 9a) (pairwise overlap *1-O* = 0.03 and 0.02 respectively). The Mesoproterozoic peaks at ca. 1.55, 1.40 and 1.20 Ga match well with those from the Brusque Complex, and the same with the Paleoproterozoic peaks between ca. 2.10–1.80 Ga and the notable absence of ca. 2.20 Ga zircon. The only significant difference between the Mesoproterozoic detrital signals of the Kaoko and Dom Feliciano Belts is the presence of a ca. 1.05 Ga peak in the Kaoko Belt rocks (Fig. 9c), which can also be found in the foreland supra-crustal rocks of the Gariep Belt (Basei et al., 2005; Hofmann et al., 2014, 2015).

The pooled unimodal group shows a prominent Paleoproterozoic peak similar to the Brusque and Porongos complexes (Fig. 9d). However, the peak is centred at 1.80 Ga, resulting in a poor pairwise overlap comparison (Fig. 9b) (*1-O* = 0.11). This age peak fits with erosion of the local Congo Craton basement (Kröner et al., 2004; Luft et al., 2011).

Konopásek et al. (2017) recognised the gradual disappearance of Mesoproterozoic zircon from the upper parts of the Kaoko Belt supracrustal sequences, and suggested that this reflects the complete erosion of Mesoproterozoic supracrustal source rocks into the lower parts of the paleobasin, with the upper sequences representing erosion of the exposed local basement. Given evident similarities in detrital zircon signatures, it is possible that the Brusque Complex protolith was deposited in the same way; the rocks with polymodal zircon distribution representing the lower strata, and those with unimodal distribution the upper strata of the basin. This interpretation would necessitate a complete revision of the current stratigraphy of the Brusque Complex (Basei et al., 2006, 2011b), as the samples with polymodal and unimodal patterns come from all known stratigraphic levels. However, given problems with exposure in the northern Dom Feliciano Belt, it remains difficult to test this hypothesis, and is otherwise beyond the scope of this study.

Data from the Port Nolloth Zone of the Gariep Belt (Andersen et al., 2018a; Hofmann et al., 2014) also fit into unimodal and polymodal groups (Fig. 9 a and b). The polymodal group contains the same late Mesoproterozoic age peaks at ca. 1.30, 1.20 and 1.10 Ga (Fig. 9c), however there is a conspicuous absence of early Mesoproterozoic ages ca. 1.50 Ga, resulting in poor pairwise overlap comparisons (*1-O*: Brusque Complex = 0.18, Porongos Complex = 0.22, Kaoko Belt = 0.22). The Namaqua Metamorphic Complex outcropping along the western edge of the Kalahari Craton contains abundant Mesoproterozoic rocks dated between ca. 1.30–1.00 Ga (Becker et al., 2006; Bial et al., 2015; Clifford et al., 2004), and has no record of 1.50 Ga events, making these rocks the most likely protosource. The Gariep unimodal group is dominated by a single Paleoproterozoic peak at 1.90 Ga, which fits with basement of the Kalahari Craton (Fig. 9d) and closely matches the Kaoko Belt unimodal group (pairwise overlap *1-O* = 0.04). Andersen et al. (2018a) interpret the Gariep Belt detrital zircon signature as the result of mixing of various protosources during sedimentary recycling events prior to Neoproterozoic rifting, similar to the inferred Mesoproterozoic sedimentary cover of Konopásek et al. (2017). However, the differences between the Gariep Belt and the rest of the orogen clearly shows there is local variation in the recycled sediment protosources,

The similarities in detrital signatures strongly suggest that the pre-orogenic supracrustal rocks of the Brusque Complex, Porongos Complex and the Kaoko Belt partly shared the same source, and that the Gariep Belt shared at least some of the same protosources. The protosources for the polymodal group are clearly of African affinity, with no clear equivalent in the South American rock record, suggesting that the sediment was sourced from Mesoproterozoic (volcano-)sedimentary sequences containing recycled African detritus.

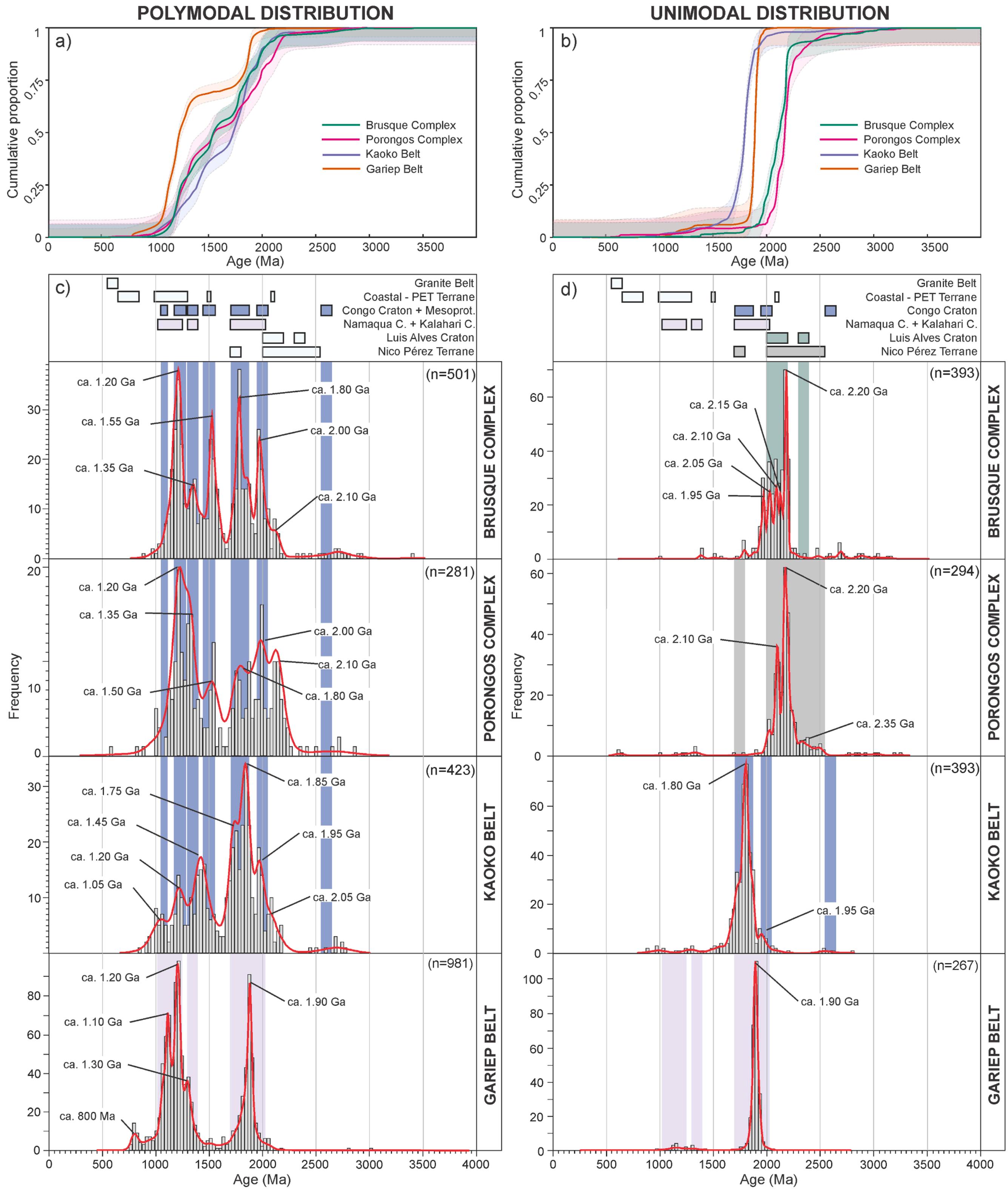

Fig. 9. Comparison between detrital zircon data of the pre-orogenic metasediments of the Brusque Complex, the Porongos Complex, the Kaoko Belt and the Gariep Belt (Porth Nolloth Zone): a) cumulative distribution curves for pooled polymodal group, b) cumulative distribution curves for pooled unimodal group, c) KDEs and histograms for polymodal group and d) KDEs and histograms for unimodal group. Data are grouped according to the patterns as identified in this study. Data sources: Brusque Complex from this study, Porongos Complex from Gruber et al. (2011); Höfig et al. (2018); Pertille et al. (2015a, 2015b, 2017), Kaoko Belt from Konopásek et al. (2014, 2017), Gariep Belt from Andersen et al. (2018a); Hofmann et al. (2014). Nico Pérez age range from Oyhantçabal et al. (2018) and references therein. See Fig. 7 for references for the remaining age-range bars.

4.8. Tectonic setting and evolution of the Schist Belt

Fig. 10 shows schematic cross sections across the northern Dom Feliciano Belt and the Kaoko Belt, outlining the proposed evolution of the Schist Belt as inferred from the Brusque Complex U–Pb zircon data and correlations with the other units. During the pre-rifting stage at ca. 1.0 Ga–850 Ma, the Congo and Luis Alves cratons were connected, accompanied by Mesoproterozoic terranes and cover sequences associated with the amalgamation of Rodinia (Fig. 10a) (Bial et al., 2015; Miller, 2012). The lack of detrital zircon close to the age of

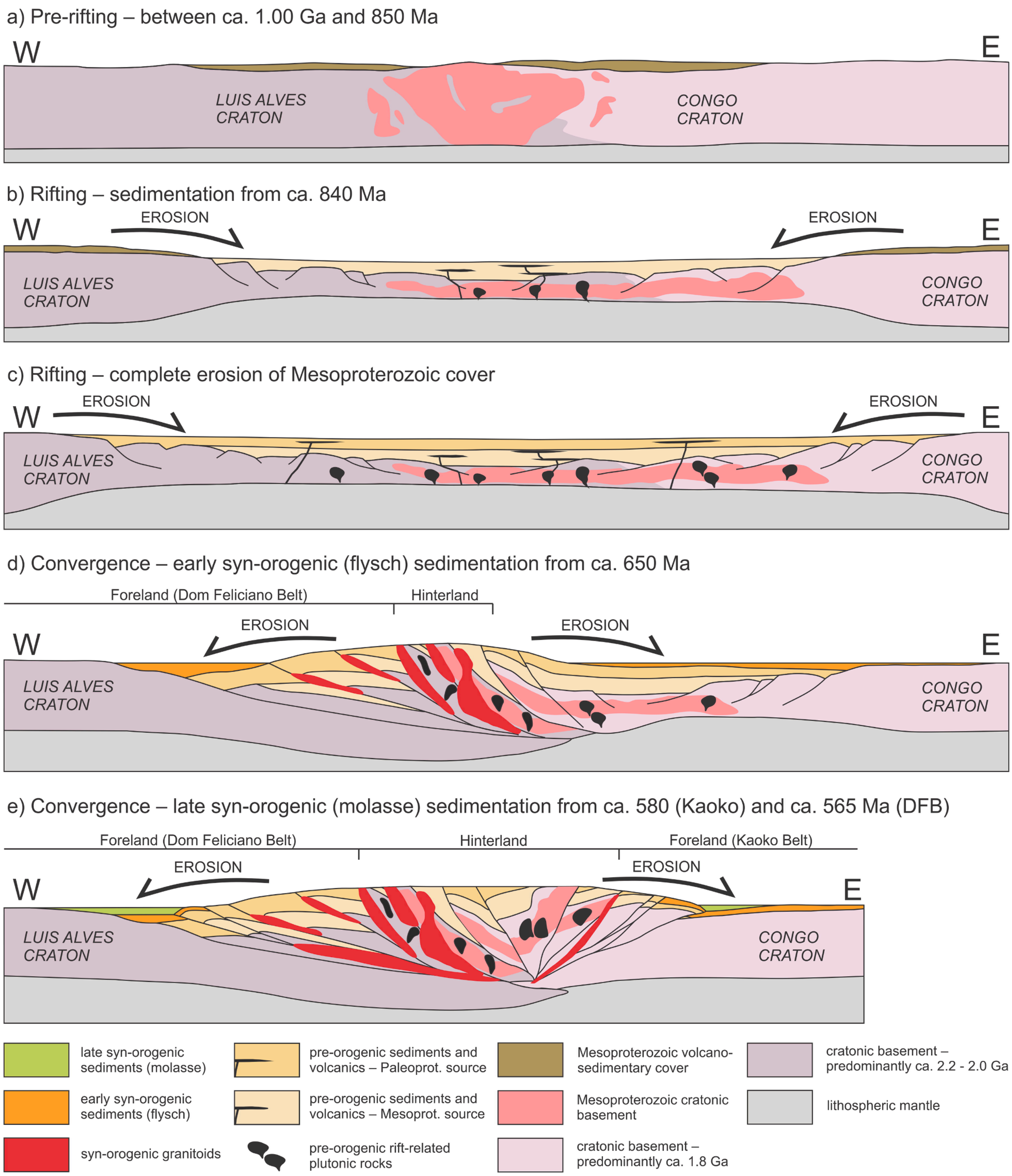

Fig. 10. Schematic cross sections outlining the proposed evolution of the Kaoko–Dom Feliciano Belt as inferred from U–Pb detrital zircon data: a) pre-rifting stage ca. 1.0 Ga–850 Ma, the Congo and Luis Alves cratons are connected, together with Mesoproterozoic terranes and cover sequences associated with Rodinia amalgamation, b) rifting from ca. 840 Ma, erosion of an extensive Mesoproterozoic cover sequence, sedimentation into the rift basin from at least ca. 810 Ma, c) rifting continues, complete erosion of the Mesoproterozoic cover and erosion of the Luis Alves and Congo Craton Basement, d) rift inversion and convergence leads to orogenesis at ca. 650, and the erosion of the rising hinterland leads to sedimentation (flysch) into *syn*-orogenic basins, e) continued convergence leads to the movement of the orogenic front towards the east and the formation of the Kaoko Belt, more sedimentation into both foreland basins, and late deformation in the west leads to deformation and metamorphism of the *syn*-orogenic sediments in the Brusque Complex.

sedimentation within the pre-orogenic sediments of the Kaoko–Dom Feliciano–Gariep Belt indicates the absence of magmatic activity on the crust of either basin margin at this time. Based on the model of Cawood et al. (2012), the pre-orogenic sediments of the Brusque Complex, Porongos Complex, Kaoko Belt and Gariep Belt best fit into an extensional setting, as the youngest 5% of zircon are>150 m.y. older than the age of sedimentation (Fig. 11). This finding supports a pure intracontinental rifting model for the formation of the Kaoko–Dom Feliciano–Gariep basin (Konopásek et al., 2018, 2020), and is in disagreement with various proposed subduction-collision models that place arc-magmatism inside and/or at the margin of the basin during or before its opening (De Toni et al., 2020a; Koester et al., 2016; Lenz et al., 2013; Martil et al., 2017). Based on this interpretation, the basin formed by intracontinental rifting from ca. 840 Ma (Basei et al., 2008b), with sedimentation into the Brusque Complex paleobasin from at least ca. 810 Ma (Fig. 10b). The complete erosion of the Mesoproterozoic cover sequences on the South American side, and the near-complete erosion on the African side, led to erosion of the Luis Alves and Congo cratons into the rift basin (Fig. 10c).

The period prior to convergence and orogenesis consisted of either 1) rift-drift transition and the development of the Adamastor Ocean (e.g. Basei et al., 2018 and references therein), or 2) continued intracontinental rifting and little to no oceanic spreading (e.g. Konopásek et al., 2020). Due to the continued lack of geochronological constraints on sedimentation into the Brusque Complex paleobasin, the duration of rifting cannot be inferred from our data. However, based on the lack of evidence of late-Neoproterozoic subduction-related metamorphism, the syn- to post- collisional nature of the Granite Belt (Bitencourt and Nardi, 1993, 2000; Florisbal et al., 2012a, 2012b), and evidence in the Kaoko Belt of crustal stretching and sedimentation up to ca. 660 Ma (Konopásek et al., 2020), the latter model is favoured for this interpretation.

Based on similarities with the Itajaí Basin, we interpret the syn-orogenic sediments of the Brusque Complex as belonging to a collisional foreland setting (Fig. 11). This suggests that, after rift inversion and convergence led to orogenesis at ca. 650 Ma (De Toni et al., 2020b), the eroding rising hinterland fed into proximal syn-orogenic basins (Fig. 10d). Finally, continued convergence led to the movement of the orogenic front towards the east (Fig. 10e), where the hinterland overrode the Congo Craton margin and led to the development of the

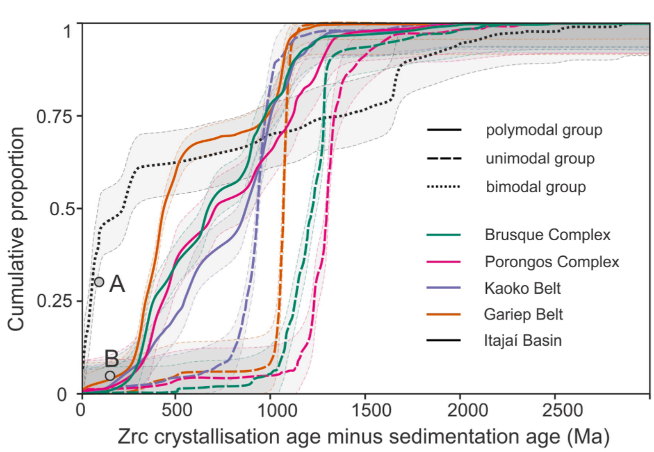

Fig. 11. Summary cumulative distribution function plot (with 95% confidence intervals) showing the difference between the detrital zircon crystallisation age and the sedimentation age of the various sample groups in this study. Point A and B are from Cawood et al. (2012), showing the points used to predict tectonic setting: A–youngest 30% of grains with $<$ 100 M.y. difference suggests convergent tectonic setting, $>$100 M.y. difference suggests collisional foreland setting; B–youngest 5% of grains with $<$ 150 M.y. difference suggests collisional foreland setting, $>$150 M.y. difference suggests extensional setting. Sedimentation ages are based on this study and from other sources in the text.

Kaoko Belt from ca. 580 Ma (Goscombe et al., 2003a; Konopásek et al., 2008). This late-stage convergence is reflected in the northern Dom Feliciano belt by the deformation of syn-orogenic sediments and their possible incorporation into the Brusque Complex (Fig. 10e).

4.9. Tectonic implications for pre-orogenic configuration

Based on pre-Atlantic plate reconstructions (Heine et al., 2013), and correlations between basement units (Konopásek et al., 2016), the Brusque Complex and Kaoko Belt foreland fold-and-thrust belts were located at approximately similar positions on either side of the orogenic hinterland (Fig. 12). The identification of a single source for significant parts of the pre-orogenic supracrustal rocks of the Dom Feliciano and Kaoko belts provides strong evidence to also correlate these rocks prior to early-Neoproterozoic rifting. Considering their deposition into a system of coeval, spatially related paleobasins, the Congo Craton, Luis Alves Craton and Nico Pérez Terrane must have been in close proximity at the onset of early-Neoproterozoic rifting (Fig. 10). Despite differences in protosources, the similarities in sedimentation history of the Gariep Belt suggests the involvement of the Kalahari Craton as well.

This means that, considering the correlation between the northern and central parts of the Schist Belt (Fig. 12), the rifting stage beginning at ca. 840–830 Ma (Basei et al., 2008b; Frimmel et al., 2001) may have involved a combined Luis Alves – Nico Pérez terrane rifting from the Congo and Kalahari cratons (Johansson, 2014; Konopásek et al., 2018). Although some authors argue that these cratonic fragments were separated by wide oceanic domains at the time of sedimentation (e.g. Foster et al., 2015), the data from this study support tectonic models that place these crustal blocks together in Rodinia at the onset of rifting (e.g. Konopásek et al., 2020; Oriolo et al., 2016; Oyhantçabal et al., 2011a; Philipp et al., 2016; Rapela et al., 2011).

The results of this study also contradict suggestions that the Major Gercino Shear Zone, and possibly the rest of the Southern Brazilian Shear Belt, separates distinct sedimentary rocks of African affinity on one side, and South American affinity on the other (Basei et al., 2000, 2008a). Although there are differences in source region for parts of the sedimentary protoliths that correlate with local African or South American basement, the Mesoproterozoic detrital zircon ages in both belts show a shared source with clear African affinity, and based on this study there is no indication that the Major Gercino Shear Zone represents a syn-sedimentary, pre-orogenic structure that separated basins with entirely different source regions.

5. Conclusions

1) U–Pb zircon dating of a felsic dyke intruding sedimentary rocks of the Brusque Complex constrains the minimum age of sedimentation into the Brusque Complex paleobasin at 811 $\pm$ 6 Ma. This age correlates with sedimentation age constraints in the Porongos Complex, Kaoko Belt and Gariep Belt, and with the age of pre-orogenic magmatism and sedimentation in the orogenic hinterland.
2) U–Pb detrital zircon dating of metamorphosed magmatic and sedimentary rocks of the Brusque Complex reveals three distinct sample groups. The first group shows a polymodal age distribution, with peaks in both the Meso- and Paleoproterozoic. The second group contains only Paleoproterozoic ages, dominated by a single age peak. The third group shows a mostly bimodal age distribution, with a major Neoproterozoic age fraction.
3) Potential protosources for the Mesoproterozoic zircon grains in the polymodal sample group are all of African affinity. The most likely source for the sediment was Mesoproterozoic sedimentary cover of the Congo Craton bearing recycled zircon grains. We suggest that the Mesoproterozoic sediment also covered the Luis Alves Craton prior to Neoproterozoic rifting. The Paleoproterozoic zircon grains from the unimodal sample group were likely sourced from local basement represented by the Luis Alves Craton and Camboriú Complex.

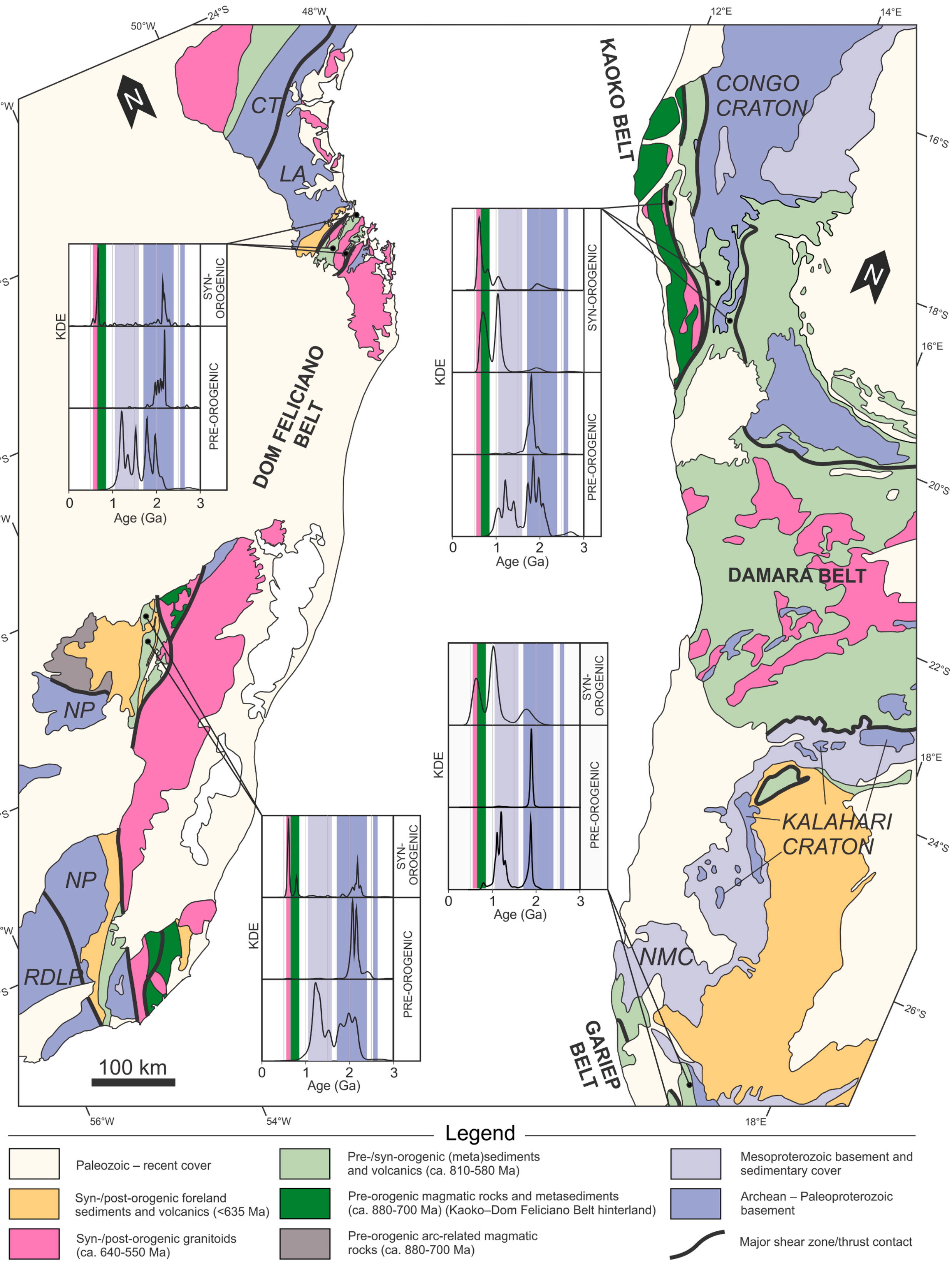

Fig. 12. Overview map showing the correlation of metasedimentary rocks of the Kaoko–Dom Feliciano Belt orogenic forelands (modified after Hueck et al., 2018b; Konopásek et al., 2017; McCourt et al., 2013; Oyhantçabal et al., 2011b; and Passarelli et al., 2018). NMC = Namaqua Metamorphic Complex, RDLP = Rio de la Plata Craton, NP = Nico Pérez Terrane, LA = Luis Alves Craton, CT = Curitiba Terrane. For KDE figures see Fig. 7 for references. Coloured bars behind KDE curves represent probable protosource regions, and the colours correspond to those regions as shown in the map.

4) The Neoproterozoic zircon grains in the bimodal sample group post-date sedimentation in the Brusque Complex paleobasin as constrained in this study, suggesting that these rocks belong to a later paleobasin formed in a different tectonic environment. Similarities with the Itajaí Basin suggest that they represent parts of a syn-orogenic foreland basin, with sediment sourced from the rising orogenic hinterland. The rocks were likely tectonically interleaved with the Brusque Complex during late-stage orogenic deformation.
5) The absence of Neoproterozoic zircon at or close to the age of sedimentation in the pre-orogenic sediments of the Brusque Complex implies that the paleobasin did not evolve within a convergent tectonic setting, supporting a pure intracontinental rifting model for basin formation.
6) Comparison of pre-orogenic Brusque Complex detrital zircon data with equivalent rocks in the Porongos Complex, Kaoko Belt and Gariep Belt indicates a shared source and/or shared basin evolution, implying that these sediments were deposited into a system of coeval and spatially related paleobasins. The data imply that the Luis Alves Craton, Congo Craton, Nico Pérez Terrane and Kalahari Craton were in close proximity at the start of Neoproterozoic rifting and the breakup of Rodinia.

CRediT authorship contribution statement

Jack James Percival: Conceptualization, Methodology, Formal analysis, Investigation, Writing - original draft, Visualization. **Jiří Konopásek:** Conceptualization, Methodology, Resources, Funding acquisition, Writing - review & editing, Project administration, Supervision. **Ragnhild Eiesland:** Conceptualization, Methodology, Formal analysis, Investigation. **Jiří Sláma:** Investigation, Formal analysis, Validation, Data curation. **Roberto Sacks de Campos:** Investigation, Writing - review & editing. **Matheus Ariel Battisti:** Investigation, Writing - review & editing. **Maria de Fátima Bitencourt:** Supervision, Writing - review & editing.

Declaration of Competing Interest

The authors declare that they have no known competing financial interests or personal relationships that could have appeared to influence the work reported in this paper.

Acknowledgements

This work was supported by the Norwegian Centre for International Cooperation in Education (SIU), the Norwegian Agency for International Cooperation and Quality Enhancement in Higher Education (Diku), and the Coordenação de Aperfeicoamento de Pessoal de Nível Superior (CAPES) in Brazil through the grant projects no. UTF-2016-CAPES-SIU10024 and UTF-2018-CAPES-Diku-10004. J. Konopásek acknowledges financial support of the Czech Science Foundation, grant no. 18-24281S. J. Sláma was supported by the ASCR institutional support RVO 67985831. Acknowledgements and thanks to D. Lyra for fieldwork assistance. The authors are grateful to T. Andersen and an anonymous reviewer for their helpful reviews.

Appendix A. Supplementary data

Supplementary data to this article can be found online at https://doi.org/10.1016/j.precamres.2020.106060.

References

Almeida, R.P., Janikian, L., Fragoso-Cesar, A.R.S., Fambrini, G.L., 2010. The Ediacaran to Cambrian Rift System of Southeastern South America: tectonic Implications. J. Geol. 118 (2), 145–161. https://www.doi.org/10.1086/649817.

Andersen, T., Elburg, M., Cawthorn-Blazeby, A., 2016. U-Pb and Lu–Hf zircon data in young sediments reflect sedimentary recycling in eastern South Africa. J. Geol. Soc. 173 (2), 337–351. https://doi.org/10.1144/jgs2015-006.

Andersen, T., Elburg, M.A., van Niekerk, H.S., Ueckermann, H., 2018a. Successive sedimentary recycling regimes in southwestern Gondwana: Evidence from detrital zircons in Neoproterozoic to Cambrian sedimentary rocks in southern Africa. Earth-Sci. Rev., vol. 181, pp. 43-60. Doi: 10.1016/j.earscirev.2018.04.001.

Andersen, T., Kristoffersen, M., Elburg, M.A., 2018b. Visualizing, interpreting and comparing detrital zircon age and Hf isotope data in basin analysis – a graphical approach. Basin Res., vol. 30, no. 1, pp. 132-147. Doi: 10.1111/bre.12245.

Andersen, T., Elburg, M.A., Magwaza, B.N., 2019. Sources of bias in detrital zircon geochronology: Discordance, concealed lead loss and common lead correction. Earth-Sci. Rev. 197, 102899 https://doi.org/10.1016/j.earscirev.2019.102899.

Basei, M.A.S., McReath, I., Siga Jr., O., 1998a. The Santa Catarina Granulite Complex of Southern Brazil: A Review. Gondwana Res. 1 (3–4), 383–391. https://www.doi.org/10.1016/S1342-937X(05)70854-6.

Basei, M.A.S., Citroni, S.B., Siga Jr, O., 1998b. Stratigraphy and age of fini-Proterozoic basins of Parana and Santa Catarina States, southern Brazil. Boletim IG-USP, Serie Cientifica 29, 195–216.

Basei, M.A.S., Siga, Jr O., Reis Neto, J.M.d., Passarelli, C.R., Prazeres, H., Kaulfuss, G., Sato, K., Lima, P.S., 1999. Paleoproterozoic granulitic belts of the Brazilian southern region (PR-SC). II South American Symposium on Isotope Geology. pp. 291-294. Cordoba, Argentina: Subsecretaría de Minería de la Nación.

Basei, M.A.S., Siga, Jr O., Masquelin, H., Harara, O.M., Reis Neto, J.M., Preciozzi, F., 2000. The Dom Feliciano Belt of Brazil and Uruguay and its Foreland Domain, the Rio de la Plata Craton: framework, tectonic evolution and correlation with similar provinces of Southwestern Africa. In Cordani U. G., et al. eds. Tectonic Evolution of South America. pp. 311-334. Rio de Janeiro, Brazil: Geological Society.

Basei, M.A.S., Frimmel, H.E., Nutman, A.P., Preciozzi, F., Jacob, J., 2005. A connection between the Neoproterozoic Dom Feliciano (Brazil/Uruguay) and Gariep (Namibia/South Africa) orogenic belts - Evidence from a reconnaissance provenance study. Precambrian Res. 139 (3–4), 195–221. https://www.doi.org/10.1016/j.precamres.2005.06.005.

Basei, M.A.S., Campos Neto, M.C., Castro, N.A., Santos, P.R., Siga, Jr. O., Passarelli, C.R., 2006. Mapa Geológico 1:100.000 das Folhas Brusque e Vidal Ramos, SC, Convênio USP-CPRM. XLII Congresso Brasileiro de Geologia, Aracaju, SE.

Basei, M.A.S., Frimmel, H.E., Nutman, A.P., Preciozzi, F., 2008a. West Gondwana amalgamation based on detrital zircon ages from Neoproterozoic Ribeira and Dom Feliciano belts of South America and comparison with coeval sequences from SW Africa. Geol. Soc. Spec. Publ. 294 (1), 239–256. https://www.doi.org/10.1144/SP294.13.

Basei, M.A.S., Grasso, C.B., Vlach, S.R.F., Nutman, A., Siga, Jr. O., Osaki, L.S., 2008b. A-type rift-related granite and the lower cryogenian age for the beginning of the Brusque Belt basin. Proceedings of South American Symposium on Isotope Geology. San Carlos de Bariloche, Argentina.

Basei, M.A.S., Nutman, A., Siga, Jr O., Passarelli, C.R., Drukas, C.O., 2009. The Evolution and Tectonic Setting of the Luis Alves Microplate of Southeastern Brazil: An Exotic Terrane during the Assembly of Western Gondwana. In Gaucher C., et al. eds. Developments in Precambrian Geology. pp. 273-291. Elsevier Doi: 10.1016/S0166-2635(09)01620-X.

Basei, M.A.S., Drukas, C.O., Nutman, A.P., Wemmer, K., Dunyi, L., Santos, P.R., Passarelli, C.R., Campos Neto, M.C., Siga Jr O., Osako, L., 2011a. The Itajaí foreland basin: A tectono-sedimentary record of the Ediacaran period, Southern Brazil. Int. J. Earth Sci., vol. 100, pp. 543–569. https://www.doi.org/10.1007/s00531-010-0604-4.

Basei, M.A.S., Campos Neto, M.C., Castro, N.A., Nutman, A.P., Wemmer, K., Yamamoto, M.T., Hueck, M., Osako, L., Siga, Jr O., Passarelli, C.R., 2011b. Tectonic evolution of the Brusque Group, Dom Feliciano belt, Santa Catarina, Southern Brazil. J. S. Am. Earth Sci., vol. 32, no. 4, pp. 324-350. https://www.doi.org/10.1016/j.jsames.2011.03.016.

Basei, M.A.S., Peel, E., Sánchez, Bettucci L., Preciozzi, F., Nutman, A.P., 2011c. The basement of the Punta del Este Terrane (Uruguay): an African Mesoproterozoic fragment at the eastern border of the South American Río de La Plata craton. Int. J. Earth Sci. 100, 289–304. https://doi.org/10.1007/s00531-010-0623-1.

Basei, M.A.S., Frimmel, H.E., Campos Neto, M.d.C., de Araujo, C.E.G., de Castro, N.A., Passarelli, C.R., 2018. The Tectonic History of the Southern Adamastor Ocean Based on a Correlation of the Kaoko and Dom Feliciano Belts. In Siegesmund S., et al. eds. Geology of Southwest Gondwana. pp. 63-85. 1st ed. Cham: Springer International Publishing Doi: 10.1007/978-3-319-68920-3_3.

Battisti, M.A., Bitencourt, M.F., De Toni, G.B., Nardi, L.V.S., Konopásek, J., 2018. Metavolcanic rocks and orthogneisses from Porongos and Várzea do Capivarita complexes: A case for identification of tectonic interleaving at different crustal levels from structural and geochemical data in southernmost Brazil. J. S. Am. Earth Sci. 88, 253–274. https://doi.org/10.1016/j.jsames.2018.08.009.

Becker, T., Schreiber, U., Kampunzu, A.B., Armstrong, R., 2006. Mesoproterozoic rocks of Namibia and their plate tectonic setting. J. Afr. Earth Sci. 46 (1–2), 112–140. https://doi.org/10.1016/j.jafrearsci.2006.01.015.

Bettucci, L.S., Cosarinsky, M., Ramos, V.A., 2001. Tectonic Setting of the Late Proterozoic Lavalleja Group (Dom Feliciano Belt). Uruguay. Gondwana Res. 4 (3), 395–407. https://doi.org/10.1016/S1342-937X(05)70339-7.

Bial, J., Büttner, S.H., Frei, D., 2015. Formation and emplacement of two contrasting late-Mesoproterozoic magma types in the central Namaqua Metamorphic Complex (South Africa, Namibia): Evidence from geochemistry and geochronology. Lithos 224–225, 272–294. https://doi.org/10.1016/j.lithos.2015.02.021.

Bitencourt, M.F., Nardi, L., 1993. Late- to Post-collisional Brasiliano Magmatism in Southernmost Brazil. Anais da Academia Brasileira de Ciências 65, 3–16.

Bitencourt, M.F., Nardi, L.V.S., 2000. Tectonic setting and sources of magmatism related to the southern Brazilian shear belt. Rev. Brasil. Geocienc. 30 (1), 186–189.
Bybee, G.M., Hayes, B., Owen-Smith, T.M., Lehmann, J., Ashwal, L.D., Brower, A.M., Hill, C.M., Corfu, F., Manga, M., 2019. Proterozoic massif-type anorthosites as the archetypes of long-lived (≥100 Myr) magmatic systems—New evidence from the Kunene Anorthosite Complex (Angola). Precambrian Res. 332, 105393 https://doi.org/10.1016/j.precamres.2019.105393.
Campos, R.S., Philipp, R.P., Massonne, H.-J., Chemale Jr, F., Theye, T., 2011. Petrology and isotope geology of mafic to ultramafic metavolcanic rocks of the Brusque Metamorphic Complex, southern Brazil. Int. Geol. Rev. 54 (6), 686–713. https://doi.org/10.1080/00206814.2011.569393.
Campos, R.S., Philipp, R.P., Massonne, H.-J., Chemale Jr, F., 2012. Early post-collisional Brasiliano magmatism in Botuverá region, Santa Catarina, southern Brazil: Evidence from petrology, geochemistry, isotope geology and geochronology of the diabase and lamprophyre dikes. J. S. Am. Earth Sci. 37, 266–278. https://doi.org/10.1016/j.jsames.2012.02.005.
Cawood, P.A., Hawkesworth, C.J., Dhuime, B., 2012. Detrital zircon record and tectonic setting. Geology 40 (10), 875–878. https://doi.org/10.1130/g32945.1.
Chemale, F., Philipp, R.P., Dussin, I.A., Formoso, M.L.L., Kawashita, K., Berttotti, A.L., 2011. Lu–Hf and U-Pb age determination of Capivarita Anorthosite in the Dom Feliciano Belt. Brazil. Precambrian Res. 186 (1–4), 117–126. https://doi.org/10.1016/j.precamres.2011.01.005.
Chemale, F., Mallmann, G., Bitencourt, M.F., Kawashita, K., 2012. Time constraints on magmatism along the Major Gercino Shear Zone, southern Brazil: Implications for West Gondwana reconstruction. Gondwana Res. 22 (1), 184–199. https://doi.org/10.1016/j.gr.2011.08.018.
Clifford, T.N., Barton, E.S., Stern, R.A., Duchesne, J.-C., 2004. U-Pb Zircon Calendar for Namaquan (Grenville) Crustal Events in the Granulite-facies Terrane of the O'okiep Copper District of South Africa. J. Petrol. 45 (4), 669–691. https://doi.org/10.1093/petrology/egg097.
Condie, K.C., 2016. Chapter 3 - Tectonic Settings. In: Condie, K.C. (Ed.), Earth as an Evolving Planetary System (Third Edition). Academic Press, pp. 43–88. https://doi.org/10.1016/B978-0-12-803689-1.00003-1.
De Toni, G.B., Bitencourt, M.F., Nardi, L.V.S., Florisbal, L.M., Almeida, B.S., Geraldes, M., 2020a. Dom Feliciano Belt orogenic cycle tracked by its pre-collisional magmatism: The Tonian (ca. 800 Ma) Porto Belo Complex and its correlations in southern Brazil and Uruguay. Precambrian Res. 342, 105702 https://doi.org/10.1016/j.precamres.2020.105702.
De Toni, G.B., Bitencourt, M.F., Konopásek, J., Martini, A., Andrade, P.H.S., Florisbal, L. M., Campos, R.S., 2020b. Transpressive strain partitioning between the Major Gercino Shear Zone and the Tijucas Fold Belt, Dom Feliciano Belt, Santa Catarina, southern Brazil. J. Struct. Geol. 136, 104058 https://doi.org/10.1016/j.jsg.2020.104058.
Dickinson, W.R., Gehrels, G.E., 2009. Use of U-Pb ages of detrital zircons to infer maximum depositional ages of strata: A test against a Colorado Plateau Mesozoic database. Earth Planet. Sci. Lett. 288 (1–2), 115–125. https://doi.org/10.1016/j.epsl.2009.09.013.
Drüppel, K., Littmann, S., Romer, R.L., Okrusch, M., 2007. Petrology and isotope geochemistry of the Mesoproterozoic anorthosite and related rocks of the Kunene Intrusive Complex. NW Namibia. Precambrian Res. 156 (1–2), 1–31. https://doi.org/10.1016/j.precamres.2007.02.005.
Evans, D.A.D., 2009. The palaeomagnetically viable, long-lived and all-inclusive Rodinia supercontinent reconstruction. Geol. Soc. Spec. Publ. 327 (1), 371. https://doi.org/10.1144/SP327.16.
Florisbal, L.M., Bitencourt, M.F., Nardi, L.V.S., Conceição, R.V., 2009. Early post-collisional granitic and coeval mafic magmatism of medium- to high-K tholeiitic affinity within the Neoproterozoic Southern Brazilian Shear Belt. Precambrian Res. 175 (1–4), 135–148. https://doi.org/10.1016/j.precamres.2009.09.003.
Florisbal, L.M., Bitencourt, M.F., Janasi, V.d.A., Nardi, L.V.S., Heaman, L.M., 2012a. Petrogenesis of syntectonic granites emplaced at the transition from thrusting to transcurrent tectonics in post-collisional setting: Whole-rock and Sr–Nd–Pb isotope geochemistry in the Neoproterozoic Quatro Ilhas and Mariscal Granites, Southern Brazil. Lithos, vol. 153, pp. 53-71. Doi: 10.1016/j.lithos.2012.04.031.
Florisbal, L.M., de Assis Janasi, V., Bitencourt, M.F., Heaman, L.M., 2012b. Space–time relation of post-collisional granitic magmatism in Santa Catarina, southern Brazil: U-Pb LA-MC-ICP-MS zircon geochronology of coeval mafic–felsic magmatism related to the Major Gercino Shear Zone. Precambrian Res. 216–219, 132–151. https://doi.org/10.1016/j.precamres.2012.06.015.
Foster, D.A., Goscombe, B.D., Newstead, B., Mapani, B., Mueller, P.A., Gregory, L.C., Muvangua, E., 2015. U-Pb age and Lu–Hf isotopic data of detrital zircons from the Neoproterozoic Damara Sequence: Implications for Congo and Kalahari before Gondwana. Gondwana Res. 28 (1), 179–190. https://doi.org/10.1016/j.gr.2014.04.011.
Frantz, J., McNaughton, N.J., Marques, J., Hartmann, L.A., Botelho, N., Caravaca, G., 2003. Shrimp U-Pb zircon ages of granitoids from southernmost Brazil: constraints on the temporal evolution on the Dorsal do Canguçu transcurrent shear zone and the eastern Dom Feliciano Belt. IV South American Symposium on Isotope Geology, pp. 174-177.
Frimmel, H.E., Hartnady, C.J.H., Koller, F., 1996. Geochemistry and tectonic setting of magmatic units in the Pan-African Gariep Belt. Namibia. Chem. Geol. 130 (1–2), 101–121. https://doi.org/10.1016/0009-2541(95)00188-3.
Frimmel, H.E., Zartman, R.E., Späth, A., 2001. The Richtersveld Igneous Complex, South Africa: U-Pb Zircon and Geochemical Evidence for the Beginning of Neoproterozoic Continental Breakup. J. Geol. 109 (4), 493–508. https://doi.org/10.1086/320795.
Frimmel, H.E., Fölling, P.G., 2004. Late Vendian Closure of the Adamastor Ocean: Timing of Tectonic Inversion and Syn-orogenic Sedimentation in the Gariep Basin. Gondwana Res. 7 (3), 685–699. https://doi.org/10.1016/S1342-937X(05)71056-X.
Frimmel, H.E., Basei, M.A.S., Gaucher, C., 2011. Neoproterozoic geodynamic evolution of SW-Gondwana: a southern African perspective. Int. J. Earth Sci. 100, 323–354. https://doi.org/10.1086/320795.
Frimmel, H.E., 2018. The Gariep Belt. In: Siegesmund, S. (Ed.), Geology of Southwest Gondwana, 1st ed. Springer International Publishing, Cham, pp. 353–386.
Gaucher, C., Frei, R., Chemale Jr, F., Frei, D., Bossi, J., Martínez, G., Chiglino, L., Cernuschi, F., 2011. Mesoproterozoic evolution of the Río de la Plata Craton in Uruguay: at the heart of Rodinia? Int. J. Earth Sci. 100 (2), 273–288. https://doi.org/10.1007/s00531-010-0562-x.
Goscombe, B., Hand, M., Gray, D., Mawby, J.O., 2003a. The Metamorphic Architecture of a Transpressional Orogen: the Kaoko Belt. Namibia. J. Petrol. 44 (4), 679–711. https://doi.org/10.1093/petrology/44.4.679.
Goscombe, B., Hand, M., Gray, D., 2003b. Structure of the Kaoko Belt, Namibia: progressive evolution of a classic transpressional orogen. J. Struct. Geol. 25 (7), 1049–1081. https://doi.org/10.1016/S0191-8141(02)00150-5.
Goscombe, B., Gray, D., Armstrong, R., Foster, D.A., Vogl, J., 2005a. Event geochronology of the Pan-African Kaoko Belt. Namibia. Precambrian Res. 140 (3–4), 103.e1–103.e41. https://doi.org/10.1016/j.precamres.2005.07.003.
Goscombe, B., Gray, D., Hand, M., 2005b. Extrusional Tectonics in the Core of a Transpressional Orogen; the Kaoko Belt. Namibia. J. Petrol. 46 (6), 1203–1241. https://doi.org/10.1093/petrology/egi014.
Gray, D.R., Foster, D.A., Meert, J.G., Goscombe, B.D., Armstrong, R., Trouw, R.A.J., Passchier, C.W., 2008. A Damara Orogen perspective on the assembly of southwestern Gondwana. In: Pankhurst, R.J. (Ed.), West Gondwana: Pre-Cenozoic Correlations Across the South Atlantic Region. Geological Society Special Publications, London, pp. 257–278. Doi: 10.1144/SP294.14.
Gross, A.O.M.S., Droop, G.T.R., Porcher, C.C., Fernandes, L.A.D., 2009. Petrology and thermobarometry of mafic granulites and migmatites from the Chafalote Metamorphic Suite: New insights into the Neoproterozoic P-T evolution of the Uruguayan—Sul-Rio-Grandense shield. Precambrian Res. 170 (3–4), 157–174. https://doi.org/10.1016/j.precamres.2009.01.011.
Gruber, L., Porcher, C., Lenz, C., Fernandes, L., 2011. Proveniência de metassedimentos das sequências Arroio Areião, Cerro Cambará e Quartzo Milonitos no Complexo Metamórfico Porongos, Santana da Boa Vista. RS. Pesquisas em Geociencias 38 (3), 205–224. https://doi.org/10.22456/1807-9806.35157.
Gruber, L., Porcher, C.C., Koester, E., Bertotti, A.L., Lenz, C., Fernandes, L.A.D., Remus, M.V.D., 2016. Isotope geochemistry and geochronology of syn-depositional volcanism in Porongos Metamorphic Complex, Santana da Boa Vista Antiform, Dom Feliciano Belt, Brazil: Onset of an 800 Ma continental arc. J. Sediment. Environ. 1 (2), 196–215. https://doi.org/10.12957/jse.2016.22722.
Guadagnin, F., Chemale Jr, F., Dussin, I.A., Jelinek, A.R., dos Santos, M.N., Borba, M.L., Justino, D., Bertotti, A.L., Alessandretti, L., 2010. Depositional age and provenance of the Itajaí Basin, Santa Catarina State, Brazil: Implications for SW Gondwana correlation. Precambrian Res. 180 (3–4), 156–182. https://doi.org/10.1016/j.precamres.2010.04.002.
Hartmann, L.A., Basei, M.A.S., Simas, M.W., 1999. Geochemistry of the Lower Proterozoic granulite-facies Grant syenite gneiss, Barra Velha, Santa Catarina State, southern Brazil. Pesquisas em Geociencias 25, 3–9.
Hartmann, L.A., Santos, J.O.S., McNaughton, N.J., Vasconcellos, M.A.Z., da Silva, L.C., 2000. Ion microprobe (SHRIMP) dates complex granulite from Santa Catarina, southern Brazil. Anais da Academia Brasileira de Ciencias 72 (4), 559–572. https://doi.org/10.1590/S0001-37652000000400007.
Hartmann, L.A., Bitencourt, M.F., Santos, J.O.S., McNaughton, N.J., Rivera, C.B., Betiollo, L., 2003. Prolonged Paleoproterozoic magmatic participation in the Neoproterozoic Dom Feliciano belt, Santa Catarina, Brazil, based on zircon U-Pb SHRIMP geochronology. J. S. Am. Earth Sci. 16 (6), 477–492. https://doi.org/10.1016/j.jsames.2003.04.001.
Hartmann, L.A., Savian, J.F., Lopes, W.R., 2015. Airborne geophysical characterization of geotectonic relationships in the southern Ribeira Belt, Luís Alves Craton, and northern Dom Feliciano Belt. Brazilian Shield. Int. Geol. Rev. 58 (4), 471–488. https://doi.org/10.1080/00206814.2015.1089424.
Heine, C., Zoethout, J., Müller, R.D., 2013. Kinematics of the South Atlantic rift. Solid Earth 4 (2), 215–253. https://doi.org/10.5194/se-4-215-2013.
Hoffman, P.F., Halverson, G.P., 2008. Otavi Group of the western Northern Platform, the Eastern Kaoko Zone and the western Northern Margin Zone. In: Miller, R.M. (Ed.), The Geology of Namibia. Geological Survey Namibia, Namibia, pp. 69–136.
Höfig, D.F., Marques, J.C., Basei, M.A.S., Giusti, R.O., Kohlrausch, C., Frantz, J.C., 2018. Detrital zircon geochronology (U-Pb LA-ICP-MS) of syn-orogenic basins in SW Gondwana: New insights into the Cryogenian-Ediacaran of Porongos Complex, Dom Feliciano Belt, southern Brazil. Precambrian Res. 306, 189–208. https://doi.org/10.1016/j.precamres.2017.12.031.
Hofmann, M., Linnemann, U., Hoffmann, K.-H., Gerdes, A., Eckelmann, K., Gärtner, A., 2014. The Namuskluft and Dreigratberg sections in southern Namibia (Kalahari Craton, Gariep Belt): a geological history of Neoproterozoic rifting and recycling of cratonic crust during the dispersal of Rodinia until the amalgamation of Gondwana. Int. J. Earth Sci. 103 (5), 1187–1202. https://doi.org/10.1007/s00531-013-0949-6.
Hofmann, M., Linnemann, U., Hoffmann, K.-H., Germs, G., Gerdes, A., Marko, L., Eckelmann, K., Gärtner, A., Krause, R., 2015. The four Neoproterozoic glaciations of southern Namibia and their detrital zircon record: The fingerprints of four crustal growth events during two supercontinent cycles. Precambrian Res. 259, 176–188. https://doi.org/10.1016/j.precamres.2014.07.021.
Hueck, M., Basei, M.A.S., Wemmer, K., Oriolo, S., Heidelbach, F., Siegesmund, S., 2018a. Evolution of the Major Gercino Shear Zone in the Dom Feliciano Belt, South Brazil,

and implications for the assembly of southwestern Gondwana. Int. J. Earth Sci. 108 (2), 403–425. https://doi.org/10.1007/s00531-018-1660-4.
Hueck, M., Oyhantçabal, P., Basei, M., Siegesmund, S., 2018b. The Dom Feliciano Belt in Southern Brazil and Uruquay. In: Siegesmund, S. (Ed.), Geology of Southwest Gondwana, 1st ed. Springer International Publishing, Cham, pp. 267–302.
Hueck, M., Basei, M.A.S., Castro, N.A.d., 2019. Tracking the sources and the evolution of the late Neoproterozoic granitic intrusions in the Brusque Group, Dom Feliciano Belt, South Brazil: LA-ICP-MS and SHRIMP geochronology coupled to Hf isotopic analysis. Precambrian Res. 338, 105566 https://doi.org/10.1016/j.precamres.2019.105566.
Johansson, Å., 2014. From Rodinia to Gondwana with the 'SAMBA' model—A distant view from Baltica towards Amazonia and beyond. Precambrian Res. 244, 226–235. https://doi.org/10.1016/j.precamres.2013.10.012.
Koester, E., Porcher, C.C., Pimentel, M.M., Fernandes, L.A.D., Vignol-Lelarge, M.L., Oliveira, L.D., Ramos, R.C., 2016. Further evidence of 777 Ma subduction-related continental arc magmatism in Eastern Dom Feliciano Belt, southern Brazil: The Chácara das Pedras Orthogneiss. J. S. Am. Earth Sci. 68, 155–166. https://www.doi.org/10.1016/j.jsames.2015.12.006.
Konopásek, J., Kosler, J., Tajcmanova, L., Ulrich, S., Kitt, S., 2008. Neoproterozoic igneous complex emplaced along major tectonic boundary in the Kaoko Belt (NW Namibia): ion probe and LA-ICP-MS dating of magmatic and metamorphic zircons. J. Geol. Soc. London 165 (1), 153–165.
Konopásek, J., Košler, J., Sláma, J., Janoušek, V., 2014. Timing and sources of pre-collisional Neoproterozoic sedimentation along the SW margin of the Congo Craton (Kaoko Belt, NW Namibia). Gondwana Res. 26 (1), 386–401. https://www.doi.org/10.1016/j.gr.2013.06.021.
Konopásek, J., Sláma, J., Košler, J., 2016. Linking the basement geology along the Africa-South America coasts in the South Atlantic. Precambrian Res. 280, 221–230. https://www.doi.org/10.1016/j.precamres.2016.05.011.
Konopásek, J., Hoffmann, K.-H., Sláma, J., Košler, J., 2017. The onset of flysch sedimentation in the Kaoko Belt (NW Namibia) – Implications for the pre-collisional evolution of the Kaoko-Dom Feliciano–Gariep orogen. Precambrian Res. 298, 220–234. https://doi.org/10.1016/j.precamres.2017.06.017.
Konopásek, J., Janoušek, V., Oyhantçabal, P., Sláma, J., Ulrich, S., 2018. Did the circum-Rodinia subduction trigger the Neoproterozoic rifting along the Congo-Kalahari Craton margin? Int. J. Earth Sci. 107 (5), 1859–1894. https://www.doi.org/10.1007/s00531-017-1576-4.
Konopásek, J., Cavalcante, C., Fossen, H., Janoušek, V., 2020. Adamastor – an ocean that never existed? Earth-Sci. Rev. 205, 103201 https://doi.org/10.1016/j.earscirev.2020.103201.
Kröner, A., Rojas-Agramonte, Y., Hegner, E., Hoffmann, K.H., Wingate, M.T.D., 2010. SHRIMP zircon dating and Nd isotopic systematics of Palaeoproterozoic migmatitic orthogneisses in the Epupa Metamorphic Complex of northwestern Namibia. Precambrian Res. 183 (1), 50–69. https://doi.org/10.1016/j.precamres.2010.06.018.
Kröner, A., Rojas-Agramonte, Y., Wong, J., Wilde, S.A., 2015. Zircon reconnaissance dating of Proterozoic gneisses along the Kunene River of northwestern Namibia. Tectonophysics 662, 125–139. https://doi.org/10.1016/j.tecto.2015.04.020.
Kröner, A., Rojas-Agramonte, Y., 2017. Mesoproterozoic (Grenville-age) granitoids and supracrustal rocks in Kaokoland, northwestern Namibia. Precambrian Res. 298, 572–592. https://doi.org/10.1016/j.precamres.2017.07.008.
Kröner, S., Konopásek, J., Kröner, A., Passchier, C.W., Poller, U., Wingate, M.T.D., Hofmann, K.H., 2004. U-Pb and Pb-Pb zircon ages for metamorphic rocks in the Kaoko Belt of Northwestern Namibia: A Palaeo- to Mesoproterozoic basement reworked during the Pan-African orogeny. S. Afr. J. Geol. 107 (3), 455–476. https://www.doi.org/10.2113/107.3.455.
Lara, P., Oyhantçabal, P., Belousova, E., 2020. Two distinct crustal sources for Late Neoproterozoic granitic magmatism across the Sierra Ballena Shear Zone, Dom Feliciano Belt, Uruguay: Whole-rock geochemistry, zircon geochronology and Sr-Nd-Hf isotope evidence. Precambrian Res. 341, 105625 https://doi.org/10.1016/j.precamres.2020.105625.
Lehmann, J., Bybee, G.M., Hayes, B., Owen-Smith, T.M., Belyanin, G., 2020. Emplacement of the giant Kunene AMCG complex into a contractional ductile shear zone and implications for the Mesoproterozoic tectonic evolution of SW Angola. Int. J. Earth Sci. 109 (4), 1463–1485. https://doi.org/10.1007/s00531-020-01837-5.
Lenz, C., Fernandes, L.A.D., McNaughton, N.J., Porcher, C.C., Masquelin, H., 2011. U-Pb SHRIMP ages for the Cerro Bori Orthogneisses, Dom Feliciano Belt in Uruguay: Evidences of a ~800Ma magmatic and ~650Ma metamorphic event. Precambrian Res. 185 (3), 149–163. https://doi.org/10.1016/j.precamres.2011.01.007.
Lenz, C., Porcher, C., Fernandes, L., Masquelin, H., Koester, E., Conceição, R., 2013. Geochemistry of the Neoproterozoic (800–767 Ma) Cerro Bori orthogneisses, Dom Feliciano Belt in Uruguay: tectonic evolution of an ancient continental arc. Mineral. Petrol. 107, 785–806. https://www.doi.org/10.1007/s00710-012-0244-4.
Li, Z.-X., Bogdanova, S.V., Collins, A.S., Davidson, A., De Waele, B., Ernst, R.E., Fitzsimons, I.C.W., Fuck, R.A., Gladkochub, D.P., Jacobs, J., Karlstrom, K.E., Lu, S., Natapov, L.M., Pease, V., Pisarevsky, S.A., Thrane, K., Vernikovsky, V., 2008. Assembly, configuration, and break-up history of Rodinia: A synthesis. Precambrian Res. 160 (1), 179–210. https://doi.org/10.1016/j.precamres.2007.04.021.
Li, Z.-X., Evans, D.A.D., Halverson, G.P., 2013. Neoproterozoic glaciations in a revised global palaeogeography from the breakup of Rodinia to the assembly of Gondwanaland. Sediment. Geol. 294, 219–232. https://doi.org/10.1016/j.sedgeo.2013.05.016.
Luft, J.L., Chemale Jr, F., Armstrong, R., 2011. Evidence of 1.7- to 1.8-Ga Collisional Arc in the Kaoko Belt. NW Namibia. Int. J. Earth Sci. 100, 305–321. https://www.doi.org/10.1007/s00531-010-0591-5.
Macey, P.H., Abrahams, Y., Miller, J.A., 2018. Lithostratigraphy of the Mesoproterozoic Stolzenfels Enderbite (Komsberg Suite), South Africa and Namibia. S. Afr. J. Geol. 121 (2), 217–226. https://www.doi.org/10.25131/sajg.121.0016.
Mallmann, G., Chemale Jr, F., Ávila, J.N., Kawashita, K., Armstrong, R.A., 2007. Isotope geochemistry and geochronology of the Nico Pérez Terrane, Rio de la Plata Craton. Uruguay. Gondwana Res. 12 (4), 489–508. https://doi.org/10.1016/j.gr.2007.01.002.
Martil, M.M.D., Bitencourt, M.F., Nardi, L.V.S., Koester, E., Pimentel, M.M., 2017. Pre-collisional, Tonian (ca. 790 Ma) continental arc magmatism in southern Mantiqueira Province, Brazil: Geochemical and isotopic constraints from the Várzea do Capivarita Complex. Lithos 274–275, 39–52. https://doi.org/10.1016/j.lithos.2016.11.011.
Martini, A., Bitencourt, M.F., Weinberg, R.F., De Toni, G.B., Lauro, V.S.N., 2019. From migmatite to magma - crustal melting and generation of granite in the Camboriú Complex, south Brazil. Lithos 340–341, 270–286. https://www.doi.org/10.1016/j.lithos.2019.05.017.
Masquelin, H., Fernandes, L., Lenz, C., Porcher, C.C., McNaughton, N.J., 2012. The Cerro Olivo Complex: A pre-collisional Neoproterozoic magmatic arc in Eastern Uruguay. Int. Geol. Rev. 54, 1161–1183. https://www.doi.org/10.1080/00206814.2011.626597.
McCourt, S., Armstrong, R., Jelsma, H., Mapeo, R., 2013. New U-Pb SHRIMP ages from the Lubango region, SW Angola: Insights into the Palaeoproterozoic evolution of the Angolan Shield, southern Congo Craton. Africa. Geol. Soc. Spec. Publ. 170 (2), 353–363. https://www.doi.org/10.1144/jgs2012-059.
Merdith, A.S., Collins, A.S., Williams, S.E., Pisarevsky, S., Foden, J.D., Archibald, D.B., Blades, M.L., Alessio, B.L., Armistead, S., Plavsa, D., Clark, C., Müller, D.R., 2017a. A Full-Plate Global Reconstruction of the Neoproterozoic. Gondwana Res. 50, 84–134. https://www.doi.org/10.1016/j.gr.2017.04.001.
Merdith, A.S., Williams, S.E., Müller, R.D., Collins, A.S., 2017b. Kinematic constraints on the Rodinia to Gondwana transition. Precambrian Res. 299, 132–150. https://doi.org/10.1016/j.precamres.2017.07.013.
Miller, R.M., 2012. Review of Mesoproterozoic magmatism, sedimentation and terrane amalgamation in southwestern Africa. S. Afr. J. Geol. 115 (4), 417–448. https://www.doi.org/10.2113/gssajg.115.4.417.
Oriolo, S., Oyhantçabal, P., Basei, M.A.S., Wemmer, K., Siegesmund, S., 2016. The Nico Pérez Terrane (Uruguay): From Archean crustal growth and connections with the Congo Craton to late Neoproterozoic accretion to the Río de la Plata Craton. Precambrian Res. 280, 147–160. https://doi.org/10.1016/j.precamres.2016.04.014.
Oriolo, S., Oyhantçabal, P., Konopásek, J., Basei, M.A.S., Frei, R., Sláma, J., Wemmer, K., Siegesmund, S., 2019. Late Paleoproterozoic and Mesoproterozoic magmatism of the Nico Pérez Terrane (Uruguay): Tightening up correlations in southwestern Gondwana. Precambrian Res. 327, 296–313. https://doi.org/10.1016/j.precamres.2019.04.012.
Oyhantçabal, P., Siegesmund, S., Wemmer, K., Frei, R., Layer, P., 2007. Post-collisional transition from calc-alkaline to alkaline magmatism during transcurrent deformation in the southernmost Dom Feliciano Belt (Braziliano–Pan-African, Uruguay). Lithos 98 (1–4), 141–159. https://doi.org/10.1016/j.lithos.2007.03.001.
Oyhantçabal, P., Siegesmund, S., Wemmer, K., Presnyakov, S., Layer, P., 2009. Geochronological constraints on the evolution of the southern Dom Feliciano Belt (Uruguay). J. Geol. Soc. 166 (6), 1075–1084. https://www.doi.org/10.1144/0016-76492008-122.
Oyhantçabal, P., Siegesmund, S., Wemmer, K., Passchier, C.W., 2011a. The transpressional connection between Dom Feliciano and Kaoko Belts at 580–550 Ma. Int. J. Earth Sci. 100, 379–390. https://www.doi.org/10.1007/s00531-010-0577-3.
Oyhantçabal, P., Siegesmund, S., Wemmer, K., 2011b. The Río de la Plata Craton: a review of units, boundaries, ages and isotopic signature. Int. J. Earth Sci. 100 (2), 201–220. https://www.doi.org/10.1007/s00531-010-0580-8.
Oyhantçabal, P., Oriolo, S., Philipp, R.P., Wemmer, K., Siegesmund, S., 2018. The Nico Pérez Terrane of Uruguay and Southeastern Brazil. In: Siegesmund, S. (Ed.), Geology of Southwest Gondwana. Springer International Publishing 10.1007/978-3-319-68920-3_7, Cham, pp. 161–188.
Passarelli, C.R., Basei, M.A.S., Siga, O., Harara, O.M.M., 2018. The Luis Alves and Curitiba Terranes: Continental Fragments in the Adamastor Ocean. In: Siegesmund, S. (Ed.), Geology of Southwest Gondwana. Springer International Publishing, Cham, pp. 189–215 https://www.doi.org/10.1007/978-3-319-68920-3_8.
Pertille, J., Hartmann, L.A., Philipp, R.P., 2015a. Zircon U-Pb age constraints on the Paleoproterozoic sedimentary basement of the Ediacaran Porongos Group, Sul-Riograndense Shield, southern Brazil. J. S. Am. Earth Sci. 63, 334–345. https://doi.org/10.1016/j.jsames.2015.08.005.
Pertille, J., Hartmann, L.A., Philipp, R.P., Petry, T.S., de Carvalho Lana, C., 2015b. Origin of the Ediacaran Porongos Group, Dom Feliciano Belt, southern Brazilian Shield, with emphasis on whole rock and detrital zircon geochemistry and U-Pb, Lu–Hf isotopes. J. S. Am. Earth Sci. 64, 69–93. https://www.doi.org/10.1016/j.jsames.2015.09.001.
Pertille, J., Hartmann, L.A., Santos, J.O.S., McNaughton, N.J., Armstrong, R., 2017. Reconstructing the Cryogenian-Ediacaran evolution of the Porongos fold and thrust belt, Southern Brasiliano Orogen, based on Zircon U-Pb–Hf–O isotopes. Int. Geol. Rev. 59 (12), 1532–1560. https://www.doi.org/10.1080/00206814.2017.1285257.
Philipp, R.P., Machado, R., 2005. The Neoproterozoic to Cambrian granitic magmatism of the Pelotas Batholith, Southern Brazil. J. S. Am. Earth Sci. 19, 461–478.
Philipp, R.P., Massonne, H.-J., de Campos, R.S., 2013. Peraluminous leucogranites of the Cordilheira Suite: A record of Neoproterozoic collision and the generation of the Pelotas Batholith, Dom Feliciano Belt, Southern Brazil. J. S. Am. Earth Sci. 43, 8–24. https://www.doi.org/10.1016/j.jsames.2012.10.006.
Philipp, R.P., Pimentel, M.M., Chemale Jr, F., 2016. Tectonic evolution of the Dom Feliciano Belt in Southern Brazil: Geological relationships and U-Pb geochronology.

Braz. J. Geol. 46, 83–104. https://www.doi.org/10.1590/2317-4889201620150016.
Porada, H., 1989. Pan-African rifting and orogenesis in southern to equatorial Africa and eastern Brazil. Precambrian Res. 44 (2), 103–136. https://doi.org/10.1016/0301-9268(89)90078-8.
Rapela, C.W., Fanning, C.M., Casquet, C., Pankhurst, R.J., Spalletti, L., Poiré, D., Baldo, E.G., 2011. The Rio de la Plata craton and the adjoining Pan-African/brasiliano terranes: Their origins and incorporation into south-west Gondwana. Gondwana Res. 20 (4), 673–690. https://doi.org/10.1016/j.gr.2011.05.001.
Saalmann, K., Remus, M.V.D., Hartmann, L.A., 2006. Structural evolution and tectonic setting of the Porongos belt, southern Brazil. Geol. Mag. 143 (1), 59–88. https://www.doi.org/10.1017/S0016756805001433.
Saalmann, K., Gerdes, A., Lahaye, Y., Hartmann, L., Remus, M., Läufer, A., 2011. Multiple accretion at the eastern margin of the Rio de la Plata craton: the prolonged Brasiliano orogeny in southernmost Brazil. Int. J. Earth Sci. 100, 355–378. https://www.doi.org/10.1007/s00531-010-0564-8.
Sánchez-Bettucci, L., Oyhantçabal, P., Loureiro, J., Ramos, V.A., Preciozzi, F., Basei, M.A.S., 2004. Mineralizations of the Lavalleja Group (Uruguay), a Probable Neoproterozoic Volcano-sedimentary Sequence. Gondwana Res. 7 (3), 745–751. https://www.doi.org/10.1016/S1342-937X(05)71060-1.
Seth, B., Kröner, A., Mezger, K., Nemchin, A.A., Pidgeon, R.T., Okrusch, M., 1998. Archaean to Neoproterozoic magmatic events in the Kaoko belt of NW Namibia and their geodynamic significance. Precambrian Res. 92 (4), 341–363. https://doi.org/10.1016/S0301-9268(98)00086-2.
Seth, B., Armstrong, R.A., Brandt, S., Villa, I.M., Kramers, J.D., 2003. Mesoproterozoic U-Pb and Pb–Pb ages of granulites in NW Namibia: reconstructing a complete orogenic cycle. Precambrian Res. 126 (1–2), 147–168. https://doi.org/10.1016/S0301-9268(03)00193-1.
Silva, L.C., Hartmann, L.A., McNaughton, N.J., Fletcher, I., 2000. Zircon U-Pb SHRIMP dating of a Neoproterozoic overprint in Paleoproterozoic granitic-gneissic terranes, southern Brazil. Am. Mineral. 85 (5–6), 649–667. https://www.doi.org/10.2138/am-2000-5-602.
Silva, L.C., McNaughton, N.J., Fletcher, I.R., 2005. SHRIMP U-Pb zircon geochronology of Neoproterozoic crustal granitoids (Southern Brazil): A case for discrimination of emplacement and inherited ages. Lithos 82 (3–4), 503–525. https://doi.org/10.1016/j.lithos.2004.09.029.
Vermeesch, P., 2012. On the visualisation of detrital age distributions. Chem. Geol. 312–313, 190–194. https://doi.org/10.1016/j.chemgeo.2012.04.021.
Vermeesch, P., Resentini, A., Garzanti, E., 2016. An R package for statistical provenance analysis. Sediment. Geol. 336, 14–25. https://doi.org/10.1016/j.sedgeo.2016.01.009.
Will, T.M., Gaucher, C., Ling, X.X., Li, X.H., Li, Q.L., Frimmel, H.E., 2019. Neoproterozoic magmatic and metamorphic events in the Cuchilla Dionisio Terrane, Uruguay, and possible correlations across the South Atlantic. Precambrian Res. 320, 303–322. https://doi.org/10.1016/j.precamres.2018.11.004.
Zimmermann, U., 2018. The Provenance of Selected Neoproterozoic to Lower Paleozoic Basin Successions of Southwest Gondwana: A Review and Proposal for Further Research. In: Siegesmund, S. (Ed.), Geology of Southwest Gondwana. Springer International Publishing, Cham, pp. 561–591. https://doi.org/10.1007/978-3-319-68920-3_7.

Paper II

Paper III